# Heart and Large Vessel interaction in Congenital Heart Disease

# Assessed by Magnetic Resonance Imaging

Heynric Bernd Grotenhuis
2009

**Heart and Large Vessel interaction in Congenital Heart Disease**
**Assessed by Magnetic Resonance Imaging**
Thesis, Leiden University Medical Center, with references and summary in Dutch.

Printed by: GVO drukkers & vormgevers B.V. | Ponsen & Looijen
Cover design by: Mirelle van Beers
ISBN/EAN: 978-90-6464-351-4

**Heart and Large Vessel interaction in Congenital Heart Disease**

Assessed by Magnetic Resonance Imaging

**Proefschrift**

ter verkrijging van de graad van Doctor aan de Universiteit Leiden
op gezag van Rector Magnificus Prof. mr. P.F. van der Heijden,
volgens besluit van het college voor Promoties te verdedigen op
donderdag 10 september 2009 klokke 15.00 uur

door

**Heynric Bernd Grotenhuis**
geboren te Zeist
in 1976

**Promotiecommissie**

| | |
|---|---|
| Promotores: | Prof. dr. A. de Roos |
| | Prof. dr. J. Ottenkamp |
| Co-promotor: | Dr. J.J.M. Westenberg |
| Referent: | Prof. dr. R. Razavi |
| | King's College / Guy's and St. Thomas Hospitals, London, UK |
| Overige leden: | Prof. dr. J. Bogaert |
| | Katholieke Universiteit Leuven, Leuven, België |
| | Prof. dr. N.A. Blom |
| | Dr. L.J.M. Kroft |

Financial support by the Netherlands Heart Foundation for the publication of this thesis is gratefully acknowledged.
Additional financial support is provided by Astra Zeneca B.V., Bayer B.V., Philips Medical Systems, Boehringer-Ingelheim B.V., J.E. Jurriaanse Stichting, Guerbet Nederland B.V., Servier Nederland Farma B.V., Medis medical imaging systems B.V., Toshiba, Laboratorium voor Klinische en Experimentele Beeldverwerking, Lily en Stichting Imago.

The research described in this thesis was carried out at the departments of Radiology (head: Prof. dr. J.L. Bloem) and Pediatrics (head: Prof. dr. H.A. Delemarre - van de Waal) of the Leiden University Medical Center.

Aan mijn ouders

## Contents

# chapter 01

**General introduction**

## General introduction

The aorta is not simply a tube or conduit, but a highly complex part of the vascular tree, originating from the left ventricular (LV) outflow tract and aortic valve and extending to its major thoracic and abdominal branches. Passing blood from the heart to the limbs and major organs is one functional aspect of the aorta; of equal importance is its capacity to distend and recoil in response to pulsatile flow, thereby reducing afterload for the LV and facilitating diastolic perfusion of the coronary arteries.

Intrinsic aortic wall abnormalities have been described in inherited connective tissue disorders like Marfan syndrome and bicuspid aortic valve disease, in which loss of fibrillin-1 microfibrils will lead to dissociation of smooth muscle cells from the medial matrix components, resulting in accelerated cell death and matrix disruption (1-3). Recent reports in literature indicate similar aortic involvement in patients with classical congenital heart disease entities such as tetralogy of Fallot, transposition of the great arteries, coarctation of the aorta and patients after the Ross procedure, suggesting a similar degenerative process that results in structural weakness of the aortic wall (1). Whether these aortic wall changes result from an intrinsic medial abnormality like in Marfan Syndrome or are secondary to hemodynamic states before and after surgical repair (or both) is unknown (1). Whatever the etiology of aortic wall pathology given this heterogeneity, aortic dilatation and reduced aortic elasticity will evolve when loss of structural support of the aortic wall progresses (1,3).

Interestingly, increased aortic dimensions and reduced aortic elasticity may be the initial steps in a negative cascade affecting aortic valve competence and LV function. Aortic elasticity is an important determinant of LV afterload, as a compliant aorta permits phasic distension and recoil in response to pulsatile flow, thereby reducing afterload for the LV (4,5). Reduced elasticity will therefore lead to increased systolic blood pressure and pulse pressure, which in turn will increase myocardial oxygen demand by increasing LV afterload (6). Furthermore, aortic stiffness proved to be an important determinant of the myocardial ischemic threshold in coronary artery disease during exercise, underlining the relation between aortic stiffness and myocardial performance (7).

Both reduced elasticity and dilatation of the aorta have a detrimental effect on aortic valve function, especially if the aortic valve is already structurally malformed by being bicuspid or quadricuspid (8). Increased dimensions of the aortic annulus lead to loss of coaptation of the aortic valve leaflets, resulting in varying degrees of central aortic regurgitation (3). In addition, aortic valve dynamics are closely related to distensibility of the aortic root. During systole, as the aortic valve opens, the aortic root should expand simultaneously (8,9). Any disturbance in this synchronized process results in increased stress on the aortic valve leaflets, which will ultimately result in degeneration of the aortic valve leaflets and consequent aortic regurgitation (8,10,11). Aortic regurgitation will then lead to a volume overload of the LV, hence increasing LV dimensions that consequently will result in decreased LV ejection fraction (12).

As life expectancy of congenital heart disease patients has significantly improved over the past decades, pediatric and adult cardiologists will be increasingly confronted with the challenge of patients with concomitant aortic sequelae. Therefore, non-invasive monitoring of aortic dimensions and elasticity, in conjunction with aortic valve competence and LV function, is clinically highly desirable in patients with potential aortic wall abnormalities. Echocardiography is widely used for routine assessment of the aortic root, aortic valve and ventricular function, but does not permit evaluation of the entire aorta (13). Magnetic resonance imaging (MRI) provides advantages such as unlimited field-of-view within the entire thorax for accurate and reproducible assessment of aortic and cardiac anatomy and function (13-15). Recently, MRI has also been established as an accurate non-invasive tool for assessment of aortic stiffness by measuring aortic distensibility and pulse wave velocity, as MRI allows for correction of through-plane motion for distensibility measurements and for direct measurement of the path length of pulse waves in the proximal and distal aorta, even in the presence of a tortuous aortic vessel (16).

The main objective of the current thesis is to assess aortic wall elasticity and aortic dimensions and their impact on aortic valve competence and LV function in patients with a bicuspid aortic valve, transposition of the great arteries, tetralogy of Fallot and patients after the Ross procedure, with the use of MRI. In addition, MRI was also used to test whether a similar interaction is present between pulmonary artery dynamics and the right ventricle in the above mentioned entities.

**Chapter 2** reviews the 5 most common entities of inherited connective tissue disorders and classical congenital heart disease with intrinsic aortic wall abnormalities, with description of the potential role of MRI in their evaluation and management. **Chapter 3** describes in vivo validation, as well as testing of reproducibility of aortic pulse wave velocity as assessed with MRI, as indicator of aortic elasticity. **Chapter 4** studies aortic elasticity, aortic valve competence and LV function in non-stenotic bicuspid aortic valve patients. **Chapter 5 and 6** describe aortic elasticity, aortic valve competence and LV function, and the results of pulmonary flow dynamics in relationship with right ventricular function in patients after the arterial switch operation, respectively. **Chapter 7** addresses aortic dimensions and elasticity in conjunction with aortic valve and LV function in patients with repaired tetralogy of Fallot after pulmonary valve replacement. **Chapter 8** describes the outcome of patients who have previously undergone the Ross procedure in our institution for a dysfunctioning aortic valve. **Chapter 9** studies aortic elasticity, aortic valve competence and LV function in patients after the Ross procedure. Finally, **Chapter 10** describes the results of pulmonary flow dynamics in relationship with right ventricular function in patients after the Ross procedure.

In **Chapter 11** all studies presented in this thesis are summarized and future directions are discussed.

## References


1. Niwa K, Perloff JK, Bhuta SM, Laks H, Drinkwater DC, Child JS, Miner PD. Structural abnormalities of great arterial walls in congenital heart disease: light and electron microscopic analyses. Circulation. 2001; 103 (3): 393-400.
2. Luciani GB, Barozzi L, Tomezzoli A, et al. Bicuspid aortic valve disease and pulmonary autograft root dilatation after the Ross procedure: a clinicopathologic study. J Thorac Cardiovasc Surg. 2001; 122 (1): 74-79.
3. Fedak PW, Verma S, David TE, Leask RL, Weisel RD, Butany J. Clinical and pathophysiological implications of a bicuspid aortic valve. Circulation. 2002; 106 (8): 900-904.
4. Mohiaddin RH, Underwood SR, Bogren HG, Firmin DN, Klipstein RH, Rees RS, Longmore DB. Regional aortic compliance studied by magnetic resonance imaging: the effects of age, training, and coronary artery disease. Br Heart J. 1989; 62 (2): 90-96.
5. O'Rourke MF, Hashimoto J. Mechanical factors in arterial aging: a clinical perspective. J Am Coll Cardiol. 2007; 50 (1): 1-13.
6. Kim GB, Kang SJ, Bae EJ, Yun YS, Noh CI, Lee JR, Kim YJ, Lee JY. Elastic properties of the ascending aorta in young children after successful coarctoplasty in infancy. Int J Cardiol. 2004; 97 (3): 471-477.
7. Kingwell BA, Waddell TK, Medley TL, Cameron JD, Dart AM. Large artery stiffness predicts ischemic threshold in patients with coronary artery disease. J Am Coll Cardiol. 2002; 40 (4): 773-779.
8. Schmidtke C, Bechtel J, Hueppe M, Noetzold A, Sievers HH. Size and distensibility of the aortic root and aortic valve function after different techniques of the ross procedure. J Thorac Cardiovasc Surg. 2000; 119 (5): 990-997.
9. Thubrikar MJ, Heckman JL, Nolan SP. High speed cine-radiographic study of aortic valve leaflet motion. J Heart Valve Dis. 1993; 2 (6): 653-661.
10. Thubrikar MJ, Nolan SP, Aouad J, Deck JD. Stress sharing between the sinus and leaflets of canine aortic valve. Ann Thorac Surg. 1986; 42 (4): 434-440.
11. Thubrikar M, Skinner JR, Aouad J, Finkelmeier BA, Nolan SP. Analysis of the design and dynamics of aortic bioprostheses in vivo. J Thorac Cardiovasc Surg. 1982; 84 (2): 282-290.
12. Bekeredjian R, Grayburn PA. Valvular heart disease: aortic regurgitation. Circulation. 2005; 112 (1): 125-134.
13. Pemberton J, Sahn DJ. Imaging of the aorta. Int J Cardiol. 2004; 97 Suppl 1: 53-60.
14. Mohrs OK, Petersen SE, Voigtlaender T, Peters J, Nowak B, Heinemann MK, Kauczor HU. Time-resolved contrast-enhanced MR angiography of the thorax in adults with congenital heart disease. AJR Am J Roentgenol. 2006; 187 (4): 1107-1114.
15. van der Geest RJ, Reiber JH. Quantification in cardiac MRI. J Magn Reson Imaging. 1999; 10 (5): 602-608.
16. Groenink M, de Roos A, Mulder BJ, et al. Changes in aortic distensibility and pulse wave velocity assessed with magnetic resonance imaging following beta-blocker therapy in the Marfan syndrome. Am J Cardiol. 1998; 82 (2): 203-208.

Heynric B. Grotenhuis
Philipp Beerbaum
Jaap Ottenkamp
Jos J.M. Westenberg
Lucia J.M. Kroft
Albert de Roos

# chapter 02

**MR Imaging of Structure and Function of the Aorta in Inherited and Congenital Aortic Disease**

In: Imaging of the Cardiovascular System. Ho V., Reddy G. (editors).

# 1. Introduction

In this chapter the 5 most common entities of inherited connective tissue disorders and classical CHD with intrinsic aortic wall abnormalities will be discussed, including Marfan syndrome, bicuspid aortic valve disease, coarctation of the aorta, tetralogy of Fallot and transposition of the great arteries, with description of the potential role of MRI in their evaluation and management.

# 2. Disease: five entities with aortic wall abnormalities

## 2.1. Marfan syndrome

### Prevalence and epidemiology

Marfan syndrome is a heritable connective tissue disorder resulting in a highly variable degree of premature aortic medial degeneration with a high risk of progressive aortic dilatation and subsequent aortic dissection or rupture (1,2). Marfan syndrome is caused by a mutation of the FBN1 gene on chromosome 15 that codes for fibrillin-1, in the absence of which elastin is more readily degraded by matrix metalloproteinases and smooth muscle cells will dissociate from the medial matrix components (3,4).

### Pathophysiology and follow-up

Aortic dilatation is the most common cause of morbidity and mortality in patients with Marfan syndrome, as dilatation of the sinus of Valsalva is found in 60 - 80% of adult patients (Figure 1) (5). The relative abundance of elastic fibers in the ascending aorta as compared to other regions of the arterial tree, coupled with the repetitive stress of LV ejection, probably account for aortic dilatation that usually occurs primarily in the aortic root (5). Therefore, the majority of patients with Marfan syndrome present with enlargement of the ascending aorta or a type A dissection and only in very rare cases with a type B dissection involving the descending aorta (1). Aortic dissection is associated with increasing aortic diameter, but may also occur in non-dilated aortas (1,2). Replacement of the aortic root with a composite-graft conduit has been recommended before the diameter exceeds 5.0 - 5.5 cm (1,2). Independent predictors of progressive aortic dilatation that will prompt the recommendation for surgery when the aorta is smaller than 5.0 cm include rapid growth of the aortic diameter (> 1 cm / year), a family history of premature aortic dissection (< 5 cm), the presence of greater-than-mild aortic regurgitation (AR), and in patients who are pregnant or contemplating pregnancy (1,2). AR may result from distortion of the aortic valve cusps' coaptation by the enlarged aortic root and occurs in 15 - 44% of patients (1). Especially in young children, progression of findings is more important as a criterion for surgery than absolute size of the aorta (1).

Figure 1.

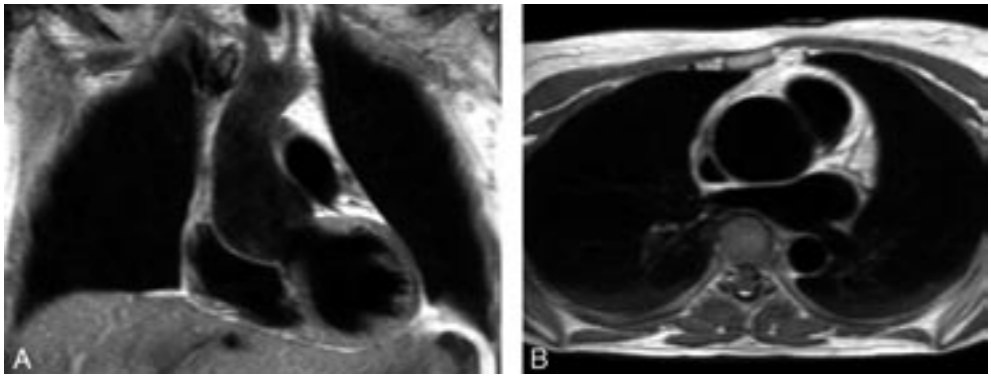


**Figure 1 a-b.** Black-blood turbo spin-echo MR coronal **(a)** and axial **(b)** images in a 46-year old female suspected for Marfan syndrome. Pear-shaped aortic root **(a)** with dilatation up to 5.1 cm, supporting the diagnosis of Marfan syndrome.

Recent MRI reports indicate that reduced aortic distensibility is an independent predictor of progressive aortic dilatation, in addition to aortic diameters (2). As elastin fragmentation in the aortic media is scattered in an irregular pattern along the aorta, regional distensibility may be sensitive in the detection of regional variations in aortic stiffness (2). For optimal risk stratification, aortic stiffness may be taken into account in combination with aortic dimensions and the previously mentioned predictors of progressive aortic dilatation (4,2,5). MRI has been recommended for routine assessment of aortic diameters and stiffness in patients with Marfan syndrome, as well as for the follow-up of aortic complications such as intramural hematoma and aortic aneurysms (4,1,2). Evaluation of aortic dilatation should be performed every 6 months to determine the rate of progression, which can be extended to annual evaluation when the aortic size is stable over time (1). MRI can also be used to adequately monitor the beneficial effect of beta-blocker administration on the progression rate of aortic dilatation and reduction of aortic complications (1).

## 2.2 Bicuspid aortic valve disease

### Prevalence and epidemiology

The bicuspid aortic valve (BAV) is the most common congenital cardiac malformation, occurring in 1 - 2% of the population (6,7). BAV is the result of abnormal aortic cusp formation due to inadequate production of fibrillin-1 during valvulogenesis (4,8) (Figure 2). Adjacent cusps fuse to form a single aberrant cusp, larger than its counterpart yet smaller than 2 normal cusps combined (8). BAV is likely the result of a complex developmental pathology rather than simply the fusion of 2 normal cusps (6-8).

Figure 2.

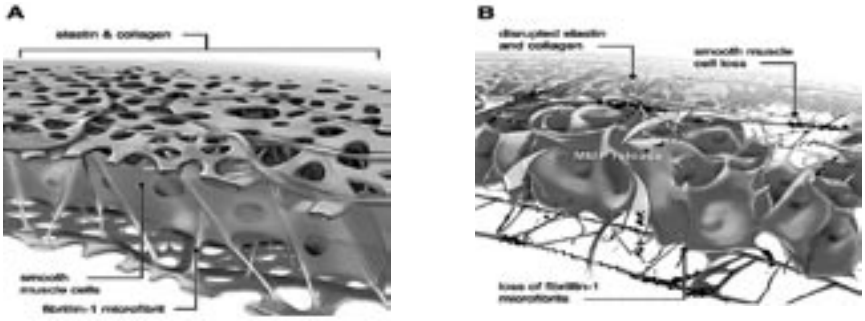


**Figure 2 a-b.** The elastic laminae of the aortic media provide structural support and elasticity to the aorta. In normal tricuspid valve patients **(a)**, fibrillin-1 microfibrils tether smooth muscle cells to adjacent elastin and collagen matrix components. In patients with BAV **(b)**, deficient microfibrillar elements result in smooth muscle cell detachment, MMP release, matrix disruption, cell death and a loss of structural support and elasticity.

Previously published in: 'Clinical and Pathophysiological Implications of a Bicuspid Aortic Valve', Fedak et al. Circulation 2002. Published with permission of Elsevier.

**Pathophysiology and follow-up**

AR is the most frequent (80%) complication in patients with BAV and usually occurs from cusp prolapse, fibrotic retraction or dilation of the sinotubular junction, in many cases requiring aortic valve replacement (4,8). BAV is also present in the majority of elderly patients with significant aortic stenosis, reflecting the propensity for premature fibrosis, stiffening and calcium deposition in these abnormally functioning valves (3,6). The vascular complications of BAV are less well understood and are associated with significant morbidity and mortality (7,8). The histology of the ascending aortic wall in patients with BAV shows strong similarities with the fibrillin-1-deficient aortas of patients with Marfan syndrome, with accelerated degeneration of the aortic media due to loss of fibrillin-1 microfibrils as well as focal abnormalities within the aortic media such as matrix disruption and smooth muscle cell loss (Figure 2) (3,6). Interestingly, BAV is present in more than 70% of patients with coarctation, and both conditions are by themselves and certainly in combination known to be associated with similar aortic wall abnormalities and concomitant aortic dilatation (3,6).

As a consequence of abnormal aortic wall composition in BAV, serious complications like progressive aortic root dilatation (50 - 60% of all patients with BAV) (Figure 3) and/or aneurysm formation may finally result in aortic dissection (5% of all patients with BAV) (7,9). Despite this lower incidence of aortic dissection than in Marfan syndrome (40%), BAV is the more common etiology in aortic dissection as Marfan syndrome is a much rarer entity (0.01% vs 1 - 2% of patients with BAV) (8). Two different phenotypes of aortic dilatation have been described. Dilatation of the mid-ascending aorta is most commonly present (70%) and is associated with aortic valve stenosis, suggesting a post-stenotic causative mechanism (7). Aortic root dilatation is much rarer (13%),

being determined by male gender and degree of AR (7). Aortic root replacement is generally more aggressively recommended for patients with BAV (i.e., 4 - 5 cm) than for those of patients with a tricuspid aortic valve (i.e., 5 - 6 cm) (8). Subdivision into the 2 existing phenotypes may further refine the surgical approach by suggesting aortic root sparing when only dilatation of the mid-ascending aorta is present (7).

Figure 3.

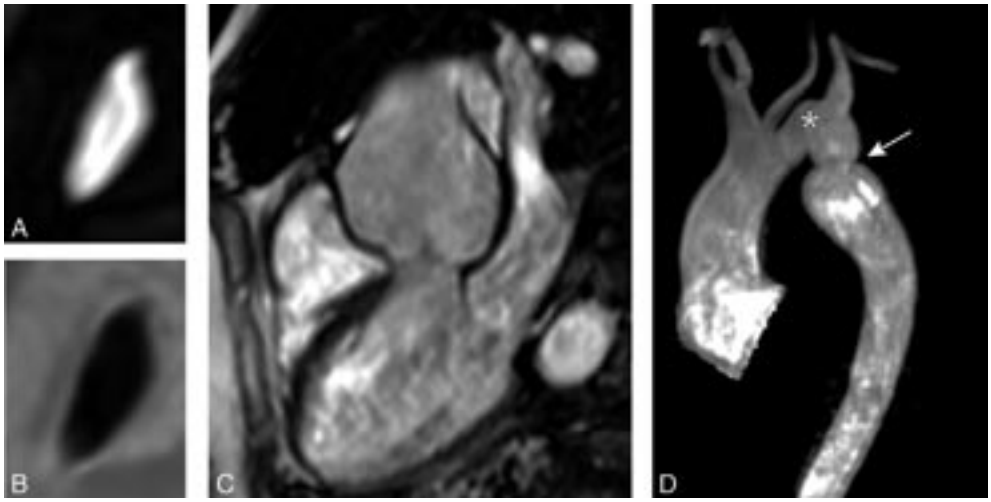


**Figure 3 a-d.** Phase contrast modulus **(a)** and phase **(b)** images of a bicuspid aortic valve, gradient-echo image of the aortic root **(c)**, and gadolinium-chelate enhanced MR angiographic image of the thoracic aorta **(d)** in a 54-year old female. Note the combination of the slit-like bicuspid aortic valve with slit flow **(a,b)** and post-stenotic dilatation that measured 4.6 cm **(c)**, together with other aortic pathology; aortic kinking **(*, d)** and pseudo coarctation **(arrow, d)**. This patient had Turner syndrome.

A recent MRI study reported frequent aortic root dilatation and reduced elasticity in the entire aorta, suggesting that not only the proximal part of the aorta is affected in BAV, but that aortic wall lesions extend into the entire aorta (10). Evaluation of the elastic properties of the ascending aorta might be useful to identify patients who are at risk of progressive aortic dilatation, analogous to patients with Marfan syndrome (2,10). Increased aortic stiffness was also associated with LV hypertrophy, as a result of increased LV afterload (10). Sustained LV hypertrophy is associated with reduced diastolic filling and therefore - as diastolic LV dysfunction is a major contributor to congestive heart failure - the presence of LV hypertrophy might pose a future risk for LV function in patients with BAV (10). As many patients with BAV will require cardiac surgery during their lifetime, close monitoring of aortic dimensions, aortic elasticity, aortic valve competence and LV function is mandatory during follow-up, to allow timely intervention (10).

## 2.3 Coarctation of the aorta

### Prevalence and epidemiology

Coarctation of the aorta accounts for 5% of all CHD and is defined as a congenital narrowing of the aorta, most commonly located in a juxtaductal position just distally to the origin of the left subclavian artery (11). A wide spectrum of narrowing of the aorta can be observed, from a discrete narrowing to a hypoplastic aortic arch, whether or not associated with intra-cardiac defects like a VSD or aortic valve pathology (10). Classic symptoms are heart failure and an increased blood pressure proximal to the narrowing, as well as a low perfusion status of the body distally to the coarctation (10). Coarctation of the aorta is associated with a significantly increased cardiovascular morbidity and reduced life expectancy even after successful surgical correction at a young age (11-16). Structural aortic wall abnormalities with reduced aortic elastic properties proximal and distal to the site of coarctation imply that coarctation of the aorta is a systemic vascular disease (4,13). Neonates with coarctation were found to have reduced elastic properties of the aorta before and after successful operation, suggesting a primary defect (15). Concomitant presence of BAV in 20 - 85% of patients with coarctation and the strong histological similarity of aortic wall abnormalities between both entities is also suggestive for an inherited origin of aortic wall pathology (3,6,9).

### Pathophysiology and follow-up

After initially successful surgical repair, complications may occur such as persistence of hypertension, recoarctation, aortic dilatation and aneurysm formation (Figure 4) (13). Persisting resting and exercise-induced hypertension have been reported in 10 - 46% and 30 - 60%, respectively, being the most important postoperative cardiovascular events (2,12). Hypertension in coarctation is accompanied by an increase in aortic medial collagen and a decrease in smooth muscle (increased stiffness) that may persist after successful repair and coincides with aortic abnormalities of a coexisting BAV (3,4). In addition, late hypertension may be caused by functional recoarctation at the site of surgical repair due to decreased distensibility (16). Impaired LV function, increased LV mass and concomitant adverse LV remodeling even in postoperative patients with normal blood pressure can be attributed to the reduced aortic elastic properties which result in increased LV afterload (17). Furthermore, arterial hypertension and a resting pressure gradient are major contributing factors to early atherosclerotic development and should therefore be primary targets for therapy (13).

Figure 4.

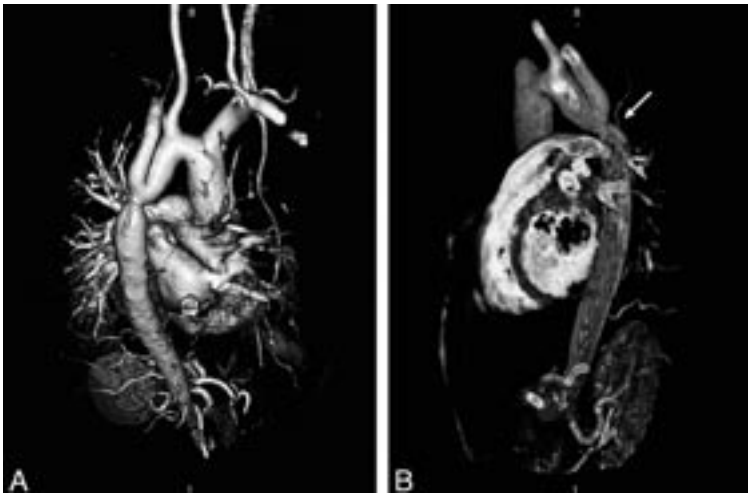


**Figure 4 a-b.** Gadolinium-chelate enhanced MR angiographic images in a 34-year old male. Follow-up study after coarctation repair. Shaded surface full volume rendering display image **(a)** and selected volume rendering display image **(b)**. Flow speed was significantly increased at the level of stenosis due to residual / re-coarctation **(arrow, a, b)**. MR phase contrast flow volume was 7.2 l/min as measured immediately distal from the level of the stenosis, and 6.0 l/min measured at the level of the diaphragm. This indicates flow decrease from the proximal to the distal descending thoracic aorta, excluding hemodynamically significant collateral flow. Note the relative normal size of the intercostal arteries; no major collaterals were observed at MR angiography.

Adults after surgical repair of coarctation, especially when associated with BAV, should be closely monitored for detection of recoarctation as well as progressive aortic dilatation (13). Risk factors for these long-term aortic complications are the presence of BAV, advanced age and hypertension (4). Systematic MRI screening performed at 2 to 5 year intervals has been found to be the most 'cost-effective' approach for the follow-up of patients after coarctation repair, with early detection of aortic complications like recoarctation (4,18). Spin-echo MRI is essential to detect abnormalities of the aortic wall and associated intracardiac abnormalities, while contrast-enhanced 3-D MR angiography provides a highly accurate view of the entire reconstructed aorta and this may obviate the need for invasive x-ray angiography by catheterization for planning of treatment (Figure 4) (14). A combination of anatomic and flow data obtained by MRI is able to predict a catheterization peak-to-peak gradient ≥ 20 mm Hg, considered to be the reference standard for hemodynamic severity of (re-) coarctation (14). The combination of narrowest aortic cross-sectional area and heart rate-corrected mean flow deceleration in the descending aorta distinguishes between those who have transcatheter pressure-gradients above and below 20 mm Hg, which can be used to determine the need for intervention (14). Velocity-encoded MRI is also useful to determine presence and hemodynamics of collateral vessels, which maintain distal aortic perfusion depending on the severity of the aortic obstruction

(19). Finally, promising utilities are MRI-guided balloon angioplasty and MRI-guided deployment of stents to repair aortic coarctation, as recent studies indicate that the combined use of MRI and X-ray imaging is effective for relieve of stenosis with a significant reduction of radiation exposure (20).

## 2.4 Tetralogy of Fallot

### Prevalence and epidemiology

Tetralogy of Fallot (TOF) is the most commonly encountered cyanotic CHD entity with a frequency of nearly 10% of all CHD patients (21). Anterior displacement of the outflow septum is the primary defect, resulting in a VSD, overriding of the aorta, RVOT obstruction and right ventricular hypertrophy (21). Patients after TOF repair frequently encounter longstanding pulmonary regurgitation and associated impaired right ventricular function after primary repair (21).

### Pathophysiology and follow-up

Progressive dilatation of the aortic root during long-term follow-up has also frequently been described after TOF repair, ranging in incidence between 15 - 88% depending on definition of aortic root dilatation (Figure 5) (21-24). Two hypotheses have been postulated to explain this observation. Increased blood flow from both ventricles to the overriding aorta before surgical repair is thought to be an underlying pathogenic mechanism, posing increased stress on the aortic wall (3,21,23,24). This premise is supported by risk factors such as longer shunt-to-repair interval and a higher prevalence of pulmonary atresia (PA) among patients with TOF and aortic root dilatation (23). Secondly, histological changes of the aortic media such as non-inflammatory loss of smooth muscle cells and fragmentation of the elastic fibers have been reported, resembling those observed in patients with Marfan syndrome and BAV (3,21).

The potential for complications of aortic root dilatation that may necessitate surgical intervention is increasingly recognized in patients after TOF repair (22). A recent study reported the progressive nature of aortic dilatation in patients with TOF, as aortic dilatation increased at a rate of 1.7 mm/year, in contrast to 0.03 mm/year in healthy controls (24). Also, more marked histological changes were observed with increasing age, suggesting that aging coupled with volume overloading on top of intrinsic aortic wall abnormalities have an additional adverse effect on the aortic histology and thus aortic dilatation (21). Additionally, AR associated with progressive dilation of the aortic root is frequently present and 15 - 18% of patients after TOF repair show mild degrees of AR (Figure 5) (24). Recent case reports of aortic dissection late after TOF repair in adults whose aortic roots exceeded 6 cm in diameter indicate that close monitoring of aortic dimensions is mandatory, especially when a dilated ascending aorta is present (25). Aortic root surgery may be considered for patients after TOF repair in case of progressive AR and aortic root dilatation exceeding 5.5 cm, particularly when the primary indication for surgery is pulmonary valve replacement and both procedures may be combined (26). At present, there is

Figure 5.

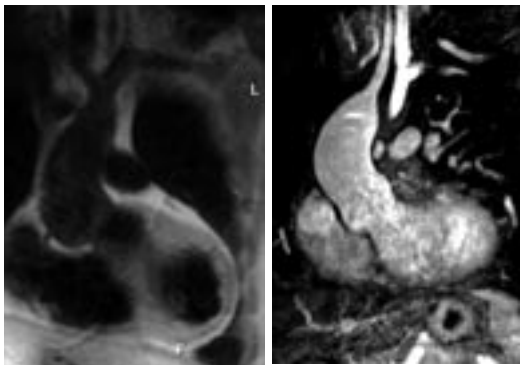

**Figure 5 a-b. (a)** Coronal black-blood turbo spin-echo MR image of the ascending aorta in a 16-year old male with tetralogy of Fallot. The dilated ascending aorta has a maximum diameter of 4.0 cm. This patient has no aortic valve regurgitation. **(b)** Coronal gadolinium-chelate enhanced maximum intensity projection angiographic MR image in a 36-year old male with tetralogy of Fallot after previous repair. The aortic root and ascending aorta are dilated (aortic root 4.8 cm, ascending aorta 4.4 cm wide). Patient has slight aortic regurgitation (9%) and moderate biventricular function.

no consensus on beta-blocker administration for prevention of progressive aortic root dilatation, nor at what stage aortic root surgery should be considered in patients after TOF repair (24).

## 2.5 Transposition of the great arteries

### Prevalence and epidemiology

Transposition of the great arteries (TGA) is defined as atrial situs solitus, normal (concordant) connection between atria and ventricles and abnormal (discordant) ventriculo-arterial connections (27). The aorta arises from the right ventricle and the pulmonary artery arises from the left ventricle. It accounts for 4.5% of all congenital cardiac malformations (27). The arterial switch operation (ASO) has become the preferred method of surgery for transposition of the great arteries (TGA) (28). Although this technique has significantly reduced the number of sequelae associated with surgical correction of TGA, completion of the ASO may still predispose patients to aortic root dilatation and AR (28-30).

### Pathophysiology and follow-up

Intrinsic aortic wall pathology in TGA has been reported due to abnormal aorticopulmonary septation, damage to the vasa vasorum, and surgical manipulations during the ASO, predisposing to aortic dilatation, aneurysm formation and even aortic dissection (Figure 6) (28,31,32). In addition, aortic distensibility may be reduced by impaired aortic elastogenesis as well as by scar formation at the site of anastomosis (28). High grade medial abnormalities in the ascending aorta have already been observed during the neonatal period, suggesting that they are inherited analogously to prototypical extremes such as in patients with Marfan syndrome or BAV (3,28).

Others concluded that aortic wall abnormalities develop due to structural differences in wall composition between the 2 great arteries, as the former pulmonary arterial wall is exposed to higher systemic pressures after the ASO, posing increased stress on the neo-aortic wall which may ultimately lead to changes in structure and function of the neo-aortic root (32,33). Whether medial abnormalities are inherent or acquired remains therefore difficult to distinguish (3).

Figure 6.

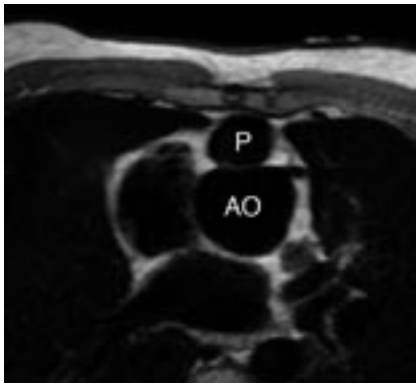


**Figure 6.** Oblique transverse black-blood turbo spin-echo MR image of the ascending aorta in a 19-year old male after the arterial switch operation with Lecompte procedure. The dilated aortic root (Ao) has a maximum diameter of 4.6 cm. Note the origin of the main coronary artery and note the anterior position of the pulmonary artery (P) to the aorta.

A high incidence of AR has been reported after ASO (30% at 6 years after ASO) and is probably the result of a multifactorial process for which aortic root geometry, surgical techniques and preoperative size discrepancy between the 2 great arteries are involved (29,34). In addition, AR appears to be functionally correlated with aortic root dilatation and reduced elasticity of the proximal aorta (30). Whether or not (previous) existence of a VSD plays an additional role remains controversial, although its hemodynamic effect might contribute to a size discrepancy between the aorta and pulmonary artery (28).

A recent MRI report described not only frequent aortic root dilatation and AR, but also a cascade of events ultimately leading to LV systolic dysfunction in patients after ASO (30). Frequent aortic root dilatation and reduced proximal aortic wall elasticity were associated with degree of AR. AR subsequently lead to increased LV dimensions, which consequently resulted in decreased LV ejection fraction. Therefore, LV systolic dysfunction as the endpoint in a sequence of events poses a prognostic risk for patients after ASO (30). Further elucidation of the underlying pathogenic substrate of aortic wall abnormalities and its clinical repercussions for patients after ASO is however required, as ASO is still a relative new surgical procedure for patients with TGA (30).

## References


1. Milewicz DM, Dietz HC, Miller DC. Treatment of aortic disease in patients with Marfan syndrome. Circulation. 2005; 111 (11): e150-e157.
2. Nollen GJ, Groenink M, Tijssen JG, van der Wall EE, Mulder BJ. Aortic stiffness and diameter predict progressive aortic dilatation in patients with Marfan syndrome. Eur Heart J. 2004; 25 (13): 1146-1152.
3. Niwa K, Perloff JK, Bhuta SM, Laks H, Drinkwater DC, Child JS, Miner PD. Structural abnormalities of great arterial walls in congenital heart disease: light and electron microscopic analyses. Circulation. 2001; 103 (3): 393-400.
4. Pemberton J, Sahn DJ. Imaging of the aorta. Int J Cardiol. 2004; 97 Suppl 1: 53-60.
5. Nollen GJ, Mulder BJ. What is new in the Marfan syndrome? Int J Cardiol. 2004; 97 Suppl 1: 103-108.
6. Fedak PW, David TE, Borger M, Verma S, Butany J, Weisel RD. Bicuspid aortic valve disease: recent insights in pathophysiology and treatment. Expert Rev Cardiovasc Ther. 2005; 3 (2): 295-308.
7. Della CA, Bancone C, Quarto C, Dialetto G, Covino FE, Scardone M, Caianiello G, Cotrufo M. Predictors of ascending aortic dilatation with bicuspid aortic valve: a wide spectrum of disease expression. Eur J Cardiothorac Surg. 2007; 31 (3): 397-404.
8. Fedak PW, Verma S, David TE, Leask RL, Weisel RD, Butany J. Clinical and pathophysiological implications of a bicuspid aortic valve. Circulation. 2002; 106 (8): 900-904.
9. Ward C. Clinical significance of the bicuspid aortic valve. Heart. 2000; 83 (1): 81-85.
10. Grotenhuis HB, Ottenkamp J, Westenberg JJ, Bax JJ, Kroft LJ, de Roos A. Reduced aortic elasticity and dilatation are associated with aortic regurgitation and left ventricular hypertrophy in nonstenotic bicuspid aortic valve patients. J Am Coll Cardiol. 2007; 49 (15): 1660-1665.
11. Rosenthal E. Coarctation of the aorta from fetus to adult: curable condition or life long disease process? Heart. 2005; 91 (11): 1495-1502.
12. Kim GB, Kang SJ, Bae EJ, Yun YS, Noh CI, Lee JR, Kim YJ, Lee JY. Elastic properties of the ascending aorta in young children after successful coarctoplasty in infancy. Int J Cardiol. 2004; 97 (3): 471-477.
13. Meyer AA, Joharchi MS, Kundt G, Schuff-Werner P, Steinhoff G, Kienast W. Predicting the risk of early atherosclerotic disease development in children after repair of aortic coarctation. Eur Heart J. 2005; 26 (6): 617-622.
14. Nielsen JC, Powell AJ, Gauvreau K, Marcus EN, Prakash A, Geva T. Magnetic resonance imaging predictors of coarctation severity. Circulation. 2005; 111 (5): 622-628.
15. Vogt M, Kuhn A, Baumgartner D, Baumgartner C, Busch R, Kostolny M, Hess J. Impaired elastic properties of the ascending aorta in newborns before and early after successful coarctation repair: proof of a systemic vascular disease of the prestenotic arteries? Circulation. 2005; 111 (24): 3269-3273.
16. Ong CM, Canter CE, Gutierrez FR, Sekarski DR, Goldring DR. Increased stiffness and persistent narrowing of the aorta after successful repair of coarctation of the aorta: relationship to left ventricular mass and blood pressure at rest and with exercise. Am Heart J. 1992; 123 (6): 1594-1600.

17. Krogmann ON, Rammos S, Jakob M, Corin WJ, Hess OM, Bourgeois M. Left ventricular diastolic dysfunction late after coarctation repair in childhood: influence of left ventricular hypertrophy. J Am Coll Cardiol. 1993; 21 (6): 1454-1460.
18. Therrien J, Thorne SA, Wright A, Kilner PJ, Somerville J. Repaired coarctation: a "cost-effective" approach to identify complications in adults. J Am Coll Cardiol. 2000; 35 (4): 997-1002.
19. Araoz PA, Reddy GP, Tarnoff H, Roge CL, Higgins CB. MR findings of collateral circulation are more accurate measures of hemodynamic significance than arm-leg blood pressure gradient after repair of coarctation of the aorta. J Magn Reson Imaging. 2003 17 (2): 177-183.
20. Krueger JJ, Ewert P, Yilmaz S, Gelernter D, Peters B, Pietzner K, Bornstedt A, Schnackenburg B, Abdul-Khaliq H, Fleck E, Nagel E, Berger F, Kuehne T. Magnetic resonance imaging-guided balloon angioplasty of coarctation of the aorta: a pilot study. Circulation. 2006; 113 (8): 1093-1100.
21. Tan JL, Davlouros PA, McCarthy KP, Gatzoulis MA, Ho SY. Intrinsic histological abnormalities of aortic root and ascending aorta in tetralogy of Fallot: evidence of causative mechanism for aortic dilatation and aortopathy. Circulation. 2005; 112 (7): 961-968.
22. Cheung YF, Ou X, Wong SJ. Central and peripheral arterial stiffness in patients after surgical repair of tetralogy of Fallot: implications for aortic root dilatation. Heart. 2006; 92 (12): 1827-1830.
23. Niwa K. Aortic root dilatation in tetralogy of Fallot long-term after repair-histology of the aorta in tetralogy of Fallot: evidence of intrinsic aortopathy. Int J Cardiol. 2005; 103 (2): 117-119.
24. Niwa K, Siu SC, Webb GD, Gatzoulis MA. Progressive aortic root dilatation in adults late after repair of tetralogy of Fallot. Circulation. 2002; 106 (11): 1374-1378.
25. Rathi VK, Doyle M, Williams RB, Yamrozik J, Shannon RP, Biederman RW. Massive aortic aneurysm and dissection in repaired tetralogy of Fallot; diagnosis by cardiovascular magnetic resonance imaging. Int J Cardiol. 2005; 101 (1): 169-170.
26. Therrien J, Gatzoulis M, Graham T, Bink-Boelkens M, Connelly M, Niwa K, Mulder B, Pyeritz R, Perloff J, Somerville J, Webb GD. Canadian Cardiovascular Society Consensus Conference 2001 update: Recommendations for the Management of Adults with Congenital Heart Disease--Part II. Can J Cardiol. 2001; 17 (10): 1029-1050.
27. Warnes CA. Transposition of the great arteries. Circulation. 2006; 114 (24): 2699-2709.
28. Hwang HY, Kim WH, Kwak JG, Lee JR, Kim YJ, Rho JR, Bae EJ, Noh CI. Mid-term follow-up of neoaortic regurgitation after the arterial switch operation for transposition of the great arteries. Eur J Cardiothorac Surg. 2006; 29 (2): 162-167.
29. Formigari R, Toscano A, Giardini A, Gargiulo G, Di Donato R, Picchio FM, Pasquini L. Prevalence and predictors of neoaortic regurgitation after arterial switch operation for transposition of the great arteries. J Thorac Cardiovasc Surg. 2003; 126 (6): 1753-1759.
30. Grotenhuis HB, Ottenkamp J, Fontein D, Vliegen HW, Westenberg JJM, Kroft LJM, de Roos A. MRI of aortic elasticity and left ventricular function after the arterial switch operation - initial experience. Radiology. 2008; 249 (3): 801-809.

31. Murakami T, Nakazawa M, Momma K, Imai Y. Impaired distensibility of neoaorta after arterial switch procedure. Ann Thorac Surg. 2000; 70 (6): 1907-1910.
32. Hourihan M, Colan SD, Wernovsky G, Maheswari U, Mayer JE, Jr., Sanders SP. Growth of the aortic anastomosis, annulus, and root after the arterial switch procedure performed in infancy. Circulation. 1993;88 (2): 615-620.
33. Schoof PH, Gittenberger-de Groot AC, de Heer E, Bruijn JA, Hazekamp MG, Huysmans HA. Remodeling of the porcine pulmonary autograft wall in the aortic position. J Thorac Cardiovasc Surg. 2000; 120 (1): 55-65.
34. Haas F, Wottke M, Poppert H, Meisner H. Long-term survival and functional follow-up in patients after the arterial switch operation. Ann Thorac Surg. 1999; 68 (5): 1692-1697.

Heynric B. Grotenhuis
Jos J.M. Westenberg
Paul Steendijk
Rob J. van der Geest
Jaap Ottenkamp
Jeroen J. Bax
J. Wouter Jukema
Albert de Roos

# chapter 03

**Validation and Reproducibility of Aortic Pulse Wave Velocity as assessed with Velocity-Encoded MRI.**

Journal of Magnetic Resonance Imaging. Accepted for publication.

## Abstract

**Purpose:** To validate magnetic resonance imaging (MRI) assessment of aortic pulse wave velocity ($PWV_{MRI}$) with PWV determined from invasive intra-aortic pressure measurements ($PWV_{INV}$) and to test reproducibility of the measurement by MRI.

**Materials and Methods:** $PWV_{MRI}$ was compared with $PWV_{INV}$ in 18 non-consecutive patients scheduled for catheterization for suspected coronary artery disease. Reproducibility of $PWV_{MRI}$ was tested in ten healthy volunteers, who underwent repeated measurement of $PWV_{MRI}$ on a single occasion. Velocity-encoded MRI was performed in all participants to assess $PWV_{MRI}$ in the total aorta ($Ao_{total}$), the proximal aorta ($Ao_{prox}$) and distal aorta ($Ao_{dist}$).

**Results:** Results are expressed as mean ± SD, Pearson correlation coefficent (PCC) and intraclass correlation (ICC). Good agreement between $PWV_{MRI}$ and $PWV_{INV}$ was found for $Ao_{total}$ (6.5 ± 1.1 m/s vs 6.1 ± 0.8 m/s; PCC = 0.53), $Ao_{prox}$ (6.5 ± 1.3 m/s vs 6.2 ± 1.1 m/s; PCC = 0.69) and for $Ao_{dist}$ (6.9 ± 1.1 m/s vs 6.1 ± 1.0 m/s; PCC = 0.71). Reproducibility of $PWV_{MRI}$ was high for $Ao_{total}$ (4.3 ± 0.5 m/s vs 4.6 ± 0.7 m/s; ICC = 0.90, $P < 0.01$), $Ao_{prox}$ (4.3 ± 0.9 m/s vs 4.7 ± 1.0 m/s; ICC = 0.87, $P < 0.01$) and $Ao_{dist}$ (4.3 ± 0.6 m/s vs 4.4 ± 0.8 m/s; ICC = 0.92, $P < 0.01$).

**Conclusion**: MRI assessment of aortic pulse wave velocity shows good agreement with invasive pressure measurements and can be determined with high reproducibility.

## Introduction

The aortic wall structure undergoes degenerative changes with advancing age, which is associated with a decline of aortic elasticity (1-5). Numerous reports emphasize the importance of aortic pulse wave velocity (PWV) as an indicator of arterial stiffness and as a prognostic indicator for future cardiovascular events (2-12). PWV is defined as the velocity of the systolic wave front propagating through the aorta and is increased when atherosclerotic degeneration of the wall and concomitant reduction of the elastic recoil are present (10).

Intra-arterial pressure measurements provide the most accurate assessment of the aortic PWV (13,14), but this modality requires an invasive procedure and is therefore not suitable for widespread clinical use. Tonometry and ultrasound are established modalities for quantification of global vascular function, but both modalities only provide an estimation of the aortic PWV, due to the limited availability to obtain acoustic windows and the inability to spatially register the distance between the acquisition sites along the length of the aorta (4,5,6). In addition, as aortic wall condition may vary along the course of the aorta, regional assessment of aortic PWV is clinically desirable, for which both techniques or not suited.

Velocity-encoded (VE) magnetic resonance imaging (MRI) allows for accurate assessment of the blood flow velocity with a sufficient temporal and spatial resolution to study the propagation of the aortic systolic flow wave (13-16). The true path length of the pulse wave along the aorta can directly be assessed with MRI, even in the presence of a tortuous course of the aorta, and regional elastic properties of the aorta can be studied, depending on the number of aortic segments studied.

To our knowledge, PWV-assessment using MRI has not been validated previously in vivo. The purpose of the current study was therefore to validate MRI assessment of aortic pulse wave velocity ($PWV_{MRI}$) with PWV determined from invasive intra-aortic pressure measurements ($PWV_{INV}$) and to test reproducibility of $PWV_{MRI}$.

## Materials and Methods

### Subjects

The local medical ethics committee approved the study and informed consent was obtained from all participants prior to their enrollment in the study. Characteristics of the participant groups are listed in Table 1.

Table 1. Characteristics of participants.

| Characteristics | group 1 (n = 18) | group 2 (n = 10) |
|---|---|---|
| male / female | 15 / 3 | 7 / 3 |
| age at MRI (years) * | 59 ± 10 | 29 ± 8 |
| height (cm) * | 174 ± 8 | 180 ± 10 |
| weight (kg) * | 83 ± 17 | 80 ± 13 |
| blood pressure systolic (mm Hg) during MRI * | 131 ± 19 | 118 ± 14 |
| blood pressure diastolic (mm Hg) during MRI * | 77 ± 13 | 73 ± 12 |
| heart rate (beats per minute) during MRI * | 66 ± 11 | 61 ± 8 |
| smoking (yes / no) | 13 / 5 | 0 / 10 |
| NYHA class II / III / IV | 8 / 8 / 2 | |

Group 1: patients for $PWV_{MRI}$ and $PWV_{INV}$ comparison.
Group 2: healthy subjects for reproducibility of $PWV_{MRI}$-assessment.

Note: unless otherwise indicated, data are number of participants and data in parentheses are percentages.
* Data are mean ± standard deviation.
Abbreviations: MRI = magnetic resonance imaging; NYHA = New York Heart Association.

Eighteen non-consecutive patients (15 male, 3 female; mean ± SD age 59 ± 10 years) with suspected coronary artery disease (group 1) - scheduled to undergo elective coronary angiography on clinical indication - were prospectively included to validate $PWV_{MRI}$-assessment by comparison with $PWV_{INV}$. The mean interval between cardiac catheterization and MRI was 15 ± 12 days.

Ten healthy non-smoking volunteers (7 male, 3 female; mean ± SD age 29 ± 8 years) without signs and symptoms of cardiovascular disease (group 2) were recruited to test reproducibility in $PWV_{MRI}$-assessment. The volunteers were studied twice (with repositioning of the subjects between the two examinations) using the same MRI protocol.

Exclusion criteria comprised of evidence of aortic valve stenosis (aortic velocity > 2.5 m/s on echocardiography), aortic coarctation and/or other forms of congenital heart disease, Marfan syndrome or a family history of Marfan syndrome and general contraindications to MRI.

**VE MRI for $PWV_{MRI}$**

MRI was performed in all participants on a 1.5-T MRI scanner with a mean acquisition time of 12 ± 2 minutes (ACS-NT15 Intera, Philips Medical Systems, The Netherlands; software release 11, Pulsar gradient system with amplitude 33 mT/m and 100 mT/m/ms slew rate, 0.33 ms rise time).

$PWV_{MRI}$ was assessed in the proximal aorta ($Ao_{prox}$) between the ascending and proximal descending aorta, and in the distal aorta ($Ao_{dist}$) between the proximal descending aorta and the abdominal aorta (Figure 1A). $PWV_{MRI}$ of the total aorta ($Ao_{total}$) was assessed using the datasets acquired at the ascending aorta and the abdominal aorta. Imaging sequences were previously described (18). In short, an oblique-sagittal single-slice segmented gradient-echo scout image was obtained to depict the full course of the aorta, with two transverse saturation-slabs applied perpendicular to the aorta (at the level of the pulmonary trunk and at the most distal level of the abdominal aorta depicted in the oblique sagittal scout) to indicate the location of the sites for subsequent through-plane VE MRI acquisition (18). One-directional through-plane non-segmented VE MRI using free breathing with retrospective ECG-gating was applied perpendicular to the aorta at the levels of the saturation-slabs in the scout image to assess the aortic flow at the 3 measurement sites (18). A maximal number of phases reconstructed during one average cardiac cycle resulted in a temporal resolution of 6-10 ms, depending on the heart rate. Arrhythmia rejection was used with an acceptance window of 15% of the set heart rate. Local phase correction filter was used to set velocity values in voxels with low magnitude to zero, in order to suppress background noise.

Figure 1. Analysis of pulse wave velocity with MRI and invasive pressure measurements.

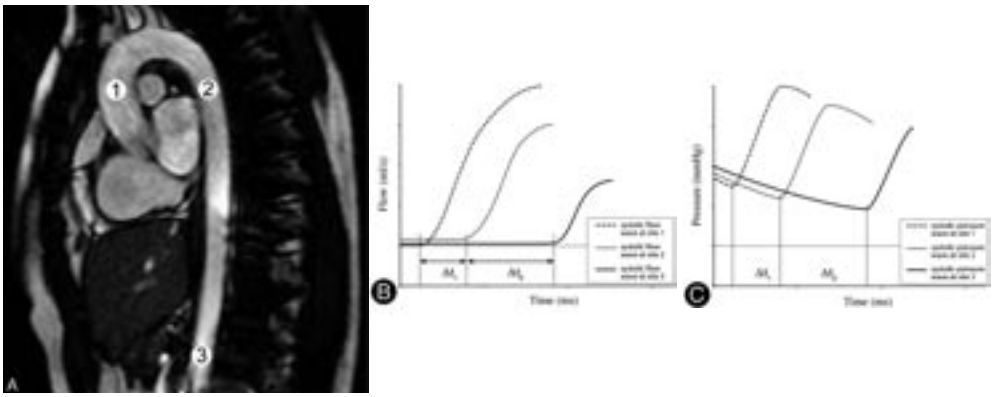


**Figure 1 a-c. (a)** An oblique sagittal scout covering the full course of the aorta, indicating the sites for the through-plane velocity-encoded PWVMRI assessments and the invasive pressure measurements for PWVINV: the ascending aorta (1), the proximal descending aorta just distal to the aortic arch (2), and the most distal level of the abdominal aorta depicted in the oblique sagittal scout (3). Determination of the onset of the three systolic flow waves for PWVMRI at the measurement sites are depicted in **(b)** while determination of the onset of the three systolic pressure waves for PWVINV at the measurement sites are depicted in **(c)**. The distance between these sites and the transit time ($\Delta t_1$ and $\Delta t_2$) between the individual onsets of the systolic flow waves **(b,c)** determine the PWV.

$PWV_{MRI}$ was calculated as $\Delta x/\Delta t$ (expressed in m/s), where $\Delta x$ is the aortic path length between the measurement sites and $\Delta t$ is the transit time between the arrival of the systolic wave front at these sites (Figure 1B) (14,18,19). The aortic path lengths between the three subsequent measurement sites were manually determined along the centerline of the aorta within the scout image by using the software package MASS (Medis, The Netherlands) (Figure 1A) (18). Aortic velocity maps were analyzed with the software package FLOW (Medis, The Netherlands) (18,20). The onset of the systolic wave front was automatically determined using custom-made software from the resulting flow graph by the intersection point of the constant horizontal diastolic flow and upslope of the systolic wave front, modeled by linear regression along the upslope. The regression line was modeled from the flow values between 20% and 80% of the total range.

**Invasive pressure measurements for $PWV_{INV}$**

In the 18 patients with suspected coronary artery disease (group 1), invasive pressure-time curves and simultaneous ECG recordings were obtained during catheterization immediately after vascular access, to avoid any interference by medication or performed procedures. Pressure measurements were acquired at three sites in the aorta, at similar locations as used for the $PWV_{MRI}$-assessments (Figure 1A). A 6 French JR4 pressure tip catheter (Cordis Corporation, USA) was introduced through a 6 French sheet (Cordis Corporation, USA) into either one of the femoral arteries and advanced through the aorta until just distal to the aortic valve, for pressure measurements at the level of the ascending aorta. During pullback, pressure waves were recorded at multiple positions, 5.8 cm apart consecutively. After MRI acquisition, the pressure measurements nearest to the MRI measurement sites 2 and 3 were used for determining $PWV_{INV.}$ Pressure-time curves and ECG were recorded with a sampling resolution of 2 kHz during at least 10 cardiac cycles. The pressure-time curves recorded in the ascending and proximal descending aorta were used to calculate the $PWV_{INV}$ of the $Ao_{prox}$, the pressure-time curves recorded in the proximal descending aorta and the abdominal aorta were used to calculate the $PWV_{INV}$ of the $Ao_{dist}$, and the pressure-time curves recorded in the ascending and the abdominal aorta were used to calculate the $PWV_{INV}$ of the $Ao_{total}$ (Figure 1C). $PWV_{INV}$ is similarly expressed by $\Delta x/\Delta t$ as for $PWV_{MRI}$, although $\Delta t$ is the transit time between the arrival of the two corresponding systolic pressure wave fronts, relative to the R-wave (Figure 1C) (19). The onset of the systolic pressure wave front was automatically determined from the time point of minimal pressure prior to the upslope of the systolic pressure wave. To minimize variation induced by respiration for assessment of the time point of the onset of the systolic pressure wave, ten consecutive cardiac cycles were analyzed and these time points were averaged. Offline analysis of the pressure-time curves was performed using custom-made software.

### Statistical analysis

Statistical analysis was performed using SPSS for Windows (version 12.0.1; SPSS, USA). All data are presented as mean values ± one standard deviation, unless stated otherwise. Variation between the $PWV_{MRI}$-assessments for validation was studied using the Pearson's correlation coefficient (PCC), while variation between the $PWV_{MRI}$-assessments reproducibility was studied using the two-way mixed intraclass correlation (ICC) for absolute agreement and the coefficients of variation (defined as the standard deviation of the differences between the two series of measurements divided by the mean of both measurements). The approach described by Bland and Altman (21) was followed to study systematic differences. Statistical significance on all tests was indicated by $P < 0.05$.

## Results

Results of $PWV_{MRI}$ and $PWV_{INV}$ assessment are listed in Table 2.

Table 2. Results of all participants.

| Parameters | group 1: | group 2: | |
|---|---|---|---|
| | | first MRI acquisition | second MRI acquisition |
| $PWV_{MRI}$ $Ao_{total}$ (m/s) | 6.5 ± 1.1 | 4.3 ± 0.5 | 4.6 ± 0.7 |
| $PWV_{MRI}$ $Ao_{prox}$ (m/s) | 6.5 ± 1.3 | 4.3 ± 0.9 | 4.7 ± 1.0 |
| $PWV_{MRI}$ $Ao_{dist}$ (m/s) | 6.9 ± 1.1 | 4.3 ± 0.6 | 4.4 ± 0.8 |
| $PWV_{INV}$ $Ao_{total}$ (m/s) | 6.1 ± 0.8 | | |
| $PWV_{INV}$ $Ao_{prox}$ (m/s) | 6.2 ± 1.1 | | |
| $PWV_{INV}$ $Ao_{dist}$ (m/s) | 6.1 ± 1.0 | | |

Group 1: patients for $PWV_{MRI}$ and $PWV_{INV}$ comparison.
Group 2: healthy subjects for reproducibility of $PWV_{MRI}$-assessment.

Note: data are expressed as mean ± standard deviation.
Abbreviations: MRI = magnetic resonance imaging; $PWV_{MRI}$ = pulse wave velocity as assessed with MRI; $PWV_{INV}$ = pulse wave velocity as assessed with invasive pressure measurements; $Ao_{total}$ = total aorta; $Ao_{prox}$ = proximal aorta; $Ao_{dist}$ = distal aorta.

### Validation of $PWV_{MRI}$

The mean distance for $PWV_{MRI}$ between site 1 (ascending aorta) and site 2 (proximal descending aorta) was 12.0 ± 1.7 cm, the mean distance between site 2 and site 3 (abdominal aorta) was 25.1 ± 3.0 cm. In Figure 2A, values for $PWV_{MRI}$ assessed in the $Ao_{total}$, $Ao_{prox}$ and $Ao_{dist}$ are presented vs $PWV_{INV}$. In Figure 2B, the differences between $PWV_{MRI}$ and $PWV_{INV}$ are presented

using Bland-Altman plots. Good agreement between $PWV_{MRI}$ and $PWV_{INV}$ was found ($Ao_{total}$: PCC = 0.53; $Ao_{prox}$: PCC = 0.69; $Ao_{dist}$: PCC = 0.71) (Figure 2A). No statistically significant bias was found in the $Ao_{total}$ and the $Ao_{prox}$, except for the $Ao_{dist}$ (mean differences between $PWV_{MRI}$ and $PWV_{INV}$ in $Ao_{total}$: 0.4 ± 1.0 m/s, P = 0.08; in $Ao_{prox}$: 0.3 ± 1.0 m/s, P = 0.16; in $Ao_{dist}$: 0.8 ± 0.8 m/s, P < 0.01). Coefficient of variation was 16% in the $Ao_{total}$ (confidence interval (CI) between -2.4 and 1.5), 16% in the $Ao_{prox}$ (CI between -2.3 and 1.6) and 13% in the $Ao_{dist}$ (CI between -2.4 and 0.8). In the Bland-Altman plots a trend is present: for high values of $PWV_{INV}$, $PWV_{MRI}$ seems to be underestimated as compared to the pressure measurements. This trend occurs for the total aorta, as well as for both segments.

Figure 2. $PWV_{MRI}$ vs $PWV_{inv}$ for the proximal, distal and total aorta.

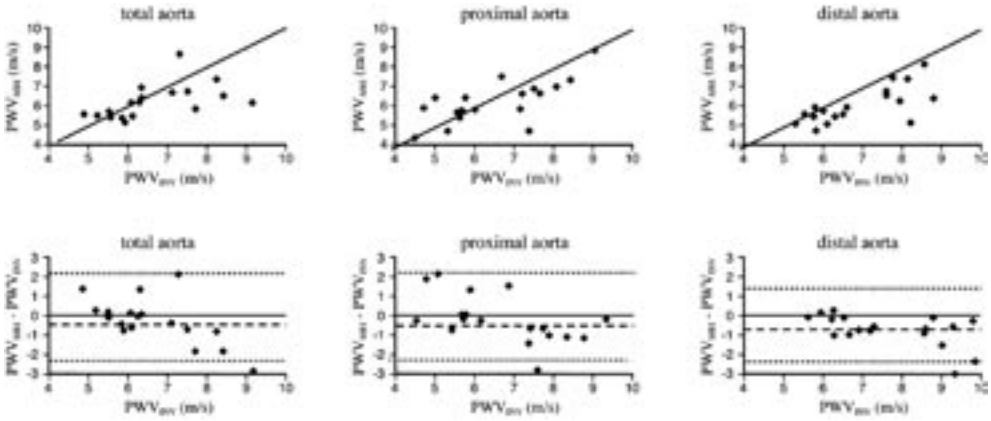


**Figure 2 a-b. (a)** Values for $PWV_{MRI}$ assessed in the proximal, distal and total aorta are shown vs $PWV_{INV}$. **(b)** The differences between $PWV_{MRI}$ and $PWV_{INV}$ are presented using a Bland-Altman plot.

### Reproducibility of $PWV_{MRI}$

Reproducibility of PWV-assessment with MRI was examined by repeating the examination on the same day. The mean distance between site 1 and 2 on the first MRI assessment was 9.4 ± 1.5 cm and on the repeated assessment 9.4 ± 1.3 cm, and both were not statistically significant different (P = 0.84). The mean distance between site 2 and 3 was 23.0 ± 3.6 cm and on the repeated assessment 22.3 ± 3.5 cm, and also these data were not statistically significant different (P = 0.38). The values for repeated $PWV_{MRI}$-assessment in the $Ao_{total}$, $Ao_{prox}$ and the $Ao_{dist}$ are presented in Figure 3A; the differences are presented in Figure 3B. Reproducibility was high, as $PWV_{MRI}$ in the $Ao_{total}$, $Ao_{prox}$ and $Ao_{dist}$ showed good intraclass correlation between the repeated examinations ($Ao_{total}$: ICC = 0.90, P < 0.01; $Ao_{prox}$: ICC = 0.87, P < 0.01; $Ao_{dist}$: ICC = 0.92, P < 0.01), with no statistically significant bias (mean difference $Ao_{total}$: 0.2 ± 0.4 m/s, P = 0.22; mean difference $Ao_{prox}$: 0.4 ± 0.6 m/s, P = 0.06; mean difference $Ao_{dist}$: 0.1 ± 0.4 m/s, P = 0.60). Coefficient of variation was 9% in the $Ao_{total}$ (CI between -0.7 and 1.5), 13% in the $Ao_{prox}$ (CI between -0.7 and 0.8) and 9% in the $Ao_{dist}$ (CI between -0.6 and 0.9).

Figure 3. Reproducibility of aortic Pulse Wave Velocity with MRI.

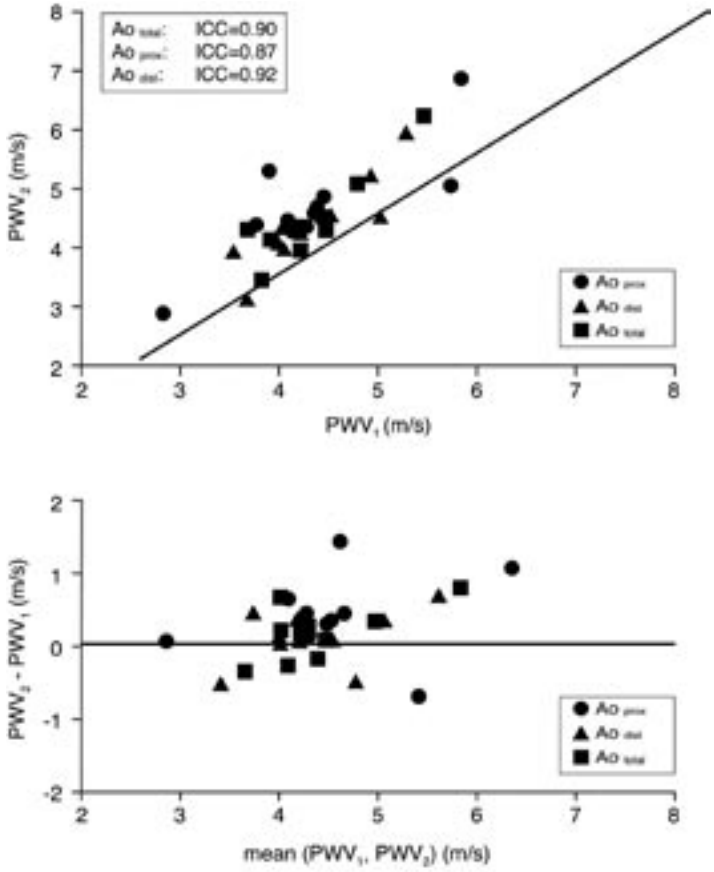


**Figure 3 a-b. (a)** The values for PWVMRI assessment in the proximal, distal and total aorta for the repeated examination. **(b)** The differences using a Bland-Altman plot.

## Discussion

The main findings of the current study are: 1. aortic pulse wave velocity as assessed with MRI ($PWV_{MRI}$) is in good agreement with aortic pulse wave velocity determined from invasive intra-aortic pressure measurements ($PWV_{INV}$); 2. reproducibility is high for $PWV_{MRI}$-assessment of the total aorta, the proximal aorta and the distal aorta.

Despite numerous reports using MRI to assess the aortic pulse wave velocity (8,10,14,18,19), $PWV_{MRI}$ has not been previously validated in vivo. Bolster et al. (14) validated $PWV_{MRI}$-

assessment in a flow phantom, showing excellent agreement with $PWV_{INV}$. However, these modelling conditions do not hold in vivo and limitations should be considered. As the aorta is not a straight tube, the bended shape of the proximal aorta and the multiple branches along the length of the aorta will produce wave reflections that may corrupt pulse wave velocity assessment, affecting both MRI and invasive pressure measurements (16,19). A similar phenomenon occurs in the abdominal aorta, with the abdominal bifurcation producing aortic wave reflections (19). In addition, the number of elastic components of the aorta is known to vary as a function of anatomic position, significantly decreasing from the elastic aortic root to the muscular peripheral vessels (15,22). In this study $PWV_{MRI}$ and $PWV_{INV}$ were acquired two weeks apart on average, so physiological variation as part of day-to-day differences in blood pressure, blood flow and sympathetic tone may have played a role in the found differences (23,24). Also, variation in the heart rate may result in a slight variation in velocity waveforms from cardiac cycle to cardiac cycle, causing errors in the assessed pulse wave velocity (14). Nevertheless, the agreement between $PWV_{MRI}$ and $PWV_{INV}$ was strong in our study, especially for the two measured aortic segments, indicating that $PWV_{MRI}$ is a reliable non-invasive imaging method especially to assess regional aortic PWV. The potential underestimation in $PWV_{MRI}$ due to the underestimation of the measured aortic distance in 2D and not in 3D, will increase for longer aortic segments. The curvature of the proximal aorta when compared to the more straight distal aorta is probably a similar potential source of error. Therefore, $PWV_{MRI}$ of the proximal and especially the distal aorta with a shorter aortic path length will probably show less underestimation and better correlation than for the total aorta. Interestingly, $PWV_{MRI}$ of all aortic segments but especially of the distal aorta underestimated the true PWV, as $PWV_{MRI}$ values showed a trend to be lower than the measured $PWV_{INV}$ values.

In this study, the onset of the systolic wave front was used to determine the time interval between the subsequent flow and pressure waves. Stefanov et al. demonstrated that usage of the onset of the systolic wave front minimizes the disruptive effect of strong wave reflections close to aortic branches, as this feature maintains its identity in the propagating wave (19). Physiological widening of the aortic wave form and the decrease of the slope of the aortic wave form along the course of the aorta due to wave reflections and damping by the aortic wall will result in artificial prolonging of the time interval between two subsequent acquisition points when the half-heights of the rising systolic flow waveforms or peak-to-peak analysis are used (19).

$PWV_{MRI}$ with repeated examination on the same day showed good agreement in our study, with an acceptable coefficient of variation (between 9% and 13%) and intraclass correlation (0.87 or higher). Differences can largely be attributed to physiological variation in PWV (22,23), as all subjects were studied under similar study conditions and our used $PWV_{MRI}$-analysis method was almost operator independent with automatic depiction of the onset of systolic wave forms. Given the coefficient of variation between 9% and 13%, a single $PWV_{MRI}$-acquisition

may over- or underestimate the representative individual $PWV_{MRI}$ by approximately 0.5 m/s. As an increase in aortic pulse wave velocity of 1 m/s is associated with a relative risk of all-cause mortality of 1.39 (24), the variation in PWV seems of acceptable relevance in the clinical interpretation of individual results. $PWV_{MRI}$ should therefore preferably be used as an indicative value for clinical purposes, and should be combined with other parameters like elevated blood pressure and MRI-assessed variables such as left ventricular function and left ventricular mass to depict cardiovascular disease (15).

Our study has limitations. $PWV_{MRI}$-assessment is based on cross-sectional data acquisition of the aortic flow, whereas $PWV_{INV}$ data are acquired locally in the aorta, namely at the tip of the catheter. Another limitation is the difficulty to exactly co-register the acquisition sites for pressure measurements and MRI-acquisition, although predefined sites were checked under fluoroscopy guidance. A potential limitation of our used analysis approach for the MRI measurements is related to the used high VENC, as measuring low velocities during the onset of the systolic wave front may become inaccurate due to the increased noise level (25). The precise determination of the onset of the systolic wave form may have been affected, although the high temporal resolution of our used sequence provided a dense set of data points along the course of the resulting flow graph. Depiction of the full course of the aorta with the single-slice scout image may be difficult in case of advanced stages of atherosclerosis or scoliosis due to elongation and a tortuous course of the aorta. Aortic imaging using 3-D MR angiography may be helpful in these cases. $PWV_{MRI}$ and $PWV_{INV}$ were acquired two weeks apart on average, so physiological variation as part of day-to-day differences in blood pressure, blood flow and sympathetic tone may have played a role in the found differences. Further studies are required to assess the value of aortic pulse wave velocity in larger cohorts of patients with vascular disease as well as in patients with different risk profiles.

In conclusion, non-invasive MRI assessment of regional and global aortic pulse wave velocity shows good agreement with the gold-standard as derived by invasive pressure measurements and can be determined with high reproducibility. In the future, evaluation with MRI of shorter aortic segments would allow for even more local identification of aortic vessel wall condition.

## References


1. Schlatmann TJ, Becker AE. Histologic changes in the normal aging aorta: implications for dissecting aortic aneurysm. Am J Cardiol. 1977; 39 (1): 13-20.
2. Sutton-Tyrrell K, Najjar SS, Boudreau RM, et al. Elevated aortic pulse wave velocity, a marker of arterial stiffness, predicts cardiovascular events in well-functioning older adults. Circulation. 2005; 111 (25): 3384-3390.
3. Willum-Hansen T, Staessen JA, Torp-Pedersen C, et al. Prognostic value of aortic pulse wave velocity as index of arterial stiffness in the general population. Circulation. 2006; 113 (5): 664-670.
4. Mitchell GF, Guo CY, Benjamin EJ, et al. Cross-sectional correlates of increased aortic stiffness in the community: the Framingham Heart Study. Circulation. 2007; 115 (20): 2628-2636.
5. Leung MT, Dumont GA, Sandor GG, Potts M, Potts JE. A novel method to estimate the aortic pressure waveform using B-mode ultrasound images acquired from a suprasternal view. Conf Proc IEEE Eng Med Biol Soc. 2008: 5286-5289.
6. Alecu C, Labat C, Kearney-Schwartz A, et al. Reference values of aortic pulse wave velocity in the elderly. J Hypertens. 2009; 27 (6): 1329-1330.
7. Pemberton J, Sahn DJ. Imaging of the aorta. Int J Cardiol. 2004; 97 Suppl 1: 53-60.
8. Bogren HG, Mohiaddin RH, Klipstein RK, et al. The function of the aorta in ischemic heart disease: a magnetic resonance and angiographic study of aortic compliance and blood flow patterns. Am Heart J .1989; 118 (2): 234-247.
9. Cruickshank K, Riste L, Anderson SG, Wright JS, Dunn G, Gosling RG. Aortic pulse-wave velocity and its relationship to mortality in diabetes and glucose intolerance: an integrated index of vascular function? Circulation. 2002; 106 (16): 2085-2090.
10. Mohiaddin RH, Underwood SR, Bogren HG, et al. Regional aortic compliance studied by magnetic resonance imaging: the effects of age, training, and coronary artery disease. Br Heart J. 1989; 62 (2): 90-96.
11. Laurent S, Cockcroft J, Van Bortel L, et al. Expert consensus document on arterial stiffness: methodological issues and clinical applications. Eur Heart J. 2006; 27 (21): 2588-2605.
12. Lehmann ED. Aortic pulse-wave velocity versus pulse pressure and pulse-wave analysis. Lancet. 2000; 355 (9201): 412.
13. Lehmann ED. Clinical value of aortic pulse-wave velocity measurement. Lancet. 1999; 354 (9178): 528-529.

    14. Bolster BD, Jr., Atalar E, Hardy CJ, McVeigh ER. Accuracy of arterial pulse-wave velocity measurement using MR. J Magn Reson Imaging. 1998; 8 (4): 878-888.
15. Latham RD, Westerhof N, Sipkema P, et al. Regional wave travel and reflections along the human aorta: a study with six simultaneous micromanometric pressures. Circulation. 1985; 72 (6):1257-1269.
16. Melina G, Rajappan K, Amrani M, Khaghani A, Pennell DJ, Yacoub MH. Aortic distensibility after aortic root replacement assessed with cardiovascular magnetic resonance. J Heart Valve Dis. 2002; 11 (1): 67-74.

17. Grotenhuis HB, Westenberg JJM, Doornbos J, et al. Aortic root dysfunctioning and its effect on left ventricular function in Ross patients, assessed with MRI. Am Heart J. 2006; 152 (5): 975 e1-8.
18. Grotenhuis HB, Ottenkamp J, Westenberg JJ, Bax JJ, Kroft LJ, de Roos A. Reduced aortic elasticity and dilatation are associated with aortic regurgitation and left ventricular hypertrophy in nonstenotic bicuspid aortic valve patients. J Am Coll Cardiol. 2007; 49 (15): 1660-1665.
19. Stevanov M, Baruthio J, Gounot D, Grucker D. In vitro validation of MR measurements of arterial pulse-wave velocity in the presence of reflected waves. J Magn Reson Imaging. 2001; 14 (2): 120-127.
20. van der Geest RJ, Niezen RA, van der Wall EE, de Roos A, Reiber JH. Automated measurement of volume flow in the ascending aorta using MR velocity maps: evaluation of inter- and intraobserver variability in healthy volunteers. J Comput Assist Tomogr. 1998; 22 (6): 904-911.
21. Bland JM, Altman DG. Statistical methods for assessing agreement between two methods of clinical measurement. Lancet. 1986; 1 (8476): 307-310.
22. Leeson CP, Robinson M, Francis JM, et al. Cardiovascular magnetic resonance imaging for non-invasive assessment of vascular function: validation against ultrasound. J Cardiovasc Magn Reson. 2006; 8 (2): 381-387.
23. Yamashina A, Tomiyama H, Takeda K, et al. Validity, reproducibility, and clinical significance of noninvasive brachial-ankle pulse wave velocity measurement. Hypertens Res. 2002; 25 (3): 359-364.
24. Blacher J, Guerin AP, Pannier B, Marchais SJ, Safar ME, London GM. Impact of aortic stiffness on survival in end-stage renal disease. Circulation. 1999; 99 (18): 2434-2439.
25. Kraft KA, Fatouros PP, Corwin FD, Fei DY. In vitro validation of rapid MR measurement of wave velocity. J Magn Reson. 1997; 126 (1): 103-109.

Heynric B. Grotenhuis
Jaap Ottenkamp
Jos J.M. Westenberg
Jeroen J. Bax
Lucia J.M. Kroft
Albert de Roos

# chapter 04

**Reduced Aortic Elasticity and Dilatation Are Associated With Aortic Regurgitation and Left Ventricular Hypertrophy in Non-stenotic Bicuspid Aortic Valve Patients**.

Journal of the American College of Cardiology. 2007; 4 (15): 1660-1665.

## Abstract

**Purpose:** Intrinsic pathology of the aortic wall is a possible explanation for reduced aortic elasticity and aortic dilatation in patients with a bicuspid aortic valve (BAV), even in the absence of a stenotic aortic valve. The relationship between aortic wall elasticity, aortic dimensions, aortic valve competence and left ventricular (LV) function in patients with BAVs has not previously been studied with magnetic resonance imaging (MRI). This study sought to assess elasticity and dimensions of the aorta and their impact on aortic valve competence and LV function in patients with a nonstenotic BAV.

**Materials and Methods:** MRI was performed in 20 patients with nonstenotic BAVs (mean ± SD, age 27 ± 11 years) and 20 matched control patients.

**Results:** The BAV patients showed reduced aortic elasticity as indicated by increased pulse wave velocity in the aortic arch and descending aorta (5.6 ± 1.3 m/s vs 4.5 ± 1.1 m/s, P = 0.01; and 5.2 ± 1.8 m/s vs 4.3 ± 0.9 m/s, P = 0.03, respectively) and reduced aortic root distensibility ($3.1 \pm 1.2*10^{-3}$ mm $Hg^{-1}$ vs $5.6 \pm 3.2*10^{-3}$ mm $Hg^{-1}$, P < 0.01). In addition, BAV patients showed aortic root dilatation as compared with control patients (mean difference 3.6 to 4.2 mm, P ≤ 0.04 at all 4 predefined levels). Minor degrees of aortic regurgitation (AR) were present in 11 patients (AR fraction 6 ± 8% vs 1 ± 1%, P < 0.01). The LV ejection fraction was normal (55 ± 8% vs 56 ± 6%, P = 0.61), whereas LV mass was significantly increased in patients (54 ± 12 $g/m^2$ vs 46 ± 12 $g/m^2$, P = 0.04). Dilatation at the level of the aortic annulus (r = 0.45, p = 0.044) and reduced aortic root distensibility (r = 0.37, P = 0.041) correlated with AR fraction. Increased pulse wave velocity in the aortic arch correlated with increased LV mass (r = 0.42, P = 0.041).

**Conclusion:** Reduced aortic elasticity and aortic root dilatation were frequently present in patients with nonstenotic BAVs. In addition, reduced aortic wall elasticity was associated with severity of AR and LV hypertrophy.

## Introduction

The bicuspid aortic valve (BAV) is the most common congenital cardiac malformation, occurring in 1% to 2% of the population (1-3). Intrinsic pathology of the aortic wall has been reported because of accelerated degeneration of the aortic media, indicating that BAV disease extends beyond the aortic valve (1,4). Given that serious complications like progressive aortic dilatation, aneurysm formation and even aortic dissection will develop in at least one-third of patients with BAVs, the bicuspid valve may be responsible for more deaths and morbidity than the combined effects of all other congenital heart defects (4).

Intrinsic aortic wall pathology in BAV disease is associated with aortic dilatation (2,4-7), but also may have a negative impact on aortic elasticity. In Marfan syndrome, increased aortic stiffness has been reported because of fragmentation of elastic wall components (8) as Marfan syndrome and BAV disease have many histological and clinical similarities (4,5), reduced aortic elasticity may be present in BAV patients as well. Distensibility and pulse wave velocity (PWV) in the aorta are markers of vessel wall integrity because they are dependent on the elastic properties of the aorta (1,9). Previous reports have indicated the clinical importance of both parameters: reduced distensibility of the aortic root increases leaflet stress and therefore predisposes for aortic valve dysfunctioning and subsequent impaired left ventricular (LV) function (10-12). Additionally, aortic PWV is an independent predictor of progressive aortic dilatation in Marfan syndrome (8) and when increased, directly leads to an increased afterload for the LV (9). Because intrinsic aortic wall abnormalities in BAV disease may be associated with impaired distensibility and PWV, both parameters might have a negative impact on aortic valve and LV function in patients with BAV disease.

Recently, magnetic resonance imaging (MRI) has been established as an accurate noninvasive tool for assessment of aortic distensibility and PWV (13-16). To our knowledge, MRI has not been used previously to study the relationship between aortic wall elasticity, aortic dimensions, aortic valve competence and LV function in patients with BAVs.

We hypothesized that intrinsic aortic wall pathology as measured by abnormal distensibility and PWV in nonstenotic BAV patients frequently occurs and that abnormal aortic elastic properties and aortic dilatation may negatively affect aortic valve and LV function. In the present study we excluded BAV patients with echocardiographic evidence of aortic valve stenosis to avoid the confounding effect on aortic elasticity of mechanical stresses placed on the aortic wall downstream of a stenotic valve (1,2).

Accordingly, the purpose of the current study was to assess aortic wall elasticity and aortic dimensions and their impact on aortic valve competence and LV function in patients with nonstenotic BAVs.

## Materials and Methods

### Patient population

Twenty patients with BAVs and 20 age- and gender-matched healthy subjects were prospectively studied with MRI at our institution. Twenty patients with BAVs were recruited from our local congenital heart disease database (mean ± SD, age 27 ± 11 years). Inclusion criteria consisted of BAV as diagnosed by echocardiography. Exclusion criteria were evidence of aortic valve stenosis (aortic velocity > 2.5 m/s on echocardiography) (17), aortic coarctation and/or other forms of congenital heart disease, Marfan syndrome or a family history of Marfan syndrome, previous surgery or intervention, usage of medication such as beta-blockers and general contraindications to MRI.

Table 1. Characteristics of BAV patients and healthy subjects.

| Characteristics | patients (n = 20) | healthy subjects (n = 20) |
|---|---|---|
| male / female | 13 (65) / 7 (35) | 13 (65) / 7 (35) |
| age at MRI (years) * | 27 ± 11 | 27 ± 12 |
| height (cm) * | 175 ± 8 | 174 ± 11 |
| weight (kg) * | 69 ± 12 | 68 ± 15 |
| Body Surface Area ($m^2$) * and † | 1.8 ± 0.2 | 1.8 ± 0.3 |
| blood pressure systolic (mm Hg) * | 128 ± 8 | 121 ± 11 |
| blood pressure diastolic (mm Hg) * | 79 ± 7 | 70 ± 11 |
| heart frequency (beats per minute) * | 71 ± 9 | 66 ± 11 |
| New York Heart Association class I | 20 | 20 |
| smoking (yes / no) | 6 / 14 | 5 / 15 |

Note: unless otherwise indicated, data are number of patients, and data in parentheses are percentages.
* Data are mean ± standard deviation.
† According to the formula: √ (height (cm) x height (kg) / 3600).
Abbreviations: BAV = bicuspid aortic valve; MRI = magnetic resonance imaging.

Age- and gender-matched healthy subjects were selected from our local database of subjects with an innocent heart murmur in the past, in whom congenital cardiac pathology had been excluded by physical examination and echocardiography. Characteristics and functional status as expressed as New York Heart Association class of the patients and healthy subjects were obtained from the patient records (Table1). The local medical ethics committee approved the study and informed consent was obtained from all participants before their enrollment in the study.

**MRI**

The MRI studies were performed with a 1.5-T system (NT 15 Gyroscan Intera; Philips Medical Systems, The Netherlands).

Aortic diameters and cross-sectional aortic areas were measured from transaxial images obtained with a gated steady-state free-precession sequence. Scan parameters encompassed field-of-view 220 mm, rectangular field-of-view percentage 90%, repetition time 3.2 ms, echo time 1.23 ms, gate width 34.2 ms, flip angle 50°, acquired voxel size 1.25 × 1.25 × 6.00 mm, reconstructed voxel size 0.43 × 0.43 × 6.00 mm, trigger delay 600 ms after the R-peak. Individual slices were obtained at the level of the annulus of the aortic valve, the sinus of Valsalva, the sinotubular junction and the proximal ascending aorta, the latter at the level of the pulmonary trunk (Figure 1).

Figure 1. Diameter Measurements of the Aortic Root.

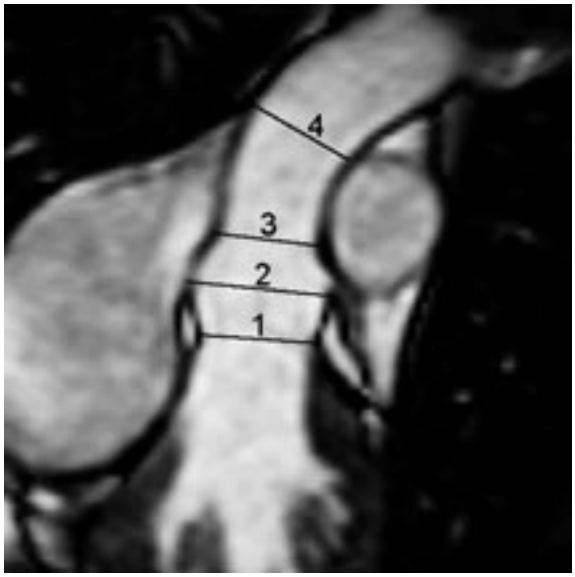


**Figure 1.** Oblique coronal image showing the 4 diameter measurements of the aortic root: at the level of the annulus of the aortic valve (1), the sinus of Valsalva (2), the sinotubular junction (3) and the ascending aorta at the level of the pulmonary trunk (4).

Aortic distensibility was measured at the level of the sinotubular junction. Distensibility (in mm $Hg^{-1}$) is calculated according to the following formula: $(A_{max} - A_{min}) / (A_{min} \times (P_{max} - P_{min}))$, with $A_{max}$ and $A_{min}$ as maximal and minimal lumen area (in $mm^2$) of the sinotubular junction, and $P_{max}$ and $P_{min}$ as systolic and diastolic blood pressure (mm Hg) (15). Maximal lumen area is expected at the peak of aortic flow and minimal lumen area is expected before the systolic flow curve (coinciding with the isovolumetric

contraction phase) (16). Minimal and maximal lumen area MRI was performed after manually positioning the acquisition planes perpendicular to the aorta at the level of the sinotubular junction (Figure 2), at time points of minimal and maximal flow through the aortic root, respectively (16). This approach enabled correction for through-plane motion of the aortic root during contraction (16). Scan parameters were identical to the diameter measurements; gate delay was individually applied for optimal timing of the acquisition (16). For timing of aortic flow, a phase-contrast sequence was used at the level of the sinotubular junction with scan parameters: field-of-view 300 mm, rectangular field-of-view percentage 90%, repetition time 4.8 ms, echo time 2.8 ms, flip angle 20°, acquired voxel size 2.34 × 2.34 × 8.00 mm, reconstructed voxel size 1.17 × 1.17 × 8.00 mm, using retrospective gating. Temporal resolution was approximately 10 ms depending on the heart rate. The sequence was encoded for a through-plane velocity up to 200 cm/s (16). The same acquisition was also used for assessment of aortic valve competence and measurement of peak flow velocity across the aortic valve. Aortic regurgitation (AR) fraction was considered significant if the regurgitant fraction was > 5% of the systolic forward flow (16). Blood pressure was noninvasively obtained using a semiautomatic MRI-compatible sphygmomanometer (Invivo Research, USA). In each patient, right brachial artery systolic and diastolic blood pressures were measured 3 times during the measurements for distensibility, and the average of the measurements was used for calculations (8).

Figure 2. Distensibility Measurements of the Aortic Root.

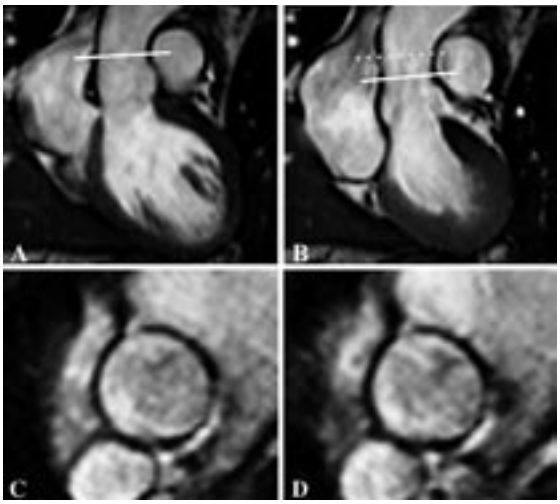


**Figure 2 a-d. (a-b)** Taken in the oblique coronal plane, these images show the slice positioning of the acquisition planes at minimal and maximal aortic flow for distensibility measurements, respectively, thus correcting for through-plane motion of the aortic root during contraction. Note the difference in position of the aortic root in both images, because of cardiac motion. **(c-d)** The corresponding area measurements in the double oblique transverse orientation.

The PWV was measured between the ascending and proximal descending aorta, and between the proximal descending aorta and aortic bifurcation (Figure 3). A retrospectively ECG-gated gradient-echo pulse sequence with velocity encoding was applied at the level of the pulmonary trunk to measure through-plane flow in the ascending aorta and proximal descending aorta (Figure 3). A second acquisition plane was positioned just above the bifurcation of the abdominal aorta (Figure 3). Scan parameters were identical to the sequence used for the distensibility measurements. During the MRI acquisition, systolic and diastolic blood pressures were measured as described for the distensibility measurements. The PWV was calculated as: $\Delta x/\Delta t$ (expressed in m/s), where $\Delta x$ is the aortic path length between 2 imaging levels and $\Delta t$ is the time delay between the arrival of the foot of the pulse wave at these levels (18).

Figure 3. Measurements of Pulse Wave Velocity of the Aorta.

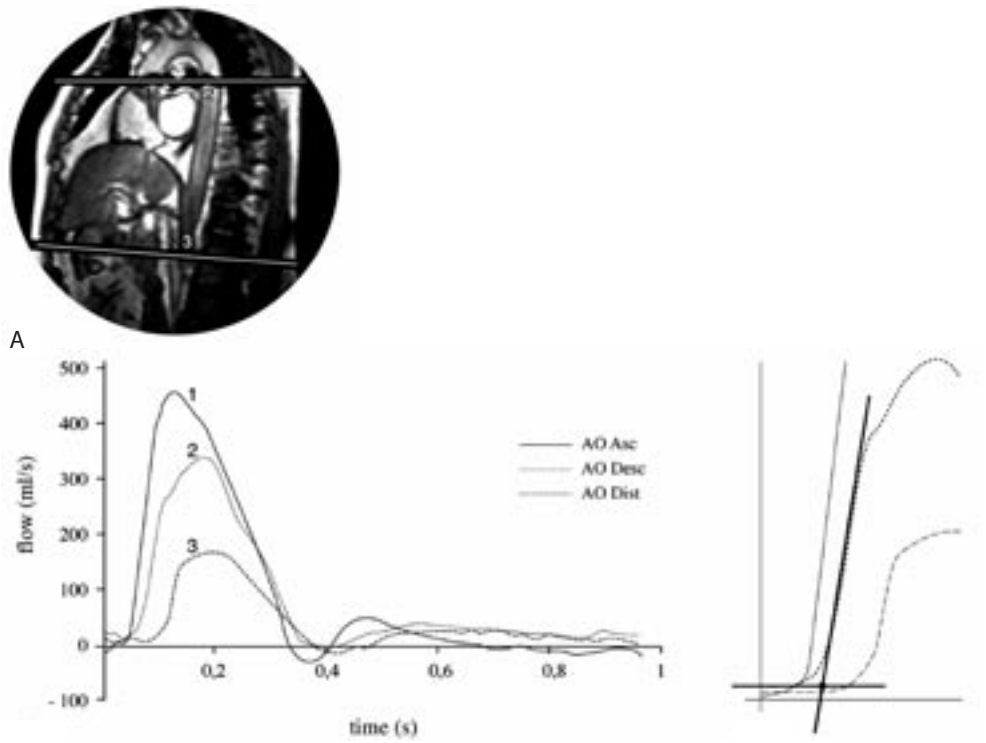


**Figure 3 a-b. (a)** The sites for the through-plane MRI pulse wave velocity (PWV) measurements: the ascending aorta (AO Asc) (1), the proximal descending aorta (AO Desc) (2), and the distal aorta (AO Dist) (3) above the aortic bifurcation. On the corresponding velocity-encoded images **(b)** (indicated by 1, 2 and 3), the arrival time of the aortic systolic pulse-wave front can be determined by measuring the through-plane flow. An example of determination of the arrival time at the site of the proximal descending aorta is depicted in **(c)**. The distance between the sampling locations and the different arrival times of the systolic flow wave determine the PWV.

Systolic LV function was assessed with a steady-state free-precession cine sequence. Scan parameters were: field-of-view 400 mm, rectangular field-of-view percentage 80%, repetition time 3.2 ms, echo time 1.6 ms, flip angle 70°, acquired voxel size 1.92 × 2.41 × 10.00 mm, reconstructed voxel size 1.56 × 1.55 × 10.00 mm, no slice gap (19). The following parameters were obtained after indexation for body surface area: LV end-diastolic volume, LV end-systolic volume, LV stroke volume, LV ejection fraction and LV mass (16,19).

All images were quantitatively analyzed on a workstation with a Pentium 4 processor (Intel, USA). The measurements for diameters and distensibility of the aortic root as well as the short-axis gradient-echo images of both ventricles were analyzed with the software package MASS (Medis, The Netherlands) (16,19). Aortic velocity maps were analyzed with the software package FLOW (Medis, The Netherlands) (20). All contours and diameters were manually drawn by one observer (3 years of experience) and were subsequently checked by a radiologist who was blinded to the patient conditions (9 years of experience).

### Statistical analysis

Statistical analysis was performed using SPSS for Windows (version 12.0.1, SPSS Inc., USA). All data are presented as mean values ± 1 SD, unless stated otherwise. The Mann-Whitney U test was used to express differences in variables between the patients and healthy subjects. Correlation between variables was expressed with the Spearman rank correlation coefficient. Linear regression analysis was used to identify predictors of variables with backward elimination procedures. Statistical significance was indicated by a P value of $< 0.05$.

## Results

### Aortic dimensions and elasticity

Patients with BAVs showed significantly increased PWV in the aortic arch and descending aorta (Table 2). In addition, distensibility at the level of the sinotubular junction was diminished in patients with BAVs as compared with the healthy subjects group (Table 2). Diameters and areas of the aortic root were significantly increased at all 4 levels in BAV patients as compared with the healthy subjects (Table 2). Dilatation was most pronounced at the levels of the sinus of Valsalva and the proximal ascending aorta (Table 2). Dilatation at the level of the sinotubular junction was significantly correlated with decreased root distensibility ($r = 0.56$, $P = 0.004$) and increased PWV in the aortic arch ($r = 0.45$, $P = 0.039$). The presence of BAV and older age at time of MRI predicted reduced root distensibility and increased PWV in the aortic arch ($r = 0.5$ to $0.7$, $P \leq 0.01$ for all).

Table 2. Results in 20 BAV Patients and 20 Age- and Gender-Matched Healthy Subjects.

| Parameters | patients | healthy subjects | P value mean | difference |
|---|---|---|---|---|
| diameter annulus (mm) | 30.1 ± 6.9 | 26.2 ± 3.3 | 0.03 | 3.9 |
| area annulus ($cm^2$) | 7.4 ± 3.5 | 5.5 ± 1.4 | 0.03 | 1.9 |
| diameter sinus of Valsalva (mm) | 33.4 ± 5.7 | 29.2 ± 3.2 | < 0.01 | 4.2 |
| area sinus of Valsalva ($cm^2$) | 9.0 ± 3.4 | 6.8 ± 1.5 | < 0.01 | 2.2 |
| diameter sinotubular junction (mm) | 30.4 ± 6.2 | 26.8 ± 3.4 | 0.04 | 3.6 |
| area sinotubular junction ($cm^2$) | 7.5 ± 3.5 | 5.7 ± 1.5 | 0.04 | 1.8 |
| diameter ascending aorta (mm) | 30.0 ± 6.3 | 25.7 ± 3.1 | < 0.01 | 4.3 |
| area ascending aorta ($cm^2$) | 7.4 ± 3.4 | 5.2 ± 1.3 | < 0.01 | 2.1 |
| distensibility (in $10^{-3}$ mm $Hg^{-1}$) * | 3.1 ± 1.2 | 5.6 ± 3.2 | < 0.01 | |
| PWV aortic arch (m/s) | 5.6 | 4.5 | 0.01 | |
| PWV descending aorta (m/s) | 5.2 | 4.3 | 0.03 | |
| aortic regurgitation fraction (%) | 6 ± 8 | 1 ± 1 | < 0.01 | |
| peak-flow velocity at STJ (m/s) | 1.68 ± 0.26 | 1.67 ± 0.33 | 0.97 | |
| LV EF (%) | 55 ± 8 | 56 ± 6 | 0.61 | |
| LV EDV ($ml/m^2$) | 101 ± 22 | 93 ± 16 | 0.29 | |
| LV ESV ($ml/m^2$) | 46 ± 17 | 41 ± 8 | 0.36 | |
| LV mass ($g/m^2$) | 54 ± 12 | 46 ± 12 | 0.04 | |

Note: data are expressed as mean ± standard deviation.
* Distensibility was measured at the level of the sinotubular junction.
Abbreviations: BAV = bicuspid aortic valve, PWV = pulse wave velocity, STJ = sinotubular junction, LV = left ventricle, EDV = end-diastolic volume indexed for body surface area, EF = ejection fraction, ESV = end-systolic volume indexed for body surface area.

**Aortic valve competence**

Patients with BAVs were characterized by frequent minor degrees of AR, as 11 of 20 patients showed AR fraction ranging between 5% and 16%. In none of the healthy subjects did AR fraction exceed 5%. The AR fraction (expressed in percentages) (Table 2) was significantly correlated with dilatation at the level of the aortic annulus ($r = 0.45$, $P = 0.044$) and reduced aortic root distensibility ($r = 0.37$, $P = 0.041$). Peak flow velocities across the aortic valve were not increased in our patient group as compared with the healthy subjects (Table 2), supporting the fact that none of the patients had aortic valve stenosis.

**LV function**

Systolic function - expressed by LV ejection fraction and LV stroke volume - was not significantly different between patients with BAVs and healthy subjects (Table 2). Also, LV dimensions (LV end-diastolic and -systolic volume) were not significantly different between the 2 groups (Table 2). Mean LV mass of the patient group was significantly larger compared with that value in healthy subjects (Table 2). Increased LV mass was significantly correlated with increased PWV in the aortic arch ($r = 0.42$, $P = 0.041$), suggesting that LV hypertrophy results from an increased LV afterload. Linear regression showed that increased PWV in the aortic arch predicted increased LV mass ($r = 0.5$, $P < 0.01$).

## Discussion

The purpose of the current study was to assess aortic wall elasticity and aortic dimensions and their impact on aortic valve competence and LV function in patients with nonstenotic BAVs. This study showed frequently reduced aortic elasticity and aortic root dilatation in patients with nonstenotic BAVs. In addition, reduced aortic wall elasticity was associated with the severity of AR and the degree of LV hypertrophy. Monitoring of aortic elasticity and aortic dimensions, in conjunction with aortic valve competence and LV function, seems therefore indicated in the long-term follow-up of patients with BAVs.

**Aortic dimensions**

Significant dilatation of the aortic root was present in our patient group with BAVs. Dilatation was most pronounced at the levels of the sinus of Valsalva and of the proximal ascending aorta, which is in agreement with previous ultrasound reports (21,22). Aortic dilatation may be caused by intrinsic pathology of the aortic wall, or hemodynamic factors caused by a stenotic aortic valve: high velocity and turbulent flow downstream of the stenosis place mechanical stress on the aortic wall (1). In this study only nonstenotic BAV patients were included, so aortic dilatation caused by stenotic mechanical stress was not suspected.

Intrinsic pathology of the aortic wall in patients with BAVs has been reported because of accelerated degeneration of the aortic media, indicating that BAV disease extends beyond the aortic valve (1,4). Inadequate production of fibrillin-1 during valvulogenesis may disrupt the formation of the aortic cusps, resulting in a bicuspid valve and a weakened aortic root (4). These lesions are similar in fibrillin-1-deficient aortas of patients with Marfan syndrome (4). The BAV should therefore be considered a disease of the entire aortic root (1,4,7).

As a consequence of intrinsic aortic wall pathology, the presence of BAV has been reported to be an independent risk factor for progressive aortic dilatation, aneurysm formation and even dissection (4,7). For the risk of aortic rupture and dissection, aortic root replacement is more aggressively recommended for patients with BAVs (i.e., 4 to 5 cm) than for those of patients

with a tricuspid aortic valve (i.e., 5 to 6 cm) (4). Long-term surveillance of aortic dimensions is therefore required (4).

**Aortic elasticity**

Significantly reduced aortic elasticity in our patient group indicated that BAV disease is not only associated with aortic dilatation (2,4-7), but also with reduced aortic elasticity. In Marfan syndrome, increased aortic stiffness has been reported because of fragmentation of elastic wall components (8). Considering the many histological and clinical similarities between both entities (4,5), intrinsic aortic wall abnormalities in BAV disease are probably responsible for reduced aortic elasticity as well. Our patient group showed diminished elasticity of the entire aorta, suggesting not only that the proximal part of the aorta is affected in BAV disease (4,21), but also that aortic wall lesions extend into the entire aorta.

In patients with Marfan syndrome, aortic stiffness has proven to be an independent predictor of progressive aortic dilatation (8). Evaluation of the elastic properties of the ascending aorta in patients with BAVs might be used analogously to identify patients who are at risk of progressive dilatation of the aorta and other aortic sequelae. Future longitudinal studies are needed to investigate whether the same predictive value of aortic stiffness is applicable for patients with BAV disease.

Arterial stiffness has also been shown to be a cardiovascular risk factor on its own (9). Augmented arterial stiffening is associated with impaired coronary blood flow and LV dysfunction (9). In addition, a strong and independent association has been shown between increased arterial stiffness and the presence of coronary artery disease (23). Therefore, prognosis of patients with increased arterial stiffness in BAV disease may be worse as compared with healthy subjects because numerous other standard risk factors such as aging, smoking, lipid profiles and gender are cumulative over a lifetime (9). Early detection of disturbances in arterial stiffness may allow for early therapeutic intervention (24). In Marfan patients, beta-blockade has a beneficial effect on the progression rate of aortic dilatation with reduction of aortic complications (8,15). Whether this is applicable for BAV patients remains to be elucidated.

**Aortic valve competence**

In the current study, minor degrees of AR were a common finding in our patients with BAVs. Inherent structural weakness of the aortic valve cusps may lead to aortic valve prolapse and subsequent AR (4). In this study the degree of AR was correlated with dilatation of the aortic annulus and decreased aortic root distensibility. Dilatation of the aortic root has been reported to have the potential to cause AR (4,7,16). In addition, distensibility of the aortic root is crucial for aortic valve dynamics: aortic valve opening occurs in concert with root expansion during the beginning of systole (10,25). Disturbance of this interrelation greatly determines the stress on valve leaflets

(10,12). We therefore hypothesize that reduced aortic root distensibility in patients with BAVs increases leaflet stress, and thus predisposes to aortic valve dysfunction in BAV disease.

**LV function**

The LV systolic function was adequately preserved in patients with BAVs. However, a significantly larger LV mass was observed in our BAV patients, indicating hypertrophy of the LV. Often LV hypertrophy is compensatory to increased LV afterload (26), which in this study was related to reduced elasticity of the proximal aorta. Myocardial stiffening may occur as a consequence of sustained LV hypertrophy, which has a negative effect on diastolic filling (26). Clinical studies have confirmed the detrimental effect of diastolic LV dysfunction, having a major contribution to congestive heart failure and diminished exercise performance (26,27). Diastolic LV dysfunction also may precede LV systolic dysfunctioning (26). Aging contributes to any diastolic dysfunction by increasing ventricular mass and loss of elastic myocardial properties over time (26,27). Therefore, LV hypertrophy might pose a future risk for LV dysfunction in our BAV patient group (26,27).

This study showed frequently reduced aortic elasticity and aortic root dilatation in patients with nonstenotic BAVs. In addition, reduced aortic wall elasticity was associated with severity of AR and degree of LV hypertrophy. Analogous to similar entities such as Marfan syndrome, intrinsic aortic wall abnormalities in BAV disease result in a negative cascade that affects aortic elasticity, aortic dimensions, aortic valve competence and LV function. Monitoring of aortic elasticity and aortic dimensions, in conjunction with aortic valve competence and LV function, seems therefore indicated in the long-term follow-up of patients with BAVs. Future longitudinal studies are required to investigate the predictive value of aortic stiffness in patients with BAV disease.

## References


1. Wilton E, Jahangiri M. Post-stenotic aortic dilatation. J Cardiothorac Surg. 2006; 3 (1): 7-18.
2. Nkomo VT, Enriquez-Sarano M, Ammash NM, Melton LJ, III, Bailey KR, Desjardins V. Bicuspid aortic valve associated with aortic dilatation: a community-based study. Arterioscler Thromb Vasc Biol. 2003; 23 (2): 351-356.
3. Warren AE, Boyd ML, O'Connell C, Dodds L. Dilation of the ascending aorta in pediatric patients with bicuspid aortic valve: frequency, rate of progression and risk factors. Heart. 2006; 92 (10): 1496-1500.
4. Fedak PW, Verma S, David TE, Leask RL, Weisel RD, Butany J. Clinical and pathophysiological implications of a bicuspid aortic valve. Circulation. 2002; 106 (8): 900-904.
5. Beroukhim RS, Roosevelt G, Yetman AT. Comparison of the Pattern of Aortic Dilation in Children With the Marfan's Syndrome Versus Children With a Bicuspid Aortic Valve. Am J Cardiol. 2006; 98 (8): 1094-1095.
6. Beroukhim RS, Kruzick TL, Taylor AL, Gao D, Yetman AT. Progression of Aortic Dilation in Children With a Functionally Normal Bicuspid Aortic Valve. Am J Cardiol. 2006; 98 (6): 828-830.
7. Cecconi M, Nistri S, Quarti A, Manfrin M, Colonna PL, Molini E. Aortic dilatation in patients with bicuspid aortic valve. J Cardiovasc Med. 2006; 7 (1): 11-20.
8. Nollen GJ, Groenink M, Tijssen JG, van der Wall EE, Mulder BJ. Aortic stiffness and diameter predict progressive aortic dilatation in patients with Marfan syndrome. Eur Heart J. 2004; 25 (13): 1146-1152.
9. Cruickshank K, Riste L, Anderson SG, Wright JS, Dunn G, Gosling RG. Aortic pulse-wave velocity and its relationship to mortality in diabetes and glucose intolerance: an integrated index of vascular function? Circulation. 2002; 106 (16): 2085-2090.
10. Schmidtke C, Bechtel J, Hueppe M, Noetzold A, Sievers HH. Size and distensibility of the aortic root and aortic valve function after different techniques of the Ross procedure. J Thorac Cardiovasc Surg. 2000; 119 (15): 990-997.
11. Thubrikar M, Skinner JR, Aouad J, Finkelmeier BA, Nolan SP. Analysis of the design and dynamics of aortic bioprostheses in vivo. J Thorac Cardiovasc Surg. 1982; 84 (2): 282-290.
12. Thubrikar MJ, Nolan SP, Aouad J, Deck JD. Stress sharing between the sinus and leaflets of canine aortic valve. Ann Thorac Surg. 1986; 42 (4): 434-440.
13. Melina G, Rajappan K, Amrani M, Khaghani A, Pennell DJ, Yacoub MH. Aortic distensibility after aortic root replacement assessed with cardiovascular magnetic resonance. J Heart Valve Dis. 2002; 11 (1): 67-74.
14. Rogers WJ, Hu YL, Coast D, Vido DA, Kramer CM, Pyeritz RE. Age-associated changes in regional aortic pulse wave velocity. J Am Coll Cardiol. 2001; 38 (4): 1123-1129.
15. Groenink M, de Roos A, Mulder BJ, et al. Changes in aortic distensibility and pulse wave velocity assessed with magnetic resonance imaging following beta-blocker therapy in the Marfan syndrome. Am J Cardiol. 1998; 82 (2): 203-208.

16. Grotenhuis HB, Westenberg JJM, Doornbos J, et al. Aortic root dysfunctioning and its effect on left ventricular function in Ross patients, assessed with MRI. Am Heart J. 2006; 152 (5): 975 e1-8.
17. Otto CM, Lind BK, Kitzman DW, Gersh BJ, Siscovick DS. Association of aortic-valve sclerosis with cardiovascular mortality and morbidity in the elderly. N Engl J Med. 1999; 341 (3): 142-147.
18. Stevanov M, Baruthio J, Gounot D, Grucker D. In vitro validation of MR measurements of arterial pulse-wave velocity in the presence of reflected waves. J Magn Reson Imaging. 2001; 14: 120-127.
19. van der Geest RJ, Reiber JH. Quantification in cardiac MRI. J Magn Reson Imaging. 1999; 10 (5): 602-608.
20. van der Geest RJ, Niezen RA, van der Wall EE et al. Automated measurement of volume flow in the ascending aorta using MR velocity maps: evaluation of inter- and intraobserver variability in healthy volunteers. J Comput Assist Tomogr. 1998; 22 (6): 904-911.
21. Cecconi M, Manfrin M, Moraca A, Zanoli R, Colonna PL, Bettuzzi MG. Aortic dimensions in patients with bicuspid aortic valve without significant valve dysfunction. Am J Cardiol. 2005; 95 (2): 292-294.
22. La Canna G, Ficarra E, Tsagalau E, Nardi M, Morandini A, Chieffo A. Progression rate of ascending aortic dilation in patients with normally functioning bicuspid and tricuspid aortic valves. Am J Cardiol. 2006; 98 (2): 249-253.
23. Arnett DK, Evans GW, Riley WA. Arterial stiffness: a new cardiovascular risk factor? Am J Epidemiol. 1994; 140 (8): 669-682.
24. Franklin SS. Blood pressure and cardiovascular disease: what remains to be achieved? J Hypertens Suppl. 2001; 19 (3): S3-S8.
25. Thubrikar MJ, Heckman JL, Nolan SP. High speed cine-radiographic study of aortic valve leaflet motion. J Heart Valve Dis. 1993; 2 (6): 653-661.
26. Mandinov L, Eberli FR, Seiler C, Hess OM. Diastolic heart failure. Cardiovasc Res. 2000; 45 (40): 813-825.
27. Singh GK, Greenberg SB, Yap YS, Delany DP, Keeton BR, Monro JL. Right ventricular function and exercise performance late after primary repair of tetralogy of Fallot with the transannular patch in infancy. Am J Cardiol. 1998; 82 (12): 1378-1382.

Heynric B. Grotenhuis
Jaap Ottenkamp
Duveken Fontein
Hubert W. Vliegen
Jos J.M. Westenberg
Lucia J.M. Kroft
Albert de Roos

# chapter 05

**Aortic Elasticity and Left Ventricular Function after Arterial Switch Operation: MR Imaging - Initial Experience.**

Radiology. 2008; 249 (3): 801-809.

## Abstract

**Purpose:** To prospectively assess aortic dimensions, aortic elasticity, aortic valve competence and left ventricular (LV) systolic function in patients after the arterial switch operation (ASO) by using magnetic resonance imaging (MRI).

**Materials and Methods:** Informed consent was obtained from all participants for this local ethics committee - approved study. Fifteen patients (11 male patients, four female patients; mean age, 16 years ± 4 (standard deviation); imaging performed 16.1 years after surgery ± 3.7) and 15 age- and sex-matched control subjects (11 male subjects, four female subjects; mean age, 16 years ± 4) were evaluated. Velocity-encoded MRI was used to assess aortic pulse wave velocity (PWV) and a balanced turbo-field-echo sequence was used to assess aortic root distensibility. Standard velocity-encoded and multisection-multiphase imaging sequences were used to assess aortic valve function, systolic LV function and LV mass. The two-tailed Mann-Whitney U test and Spearman rank correlation coefficient were used for statistical analysis.

**Results:** Patients treated with the ASO showed aortic root dilatation at three predefined levels (mean difference, 5.7 - 9.4 mm; $P = 0.007$) and reduced aortic elasticity (PWV of aortic arch, 5.1 m/s ± 1.2 vs 3.9 m/s ± 0.7, $P = 0.004$; aortic root distensibility, $2.2*10^{-3}$ mm $Hg^{-1}$ ± 1.8 vs $4.9*10^{-3}$ mm $Hg^{-1}$ ± 2.9, $P < 0.01$) compared with control subjects. Minor degrees of aortic regurgitation (AR) were present (AR fraction, 5% ± 3 in patients vs 1% ± 1 in control subjects; $P < 0.001$). Patients had impaired systolic LV function (LV ejection fraction (LV EF), 51% ± 6 vs 58% ± 5 in control subjects; $P = 0.003$), in addition to enlarged LV dimensions (end-diastolic volume (EDV), 112 ml/$m^2$ ± 13 vs 95 ml/$m^2$ ± 16, $P = 0.007$; end-systolic volume (ESV), 54 ml/$m^2$ ± 11 vs 39 ml/$m^2$ ± 7, $P < 0.001$). Degree of AR predicted decreased LV EF ($r = 0.41$, $P = 0.026$) and was correlated with increased LV dimensions (LV EDV: $r = 0.48$, $P = 0.008$; LV ESV: $r = 0.67$, $P < 0.001$).

**Conclusion:** Aortic root dilatation and reduced elasticity of the proximal aorta are frequently observed in patients who have undergone the ASO, in addition to minor degrees of AR, reduced LV systolic function and increased LV dimensions.

## Introduction

The arterial switch operation (ASO) has become the preferred method of surgery for transposition of the great arteries (TGA) (1-3). The operation consists of transection and reanastomosis of the aorta and pulmonary trunk above the sinuses, as well as relocation of the coronary arteries (1). Although this technique has substantially reduced the number of sequelae associated with surgical correction of TGA, completion of the ASO may still leave patients with complications such as aortic root dilatation and aortic regurgitation (AR) (1-5).

Aortic wall abnormalities in TGA have been reported that are due to abnormal aorticopulmonary septation, damage to the vasa vasorum, and surgical manipulations during the ASO, predisposing patients to aortic dilatation, aneurysm formation and even aortic dissection (4-7). In addition, aortic distensibility may be reduced by impaired aortic elastogenesis, as well as by scar formation at the site of anastomosis (8,9). Distensibility and pulse wave velocity (PWV) in the aorta have been shown to be markers of vessel wall elasticity, as they are mainly related to the elastic properties of the aorta (10-12).

Both aortic distensibility and aortic dimensions are crucial for aortic valve dynamics. Aortic valve opening occurs in concert with root expansion during the beginning of systole (13,14). Decreased distensibility of the aortic root increases leaflet stress and therefore predisposes for aortic valve dysfunction (14-16). Aortic dilatation contributes to aortic valve dysfunction through loss of coaptation of the aortic valve leaflets (10,17). As a consequence, impaired distensibility and dilatation of the aorta may lead to aortic valve dysfunction and subsequent impairment of left ventricular (LV) function in patients after surgical repair of TGA (10,14-16).

Magnetic resonance imaging (MRI) has been established as an accurate noninvasive tool for assessment of aortic distensibility and PWV (10,12,18-20). To our knowledge, MRI has not previously been used to study the relationship between aortic dimensions, aortic wall elasticity, aortic valve competence and LV function in patients after the ASO. We hypothesized that intrinsic aortic wall dysfunction, as indicated by abnormal distensibility and PWV, in patients after the ASO frequently occurs and that abnormal aortic elastic properties and aortic dilatation may be associated with reduced aortic valve and LV function. Thus, the objective of our study was to prospectively assess aortic dimensions, aortic elasticity, aortic valve competence and LV systolic function in patients after the ASO by using MRI.

## Materials and Methods

### Patients

The medical ethics committee of Leiden University Medical Center (Leiden, The Netherlands) approved this study and informed consent was obtained from all participants prior to their enrollment in the study. Fifteen patients who had undergone the ASO (mean age, 16 years ± 4 (standard deviation); imaging performed 16.1 years after surgery ± 3.7) and 15 age- and sex-matched healthy control subjects (mean age, 16 years ± 4) were prospectively examined with MRI at our institution. Characteristics of all participants are listed in Table 1. None of the patients who had undergone the ASO used medication.

Table 1. Characteristics of Patients Who Had Undergone the ASO and Healthy Control Subjects .

| Characteristics | patients (n = 15) | healthy controls (n = 15) |
|---|---|---|
| male / female * | 11 (73) / 4 (27) | 11 (73) / 4 (27) |
| age at MRI (years) | 16 ± 4 | 16 ± 4 |
| height (cm) | 167 ± 14 | 168 ± 12 |
| weight (kg) | 55 ± 17 | 60 ± 15 |
| body surface area ($m^2$) † | 1.6 ± 0.3 | 1.7 ± 0.3 |
| blood pressure systolic (mm Hg) | 116 ± 16 | 121 ± 13 |
| blood pressure diastolic (mm Hg) | 66 ± 12 | 68 ± 11 |
| cardiac frequency (beats per minute) | 71 ± 13 | 69 ± 9 |
| New York Heart Association class (I/ II) | 13 / 2 | 15 / 0 |
| smoking (yes / no) | 0 / 15 | 0 / 15 |

Note: Unless otherwise indicated, data are means ± standard deviations, with ranges in parentheses. No patient or control subject had a history of smoking.

* Data are numbers of patients, with percentages in parentheses.

† Calculated with the following formula: $\sqrt{}$ (height (cm) × weight (kg) / 3600).

Twenty-three patients who had undergone the ASO, as reported in our local congenital heart disease database, were initially approached for this study. Inclusion criteria comprised TGA corrected with the ASO, current age between 12 and 25 years, willingness to comply with the study procedures and written informed consent. Exclusion criteria comprised TGA corrected with the Jatene procedure (this procedure includes insertion of an artificial tunnel to connect the right ventricle with the pulmonary artery, creating a different type of configuration of the great arteries) (n = 1), evidence of aortic valve stenosis (aortic velocity > 2.5 m/s at echocardiography) (21), coarctation of the aorta and/or other forms of congenital heart

disease, Marfan syndrome or a family history of Marfan syndrome, repeat ASO or surgery and/or intervention other than the ASO, usage of medication such as beta-blockers and general contraindications to cardiovascular MRI. Seven patients declined to participate for personal reasons. Age- and sex-matched healthy control subjects were selected from our database of individuals with a harmless heart murmur in whom congenital cardiac disease had been excluded in the past with physical examination and echocardiography.

Previously, data in the same patients who had undergone the ASO and control subjects were included in a report on right ventricular function and pulmonary flow analysis (22).

**Surgical technique**

The ASO was performed in patients with TGA (median age at surgery, 7 days; range, 3 - 21 days) by using cardiopulmonary bypass and moderate hypothermia by one surgeon with 20 years of experience with the ASO. The operation included transection of the aorta above the sinotubular junction and the pulmonary trunk above the pulmonary root, transplantation of the coronary arteries into the root of the pulmonary trunk, switching of the aorta and pulmonary trunk and subsequent reconstruction of the pulmonary trunk with a pericardial patch (Figure 1). The Lecompte maneuver was performed in all 15 patients (23). Associated procedures during the ASO were ventricular septal defect closure in five patients, atrial septal defect closure in six patients and closure of the ductus arteriosus in 10 patients. No perioperative ischemic events were observed.

Figure 1.

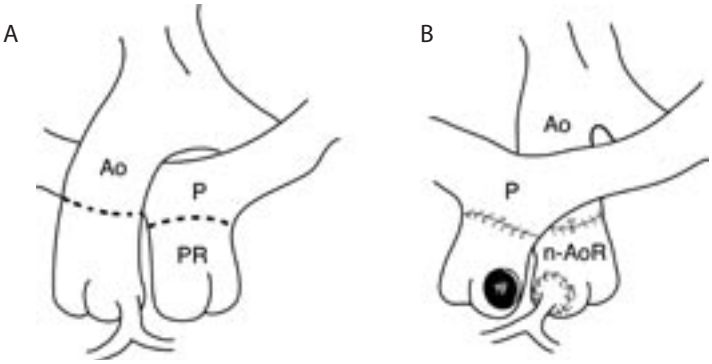


**Figure 1a-b. (a)** Great artery configuration in TGA before surgical repair. Ao = aorta, P = pulmonary trunk, PR = pulmonary root. **(b)** Great artery configuration after the ASO, which involves transection of the aorta (Ao) above the sinotubular junction and the pulmonary trunk (P) above the pulmonary root, transplantation of the coronary arteries into the root of the pulmonary trunk, switching of the aorta and pulmonary trunk with anterior positioning of the pulmonary trunk (Lecompte maneuver) and subsequent reconstruction of the former aortic root with a pericardial patch. The former pulmonary root has now become the neoaortic root (n-AoR).

**MRI**

MRI studies were performed with a 1.5-T system (NT 15 Gyroscan Intera; Philips Medical Systems, The Netherlands).

Aortic root dimensions were assessed by using double-oblique transverse images perpendicular to the aorta at the levels of the annulus of the aortic valve, the sinus of Valsalva, the sinotubular junction and the ascending aorta (the latter at the level of the crossing of the right pulmonary artery) (Figure 2) (10). Two sets of orthogonal scout cine images of the aortic root were initially obtained for planning of these acquisition planes. Imaging parameters with the ECG gated steady-state free precession (balanced turbo-field-echo) pulse sequence are listed in (Table 2) (10). Diameter measurements were acquired during diastole, with a trigger delay for all measurements set at 600 ms (10).

Figure 2.

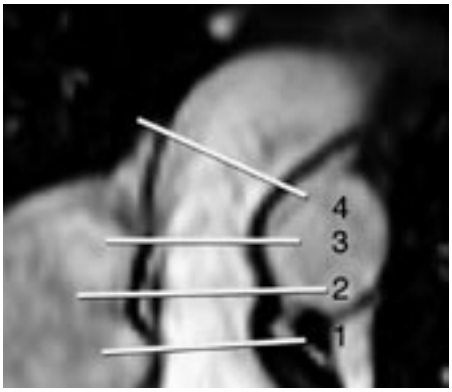


**Figure 2.** MR image obtained with steady-state free precession cine sequence in 16-year-old healthy male control subject shows four diameter measurements of the aortic root performed at (1) the level of the annulus of the aortic valve, (2) the sinus of Valsalva, (3) the sinotubular junction and (4) the ascending aorta (at the level of the crossing of the right pulmonary artery).

Table 2. MRI Sequence Characteristics.

| Sequence | repetition time* | echo time* | gate width* | field of view† | voxel size† | flip angle |
|---|---|---|---|---|---|---|
| Diameter and distensibility measurements | 3.2 | 1.23 | 34.2 | 220 | 1.25×1.25×6.00 | 50° |
| Aortic flow measurement | 4.8 | 2.8 | | 300 | 1.17×1.17× 8.00 | 20° |
| Short axis imaging | 3.2 | 1.6 | 34.2 | 400 | 1.60×1.60× 8.00 | 50° |

* expressed in ms.
† expressed in mm.

Aortic distensibility was measured at the level of the sinotubular junction, at the site of anastomosis of the ASO, as previously described (10). Distensibility (in mm $Hg^{-1}$) is defined by the following equation: $(A_{max} - A_{min}) / (A_{min} \times (P_{max} - P_{min}))$, where $A_{max}$ and $A_{min}$ are the maximal and minimal lumen areas (in square mm) of the sinotubular junction, respectively, and $P_{max}$ and $P_{min}$ are the systolic and diastolic blood pressures (in mm of mercury), respectively (10,12). The minimal lumen area is to be expected early in the cardiac cycle during the isovolumetric contraction phase (just before the beginning of the systolic upslope), while the maximal area is to be expected when the peak of aortic flow passes through the ascending aorta (10). First, the aortic flow was measured just distal to the aortic valve with a velocity-encoded MRI sequence, for timing of the acquisition of the cross-sectional minimal and maximal area measurements. The velocity-encoded sequence was encoded for a fixed velocity-encoding sensitivity of up to 200 cm/s (24). None of the participants showed aliasing on the acquired images, so the velocity-encoded acquisition did not need to be repeated with a higher velocity-encoding sensitivity.

The high temporal resolution (ranging between 7 and 12 ms) enabled optimal timing of the acquisition of the minimal and maximal cross-sectional areas (10). The same acquisition was also used for determination of aortic valve competence (AR fraction) and the measurement of peak flow velocity across the aortic valve. The AR fraction was calculated with the following formula: RV / SFV × 100%, where RV is regurgitant volume in milliliters and SFV is systolic forward volume in milliliters. Minimal and maximal lumen area MRI was subsequently performed after the acquisition planes were manually positioned perpendicular to the aorta at the level of the sinotubular junction at time points of minimal and maximal flow through the aortic root, respectively (10). This approach enabled correction for through-plane motion of the aortic root during contraction. Gate delay was individually applied for optimal timing of the acquisition (10).

Simultaneous blood pressure measurements were noninvasively obtained by using a semiautomatic MRI-compatible sphygmomanometer (Invivo Research, USA) (25).

The PWV of the aorta was measured between the ascending and the proximal descending aorta and between the proximal descending aorta and the abdominal aorta just proximal to the iliac bifurcation (Figure 3). A retrospectively electrocardiographically gated gradient-echo pulse sequence with velocity encoding was applied at the level of the pulmonary trunk to measure through-plane flow in the ascending aorta and proximal descending aorta. A second section was prescribed in the abdominal aorta just proximal to the iliac bifurcation. Imaging parameters were identical to those of the phase-contrast sequence used for timing of the distensibility measurements (18). During MR image acquisition, systolic and diastolic blood pressures were measured as described for the distensibility measurements. PWV was calculated as $\Delta x/\Delta t$ (expressed in meters per second), where $\Delta x$ is the aortic path length between two imaging levels and $\Delta t$ is the transit time between the arrival of the foot of the pulse wave at these levels (Figure 3) (18).

Figure 3.

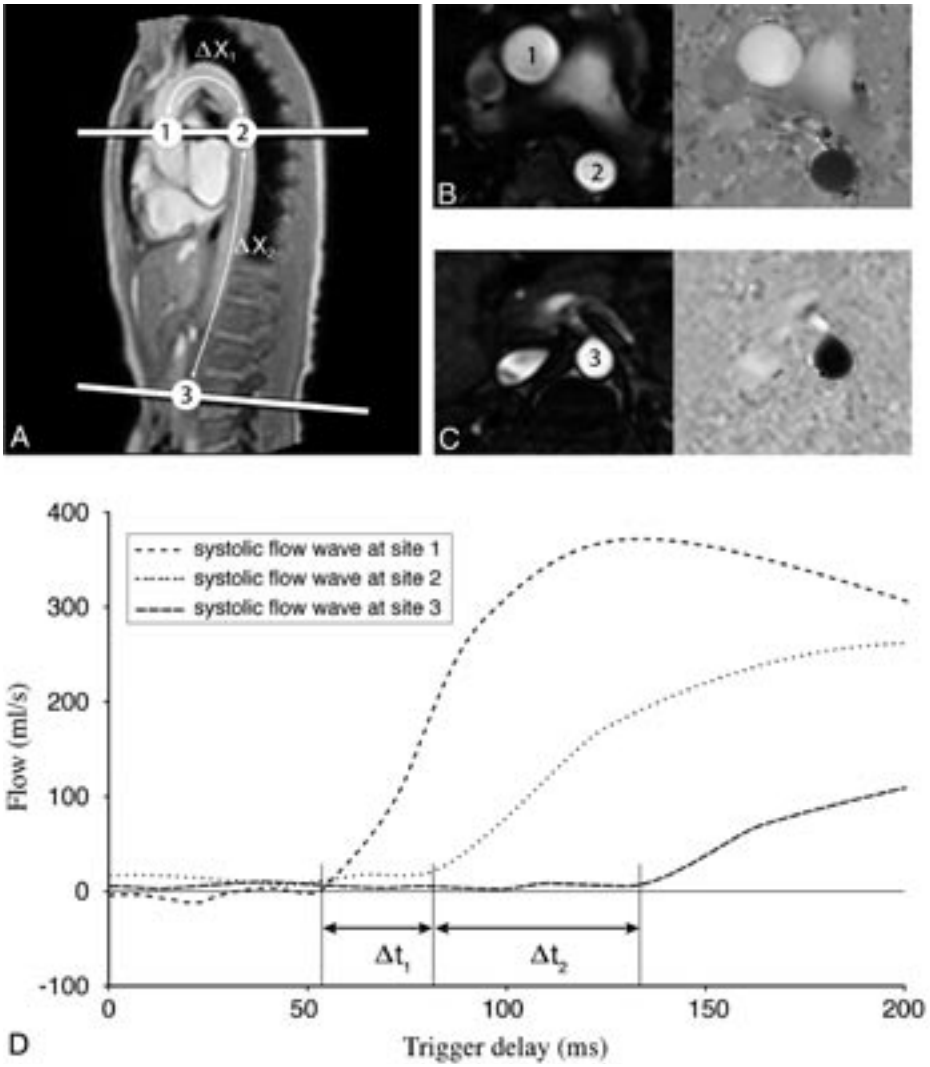


**Figure 3 a-d.** PWV in the aorta. **(a)** Sagittal MR image shows sites for through-plane velocity-encoded PWV measurements in 16-year-old male healthy control subject: the ascending aorta (1), the proximal descending aorta just distal to the aortic arch (2), and the abdominal aorta just proximal to the iliac bifurcation (3). $\Delta X_1$ = distance between measurement sites 1 and 2, $\Delta X_2$ = distance between measurement sites 2 and 3. **(b,c)** On the corresponding velocity-encoded images, the arrival time of the aortic systolic pulse-wave front can be determined by measuring the through-plane flow. **(d)** Graph shows determination of the arrival times of the three systolic flow waves at the measurement sites. The distance between the sampling sites (derived from **a**) and the transit times ($\Delta t_1$ and $\Delta t_2$) between the individual arrival times of the systolic flow waves (in **d**) determines the PWV.

Systolic LV function was assessed with a steady-state free precession cine sequence in the short-axis plane by using breath holds. A total of 12 consecutive sections were obtained (40 phases per cardiac cycle) without a section gap (26).

**Postprocessing**

Diameter and distensibility measurements of the aortic root, as well as systolic LV function images, were analyzed by using the software package MASS (Medis, The Netherlands) (26). LV end-diastolic volume and end-systolic volume were assessed by drawing the LV endocardial contours at end-diastole and end-systole in all sections, as previously described (10,18,26). At end-diastole, the epicardial borders of the LV were drawn to obtain the LV mass with inclusion of the interventricular septum (10,18,26). Indexing was performed according to the Mosteller formula: BSA = $\sqrt{}$ (height (cm) $\times$ weight (kg) / 3600), where BSA is the body surface area in square meters. The following parameters were then determined: end-diastolic volume, end-systolic volume, stroke volume, LV ejection fraction (LV EF) and LV mass (10,26).

Flow velocity - encoded MRI data were analyzed with the software package FLOW (Medis, The Netherlands) (24). Flow curves were obtained with this method for aortic flow during the cardiac cycle. Contours were drawn for the aortic lumen and flow data were subsequently obtained from the velocity data of each voxel in all phases. Peak flow velocity was determined with a time-velocity analysis that revealed the voxel with maximum peak flow throughout the cardiac cycle.

The manual drawing of all MRI contours and analysis of the other results was performed by one researcher (H.B.G., with 3 years of experience in cardiac MRI); these results were subsequently checked by a radiologist (L.J.M.K., with 9 years of experience in cardiac MRI) who was unaware of the patients' conditions.

**Statistical analysis**

Statistical analysis was performed by using software (SPSS for Windows, version 12.0.1; SPSS, USA). All data are presented as mean $\pm$ 1 standard deviation, unless stated otherwise. The two-tailed Mann-Whitney U test was used to express differences between the patients and control subjects. Correlation between variables was expressed with the Spearman rank correlation coefficient. Linear regression analysis was used to identify predictors of variables with backward elimination procedures. Statistical significance was indicated by $P < 0.05$.

## Results

### Aortic dimensions and elasticity

Diameters of the aortic root were significantly increased in patients after the ASO as compared with those in the healthy control subjects (Table 3). Dilatation was most pronounced at the level of the sinus of Valsalva, whereas diameters at the level of the ascending aorta were within normal limits. Elasticity of the proximal aorta was found to be reduced, as distensibility at the level of the sinotubular junction was significantly decreased and PWV in the aortic arch was significantly increased in patients after the ASO. PWV in the descending aorta was relatively normal. Aortic dilatation at the level of the sinus of Valsalva was significantly correlated with increased PWV in the aortic arch ($r = 0.36$, $P = 0.049$).

Table 3. Results in 15 Patients Who Had Undergone the ASO and 15 Age- and Sex-matched Healthy Control Subjects .

| Parameters | patients | healthy controls | P value mean | difference |
|---|---|---|---|---|
| diameter annulus (mm) | 30.6 ± 5.3 | 24.3 ± 3.0 | 0.001 | 6.3 |
| diameter sinus of Valsalva (mm) | 36.4 ± 6.1 | 27.0 ± 3.6 | < 0.001 | 9.4 |
| diameter sinotubular junction (mm) | 29.6 ± 6.0 | 23.9 ± 2.9 | 0.007 | 5.7 |
| diameter ascending aorta (mm) | 25.2 ± 5.3 | 22.6 ± 2.4 | 0.18 | 2.6 |
| distensibility (in $10^{-3}$ mm $Hg^{-1}$) * | 2.2 ± 1.8 | 4.9 ± 2.9 | < 0.01 | |
| PWV aortic arch (m/s) | 5.1 ± 1.2 | 3.9 ± 0.7 | 0.004 | |
| PWV descending aorta (m/s) | 4.1 ± 0.7 | 3.6 ± 0.3 | 0.06 | |
| aortic regurgitation fraction (%) | 5 ± 3 | 1 ± 1 | < 0.001 | |
| peak-flow velocity at STJ (m/s) | 1.63 ± 0.21 | 1.50 ± 0.32 | 0.21 | |
| LV EF (%) | 51 ± 6 | 58 ± 5 | 0.003 | |
| LV EDV ($ml/m^2$) | 112 ± 13 | 95 ± 16 | 0.007 | |
| LV ESV ($ml/m^2$) | 54 ± 11 | 39 ± 7 | < 0.001 | |
| LV mass ($g/m^2$) | 49 ± 11 | 43 ± 12 | 0.17 | |

Note: data are expressed as mean ± standard deviation.
* Distensibility was measured at the level of the sinotubular junction.
Abbreviations: ASO = arterial switch operation, PWV = pulse wave velocity, STJ = sinotubular junction, LV = left ventricle, EF = ejection fraction, EDV = end-diastolic volume indexed for body surface area, ESV = end-systolic volume indexed for body surface area.

### Aortic Valve Competence

Minor to mild degrees of AR were found in 6 of 15 patients after the ASO, with AR fraction ranging between 5% and 15%. In none of the healthy control subjects did AR fraction exceed

5%. Aortic root dilatation and reduced elasticity of the proximal aorta were associated with the degree of AR, as aortic root dilatation (r ranging between 0.32 and 0.66, $P \leq 0.01$ for all four levels), reduced aortic root distensibility ($r = 0.45$, $P = 0.01$) and increased PWV in the aortic arch ($r = 0.39$, $P = 0.03$) were all correlated with degree of AR fraction. Peak flow velocities across the aortic valve were not increased in our patient group as compared with those in the healthy control subjects (Table 3), supporting the fact that none of the examined individuals had aortic valve stenosis.

**LV function**

Systolic LV function - expressed by LV EF - was found to be significantly decreased in patients after the ASO as compared with that in the healthy control subjects (Table 3). Linear regression analysis revealed that degree of AR predicted decreased LV EF ($r = 0.41$, $P = 0.026$). LV dimensions (LV end-diastolic volume and LV end-systolic volume) were significantly enlarged in the patient group and were also related to AR fraction ($r = 0.48$, $P = 0.008$ and $r = 0.67$, $P < 0.001$, respectively). Mean LV mass in the patient group was slightly but not significantly larger than that in the healthy control subjects. Mean LV mass was significantly correlated with increased PWV at the level of the aortic arch ($r = 0.48$, $P = 0.008$) and increased LV end-diastolic and LV end-systolic volume ($r = 0.81$, $P < 0.001$ and $r = 0.48$, $P = 0.007$, respectively).

## Discussion

Our study revealed aortic root dilatation and reduced elasticity of the proximal aorta, associated with minor degrees of AR, in patients after the ASO. AR was associated with reduced LV systolic function and enlarged LV dimensions in these patients.

**Aortic dimensions and elasticity**

Patients after the ASO showed dilatation of the aortic root and reduced proximal aortic elasticity as compared with healthy control subjects; these findings are in agreement with those of previous studies (2-5,7). Structural differences between the walls of the two arterial roots have been reported to result in aortic root dilatation and reduced distensibility (7). After the ASO, the former pulmonary arterial wall (the neoaorta after the ASO) is exposed to higher systemic pressures, posing increased stress on the neoaortic wall that may ultimately lead to changes in the structure and function of the neoaortic root. Schoof et al. (27) reported that dilatation was the result of a pulmonary wall adapting to higher systemic pressures. Others have observed structural neoaortic wall abnormalities in patients with TGA even during the neonatal period, suggesting that these wall abnormalities are inherited, analogous to prototypical extremes such as Marfan syndrome and bicuspid aortic

valve disease (5). Whether medial abnormalities of the neoaortic wall are inherent or acquired remains, however, difficult to distinguish (5). Murakami et al. (4) proposed a relationship between neoaortic dilatation and decreased distensibility and damage to the vasa vasorum. The vasa vasorum are a fine network of vessels that supply the outer wall of a larger blood vessel (4). During the ASO, the vasa vasorum are transected and blood flow is inhibited, causing necrosis that may be followed by dilatation and impaired distensibility of the neoaorta (4). Manipulations during the ASO - such as the reimplantation of the coronary arteries - can also lead to changes in the neoaortic root wall that may result in progressive aortic dilatation (7), whereas aortic distensibility may be reduced by impaired aortic elastogenesis, as well as by scar formation at the site of anastomosis (8,9).

Arterial stiffness has been shown to be a cardiovascular risk factor on its own (11). Augmented arterial stiffening is associated with impaired coronary blood flow and LV dysfunction (11). In addition, a strong and independent association has been demonstrated between increased arterial stiffness and the presence of coronary artery disease (28). Therefore, the prognosis of patients with increased arterial stiffness may be worse as compared with healthy control subjects, because numerous other standard risk factors, such as aging, smoking, lipid profiles and sex, act cumulatively over a lifetime (11,28). Early detection of disturbances in arterial stiffness may allow for early therapeutic intervention (29). In patients with Marfan syndrome, beta-blockade has a beneficial effect on the progression rate of aortic dilatation, with reduction of aortic complications (12,25). Whether this is applicable for patients who have undergone the ASO remains to be elucidated.

**Aortic Valve Competence**

Aortic root dilatation and decreased aortic distensibility are closely related to aortic valve function, with the potential to cause AR (10,18,27,30). Although fewer than half of our patients who had undergone the ASO exhibited minor to mild degrees of AR, dilatation of the aortic root and reduced elasticity of the proximal aorta were found to be significantly correlated with degree of AR. Increased dimensions of the aortic annulus lead to loss of coaptation of the aortic valve leaflets, resulting in varying degrees of central AR (31-33). In addition, aortic valve dynamics are closely related to distensibility of the aortic root. During systole, as the aortic valve opens, the aortic root should expand simultaneously (13,14). Any disturbance in this synchronized process results in increased stress on the aortic valve leaflets (14-16), which will ultimately result in degeneration of the aortic valve leaflets and, consequently, AR.

**LV Function**

LV systolic function was significantly reduced in our patients after the ASO, despite most patients having New York Heart Association class I cardiac function. LV dysfunction has been suggested to be related to ischemic damage caused by coronary insufficiency or perioperative ischemia. A previous study (3), however, demonstrated no areas of myocardial infarction in patients

after the ASO without ischemic events. As in our patient group, no previous ischemic events were reported, and myocardial scar and coronary imaging were not included in the imaging protocol. In our study, LV dysfunction and increased LV dimensions appeared to be associated with degree of AR, which may be considered as the end point in a sequence of events (30). As a consequence of AR, increased LV mass occurs to maintain normal LV filling pressures (30). A normal LV volume-to-mass ratio is initially maintained, with adequate preservation of LV EF because of the increased preload, but, as AR continues to progress and the LV continues to dilate, increased wall stress may result in LV systolic dysfunction and, consequently, decreased LV EF (30). AR also leads to a volume overload of the LV, hence increasing LV dimensions, which consequently results in decreased LV EF.

Our study had limitations. We used a limited number of patients and control subjects, although the low inter- and intraobserver variability of MRI allows relatively small sample sizes (34). No preoperative or follow-up measurements were available in our observational study, so progression of findings could not be documented. Future longitudinal follow-up studies with larger numbers of patients may further elucidate the predictive value of our findings in patients after the ASO, allowing for multivariate analysis and subgroup analysis, as other parameters may additionally be involved in our findings.

In conclusion, our study revealed aortic root dilatation and reduced elasticity of the proximal aorta in patients after the ASO, in addition to minor degrees of AR, reduced LV systolic function and enlarged LV dimensions. Therefore, despite the fact that the ASO has substantially reduced the number of sequelae associated with surgical correction of TGA, the current findings might pose a prognostic risk for patients after the ASO. Our study showed the feasibility of MRI as an integrated imaging tool for monitoring aortic and LV function parameters, which may facilitate the early detection of aortic and LV dysfunction in patients after the ASO.

## References


1. del Nido PJ, Schwartz ML. Aortic regurgitation after arterial switch operation. J Am Coll Cardiol. 2006; 47 (10): 2063-2064.
2. Formigari R, Toscano A, Giardini A, et al. Prevalence and predictors of neoaortic regurgitation after arterial switch operation for transposition of the great arteries. J Thorac Cardiovasc Surg. 2003; 126 (6): 1753-1759.
3. Taylor AM, Dymarkowski S, Hamaekers P, et al. MR coronary angiography and late-enhancement myocardial MR in children who underwent arterial switch surgery for transposition of great arteries. Radiology. 2005; 234 (2): 542-547.
4. Murakami T, Nakazawa M, Momma K, Imai Y. Impaired distensibility of neoaorta after arterial switch procedure. Ann Thorac Surg. 2000; 70 (6): 1907-1910.
5. Niwa K, Perloff JK, Bhuta SM, et al. Structural abnormalities of great arterial walls in congenital heart disease: light and electron microscopic analyses. Circulation. 2001; 103 (3): 393-400.
6. Mersich B, Studinger P, Lenard Z, Kadar K, Kollai M. Transposition of great arteries is associated with increased carotid artery stiffness. Hypertension. 2006; 47 (6): 1197-1202.
7. Hourihan M, Colan SD, Wernovsky G, Maheswari U, Mayer JE Jr, Sanders SP. Growth of the aortic anastomosis, annulus, and root after the arterial switch procedure performed in infancy. Circulation. 1993; 88 (2): 615-620.
8. Hwang HY, Kim WH, Kwak JG, et al. Mid-term follow-up of neoaortic regurgitation after the arterial switch operation for transposition of the great arteries. Eur J Cardiothorac Surg. 2006; 29 (2): 162-167.
9. Verhaaren H, De Mey S, Coomans I, et al. Fixed region of nondistensibility after coarctation repair: in vitro validation of its influence on Doppler peak velocities. J Am Soc Echocardiogr. 2001; 14 (6): 580-587.
10. Grotenhuis HB, Westenberg JJ, Doornbos J, et al. Aortic root dysfunctioning and its effect on left ventricular function in Ross procedure patients assessed with magnetic resonance imaging. Am Heart J. 2006; 152 (5): 975-978.
11. Cruickshank K, Riste L, Anderson SG, Wright JS, Dunn G, Gosling RG. Aortic pulse-wave velocity and its relationship to mortality in diabetes and glucose intolerance: an integrated index of vascular function? Circulation. 2002; 106 (16): 2085-2090.
12. Groenink M, de Roos A, Mulder BJ, Spaan JA, van der Wall EE. Changes in aortic distensibility and pulse wave velocity assessed with magnetic resonance imaging following beta-blocker therapy in the Marfan syndrome. Am J Cardiol. 1998; 82 (2): 203-208.
13. Thubrikar MJ, Heckman JL, Nolan SP. High speed cine-radiographic study of aortic valve leaflet motion. J Heart Valve Dis. 1993; 2 (6): 653-661.
14. Schmidtke C, Bechtel J, Hueppe M, Noetzold A, Sievers HH. Size and distensibility of the aortic root and aortic valve function after different techniques of the Ross procedure. J Thorac Cardiovasc Surg. 2000; 119 (5): 990-997.

15. Thubrikar M, Skinner JR, Aouad J, Finkelmeier BA, Nolan SP. Analysis of the design and dynamics of aortic bioprostheses in vivo. J Thorac Cardiovasc Surg. 1982; 84 (2): 282-290.
16. Thubrikar MJ, Nolan SP, Aouad J, Deck JD. Stress sharing between the sinus and leaflets of canine aortic valve. Ann Thorac Surg. 1986; 42 (4): 434-440.
17. Fedak PW, Verma S, David TE, Leask RL, Weisel RD, Butany J. Clinical and pathophysiological implications of a bicuspid aortic valve. Circulation. 2002; 106 (8): 900-904.
18. Grotenhuis HB, Ottenkamp J, Westenberg JJ, Bax JJ, Kroft LJ, de Roos A. Reduced aortic elasticity and dilatation are associated with aortic regurgitation and left ventricular hypertrophy in nonstenotic bicuspid aortic valve patients. J Am Coll Cardiol. 2007; 49 (15): 1660-1665.
19. Mohiaddin RH, Underwood SR, Bogren HG, et al. Regional aortic compliance studied by magnetic resonance imaging: the effects of age, training, and coronary artery disease. Br Heart J. 1989; 62 (2): 90-96.
20. Bogren HG, Klipstein RH, Mohiaddin RH, et al. Pulmonary artery distensibility and blood flow patterns: a magnetic resonance study of normal subjects and of patients with pulmonary arterial hypertension. Am Heart J. 1989; 118 (5): 990-999.
21. Otto CM, Lind BK, Kitzman DW, Gersh BJ, Siscovick DS. Association of aortic-valve sclerosis with cardiovascular mortality and morbidity in the elderly. N Engl J Med. 1999; 341 (3): 142-147.
22. Grotenhuis HB, Kroft LJ, van Elderen SG, et al. Right ventricular hypertrophy and diastolic dysfunction in arterial switch patients without pulmonary artery stenosis. Heart. 2007; 93 (12): 1604-1608.
23. Lecompte Y, Zannini L, Hazan E, et al. Anatomic correction of transposition of the great arteries. J Thorac Cardiovasc Surg. 1981; 82 (4): 629-631.
24. van der Geest RJ, Niezen RA, van der Wall EE, de Roos A, Reiber JH. Automated measurement of volume flow in the ascending aorta using MR velocity maps: evaluation of inter- and intraobserver variability in healthy volunteers. J Comput Assist Tomogr. 1998; 22 (6): 904-911.
25. Nollen GJ, Groenink M, Tijssen JG, van der Wall EE, Mulder BJ. Aortic stiffness and diameter predict progressive aortic dilatation in patients with Marfan syndrome. Eur Heart J. 2004; 25 (13): 1146-1152.
26. van der Geest RJ, Reiber JH. Quantification in cardiac MRI. J Magn Reson Imaging. 1999; 10 (5): 602-608.
27. Schoof PH, Gittenberger-de Groot AC, de Heer E, Bruijn JA, HazekampMG, Huysmans HA. Remodeling of the porcine pulmonary autograft wall in the aortic position. J Thorac Cardiovasc Surg. 2000; 120 (1): 55-65.
28. Arnett DK, Evans GW, Riley WA. Arterial stiffness: a new cardiovascular risk factor? Am J Epidemiol. 1994; 140 (8): 669-682.
29. Franklin SS. Blood pressure and cardiovascular disease: what remains to be achieved? J Hypertens Suppl. 2001; 19 (3): S3-S8.
30. Bekeredjian R, Grayburn PA. Valvular heart disease: aortic regurgitation. Circulation. 2005; 112 (1): 125-134.
31. Thubrikar MJ, Labrosse MR, Zehr KJ, Robicsek F, Gong GG, Fowler BL. Aortic root dilatation may alter the dimensions of the valve leaflets. Eur J Cardiothorac Surg. 2005; 28 (6): 850-855.

32. Chong WY, Wong WH, Chiu CS, Cheung YF. Aortic root dilation and aortic elastic properties in children after repair of tetralogy of Fallot. Am J Cardiol. 2006; 97 (6): 905-909.
33. Tafreshi RI, Shahmohammadi A, Davari PN. Predictors of left ventricular performance after valve replacement in children and adolescents with chronic aortic regurgitation. Pediatr Cardiol. 2005; 26 (4): 331-337.
34. Bellenger NG, Davies LC, Francis JM, Coats AJ, Pennell DJ. Reduction in sample size for studies of remodeling in heart failure by the use of cardiovascular magnetic resonance. J Cardiovasc Magn Reson. 2000; 2 (4): 271-278.

Heynric B. Grotenhuis
Lucia J.M. Kroft
Saskia G.C. van Elderen
Jos J.M. Westenberg
Joost Doornbos
Mark G. Hazekamp
Hubert W. Vliegen
Jaap Ottenkamp
Albert de Roos

# chapter 06

**Right Ventricular Hypertrophy and Diastolic Dysfunction in Arterial Switch Patients without Pulmonary Artery Stenosis.**

Heart. 2007; 93 (12): 1604-1608

## Abstract

**Purpose:** To assess pulmonary flow dynamics and right ventricular (RV) function in patients without significant anatomical narrowing of the pulmonary arteries late after the arterial switch operation (ASO) by using magnetic resonance imaging (MRI).

**Materials and Methods:** 17 patients (mean (SD), 16.5 (3.6) years after ASO) and 17 matched healthy subjects were included. MRI was used to assess flow across the pulmonary trunk, RV systolic and diastolic function and RV mass.

**Results:** Increased peak flow velocity (> 1.5 m/s) was found across the pulmonary trunk in 14 of 17 patients. Increased RV mass was found in ASO patients: 14.9 (3.4) vs 10.0 (2.6) g/m2 in normal subjects ($P < 0.01$). Delayed RV relaxation was found after ASO: mean tricuspid valve E/A peak flow velocity ratio = 1.60 (0.96) vs 1.92 (0.61) in normal subjects ($P = 0.03$) and E-deceleration gradients = -1.69 (0.73) vs -2.66 (0.96) ($P < 0.01$). After ASO, RV mass correlated with pulmonary trunk peak flow velocity ($r = 0.49$, $P < 0.01$) and tricuspid valve E-deceleration gradients ($r = 0.35$, $P = 0.04$). RV systolic function was well preserved in patients (ejection fraction = 53 (7)% vs 52 (8)% in normal subjects, $P = 0.72$).

**Conclusions:** Increased peak flow velocity in the pulmonary trunk was often observed late after ASO, even in the absence of significant pulmonary artery stenosis. Hemodynamic consequences were RV hypertrophy and RV relaxation abnormalities as early markers of disease, while systolic RV function was well preserved.

## Introduction

The arterial switch operation (ASO) has become the standard procedure of choice for repair of transposition of the great arteries (1-3). The ASO consists of translocation of the pulmonary trunk and the aorta, and subsequent relocation of the coronary arteries in the neonatal period (4). The advantages of the ASO compared with the previous intra-atrial repair are related to creation of the left ventricle as the systemic ventricle and the maintenance of normal sinus node function (5-7).

Supravalvar pulmonary artery stenosis is the most frequent complication after ASO (5-7). Reduction of the cross sectional area due to stretching of the pulmonary arteries is induced by the Lecompte maneuver (5-7), while compression of the proximal pulmonary branches may occur because of the close anatomical relation with the aorta (1,5,7,8). As a result, supravalvar pulmonary artery stenosis in ASO patients is associated with right ventricular hypertrophy and dysfunction from the increased afterload (9). These stenoses are well visualized by magnetic resonance imaging (MRI): a fixed stenosis can easily be recognized using spin-echo or gradient-echo sequences, and increased peak flow velocity across a significant stenosis can be detected by velocity encoded MRI (1,7,9).

In patients with repaired coarctation, increased peak flow velocities across vascular segments may also be observed, because of scar formation at the site of anastomosis, even in the absence of overt narrowing (10,11). Scar tissue at the site of anastomosis may lead to decreased distensibility - thereby increasing local peak-flow velocity - as may also be the case in ASO patients (10,11). In addition, minor degrees of stenosis or hypoplasia of the pulmonary vascular bed may lead to increased flow velocities in the pulmonary trunk (10), thereby increasing the hemodynamic burden for the right ventricle.

We hypothesized that in ASO patients without significant pulmonary artery stenosis, increased peak flow velocities are present in the pulmonary trunk, with a potential negative impact on right ventricular function. In the present study we excluded ASO patients with significant pulmonary artery stenosis as shown by anatomical imaging.

We tested these hypotheses by studying pulmonary flow dynamics and right ventricular function in patients without significant anatomical narrowing of the pulmonary trunk or pulmonary arteries late after the ASO, compared with matched healthy subjects.

## Methods

### Patient population

The local medical ethics committee approved the study and informed consent was obtained from all participants before their enrollment. Twenty-two ASO patients and 22 healthy subjects were studied prospectively with MRI at our institution. All patients were recruited from our local pediatric cardiology database. Inclusion criteria included transposition of the great arteries corrected by ASO (including the Lecompte maneuver) in the past, current age between 10 and 20 years, willingness to comply with the study procedures and written informed consent. Exclusion criteria comprised ASO using the Jatene procedure, pulmonary stenting, general contraindications to MRI and pulmonary artery stenosis shown by echocardiography, based on local tailoring of the pulmonary trunk of at least 50% or a peak systolic gradient of at least 60 mm Hg in the pulmonary arteries, or both.

Visual inspection of the pulmonary arteries on MRI confirmed that only ASO patients without pulmonary artery stenosis were enrolled in the study. A vessel diameter reduction of more than 50% gives rise to a reduction in blood volume flow and was considered significant (12). Two patients who had a main pulmonary artery stenosis that was visually greater than 50% were thus excluded from further analysis. Three patients failed to complete the MRI study because of problems with breath holding. In all, 17 patients and 17 healthy subjects were included for final analysis.

Age and sex matched healthy subjects were selected from our database and comprised subjects in whom congenital cardiac pathology had been excluded in the past by physical examination and echocardiography. Characteristics of the two groups (Table 1) and their functional status, expressed as New York Heart Association functional class, were obtained from the patient records.

Table 1: Patient and healthy subject characteristics.

| Characteristics | patients (n = 17) | healthy subjects (n = 17) |
|---|---|---|
| male / female | 13 (76%) / 4 (24%) | 13 (76%) / 4 (24%) |
| age at ASO (days) * | 16 ± 23 | |
| age at MRI (years) * | 16.4 ± 3.2 | 16.5 ± 3.6 |
| height at MRI (cm) * | 169 ± 13 | 169 ± 12 |
| weight at MRI (kg) * | 61 ± 17 | 60 ± 13 |
| body surface area at MRI ($m^2$) * and † | 1.7 ± 0.3 | 1.7 ± 0.2 |
| systolic / diastolic BP at MRI (mm Hg) * | 124 / 74 ± 20 / 18 | 121 / 69 ± 12 / 10 |
| cardiac frequency (beats per minute) * | 74 ± 16 | 69 ± 9 |

* Data are mean ± standard deviation.
† According to the Mosteller formula: √ (height (cm) × weight (kg) / 3600).
Abbreviations: ASO = arterial switch operation; MRI = magnetic resonance imaging; BP = blood pressure.

**Operation technique**

Nine patients had undergone balloon atrial septostomy (that is, the Rashkind procedure) and 11 had received prostaglandin E1 infusions before the ASO. The ASO was carried out in patients with transposition of the great arteries (median age at surgery = 6 days) using cardiopulmonary bypass and moderate hypothermia. The operation included transection of the aorta and pulmonary trunk above their roots, transplantation of the coronary arteries into the root of the pulmonary trunk, switching of the aorta and pulmonary trunk and subsequent reconstruction of the pulmonary trunk with a pericardial patch. The Lecompte maneuver was undertaken in all 17 patients (8). Associated procedures during the ASO were closure of a ventricular septal defect in 5 patients, closure of an atrial septal defect in 7 and closure of the ductus arteriosus in 12. No perioperative ischemic events were recorded.

**MRI**

MRI studies were done using a 1.5-T system (NT 15 Gyroscan Intera; Philips Medical Systems, The Netherlands). Initial scout images were obtained in transverse, coronal and sagittal planes using a standard multislice turbo spin-echo sequence.

To visualize the pulmonary vessel anatomy a black-blood static sequence and contrast enhanced magnetic resonance angiography were used. Black-blood turbo spin-echo imaging using sensitivity encoding (13) was acquired in the double oblique transverse plane, axial to the pulmonary trunk, with the following scan parameters: field of view 350 mm, repetition time two heart beats, with actual time depending on the individual heart rate, echo time 8.6 ms, flip angle 90°, slice gap 0.8 mm, voxel size 1.37 × 2.12 × 8.00 mm (1). Contrast enhanced magnetic resonance angiography by using Magnevist (0.2 mmol/kg; Schering, Germany) was carried out with the following scan parameters: field of view 400 mm, repetition time 5.1 ms, echo time 1.44 ms, voxel size 1.56 × 3.13 × 4.00 mm.

Pulmonary valve function and flow dynamics across the pulmonary trunk were assessed using velocity encoded MRI in the proximal pulmonary trunk (14). Scan parameters were field of view 400 mm, repetition time 8.6 ms, echo time 5.3 ms, flip angle 20°, voxel size 2.34 × 2.61 × 8.00 mm. The sequence was encoded for a through-plane velocity up to 150 cm/s. Temporal resolution was 25.6 ms.

Systolic right ventricular function was assessed using a prospectively ECG triggered balanced gradient-echo sequence. A short-axis stack of 14 to 18 contiguous slices was used, covering the base of the heart to the apex (14), with the following scan parameters: field of view 350 mm, repetition time 3.2 ms, echo time 1.62 ms, flip angle 70°, voxel size 2.19 × 1.62 × 8.00 mm.

Velocity mapping across the tricuspid valve was used for assessment of diastolic right ventricular function (14,15). Scan parameters were: field of view 300 mm, repetition time

9.4 ms, echo time 6 ms, flip angle 20°, voxel size 2.34 × 2.61 × 8.00 mm. The sequence was encoded for a through-plane velocity up to 100 cm/s. Temporal resolution was 25.6 ms.

**Postprocessing**

All images were quantitatively analyzed on a workstation with a Pentium 4 processor (Intel, USA). Contrast enhanced magnetic resonance angiography and black-blood images of the pulmonary vessels were used to exclude significant pulmonary artery stenoses. The gradient-echo right ventricular dataset was analyzed with the software package MASS (Medis, The Netherlands) (14). Flow velocity encoded MRI data were analyzed using the software package FLOW (Medis, The Netherlands) (14). All contours were manually drawn by two observers (both with one year of experience) and were subsequently checked by a radiologist (with nine years of experience), who was unaware of the patient conditions.

Vascular contours were drawn for the pulmonary trunk to generate flow curves throughout the cardiac cycle (16). The presence of substantial pulmonary valve regurgitation was assessed (> 5%). Increased peak flow velocity in the pulmonary trunk was defined as maximum blood flow velocity ($V_{max}$) exceeding 1.5 m/s (1). The duration of the forward flow wave during systole across the pulmonary trunk was divided in a first and second half, with subsequent comparison of the flow/volume ratios (flow through first half of systole divided by flow through second half of systole) as a marker of flow propagation (17).

Right ventricular systolic function was assessed by drawing endocardial right ventricular contours at end-diastole and end-systole in all sections of the cine short axis data (16). Right ventricular end-diastolic volumes (RV EDV) and right ventricular end-systolic volumes (RV ESV) were obtained and indexed for body surface area according to the Mosteller formula: √ (height (cm) × weight (kg) / 3600). Right ventricular stroke volume indexed for body surface area (RV SV) was calculated by subtracting RV ESV from RV EDV. The right ventricular ejection fraction (RV EF) was calculated by dividing RV SV by RV EDV. Right ventricular mass was calculated as previously described after drawing right ventricular endocardial and epicardial contours, with subsequent indexation for body surface area (indicated by right ventricular mass) (16).

For evaluation of right ventricular diastolic function, tricuspid valve contours were drawn throughout the cardiac cycle (18). Flow vs time curves of the tricuspid flow were subsequently analyzed using Microsoft Excel (version 2003) (19) for calculation of the following indices of diastolic right ventricular function: early filling phase (E), atrial kick phase (A) and E/A peak flow velocity ratios (18). Analysis of E slopes was done by calculation of mean deceleration gradients of E (18). Times of E, A and diastasis were also measured (18).

**Statistical analysis**

Statistical analysis was carried out by using SPSS for Windows (version 12.0.1; SPSS, USA). All data are expressed as mean (SD), unless stated otherwise. The Mann-Whitney U test was used to express differences in variables between patients and healthy subjects. Correlations between variables are expressed using Spearman's rank correlation coefficient. Statistical significance was indicated by a probability P value of less than 0.05.

## RESULTS

Patients and healthy subjects were matched for age and sex. Subject characteristics were comparable between both groups (Table 1). All patients were in New York Heart Association functional class 1, without drug treatment.

**Pulmonary artery characteristics**

Cross sectional diameters of the pulmonary trunk were slightly smaller in the ASO patients than in the controls, with a mean difference of 3.5 mm between the two groups (Table 2). In 14 of the 17 ASO patients (82%), the pulmonary trunk $V_{max}$ exceeded 1.5 m/s, compared with none in the healthy subject group, indicating frequently increased peak flow velocities at the level of the pulmonary trunk (Table 2). In the ASO patients, the ratio of pulmonary trunk forward flow volume during the first half of systole to that in the second half was significantly smaller than in the healthy subjects, reflecting delayed propagation of pulmonary flow through the pulmonary trunk. Within the patient group, a positive correlation was found between this pulmonary trunk forward flow volume ratio and the pulmonary trunk $V_{max}$ ($r = -0.42$, $P = 0.02$), indicating that delayed flow propagation was associated with higher maximum flow velocities. No substantial pulmonary regurgitation (> 5%) was present in any patient or healthy subject.

Table 2: Results in 17 ASO patients and 17 age/gender matched healthy subjects.

| Parameters | patients | healthy subjects | P value |
|---|---|---|---|
| PT crossectional diameter (mm) | 25.6 ± 3.4 | 29.1 ± 3.5 | 0.01 |
| PT $V_{max}$ (m/s) | 1.88 ± 0.56 | 0.93 ± 0.19 | < 0.01 |
| PT volume-ratio systole1 / systole2 | 1.16 ± 0.15 | 0.35 ± 0.26 | 0.01 |
| RV EF (%) | 53 ± 7 | 52 ± 8 | 0.84 |
| RV SV (ml/$m^2$) | 56 ± 8 | 50 ± 13 | 0.06 |
| RV EDV (ml/$m^2$) | 108 ± 18 | 96 ± 16 | 0.06 |
| RV ESV (ml/$m^2$) | 51 ± 14 | 46 ± 10 | 0.41 |
| RV mass (gr/$m^2$) | 14.9 ± 3.4 | 10.0 ± 2.6 | < 0.01 |
| TV E/A peak-flow ratio | 1.60 ± 0.96 | 1.92 ± 0.61 | 0.03 |
| TV mean dec gradient of E phase (l/$s^2$) | -1.69 ± 0.73 | -2.66 ± 0.96 | < 0.01 |
| TV diastasis time (ms) | 19 ± 30 | 53 ± 64 | 0.04 |

Note: data are expressed as mean ± standard deviation.
Abbreviations: ASO = arterial switch operation; PT = pulmonary trunk; $V_{max}$ = maximum velocity; RV = right ventricle; EF = ejection fraction; SV = stroke volume indexed for body surface area; EDV = end-diastolic volume indexed for body surface area; ESV = end-systolic volume indexed for body surface area; TV = tricuspid valve; E = early filling phase; A = atrial kick phase; dec = deceleration.

**Right ventricular function**

Systolic function, expressed by RV EF and RV SV, did not differ between ASO patients and healthy subjects (Table 2). Right ventricular dimensions (RV EDV and RV ESV) were also not different between the two groups (Table 2).

Mean right ventricular mass in the ASO patient group was significantly greater than in the healthy subjects (Table 2). In the patient group a significant correlation was found between right ventricular mass and pulmonary trunk $V_{max}$ ($r = 0.49$, $P < 0.01$), indicating that right ventricular hypertrophy is associated with increased peak flow velocities in the pulmonary trunk.

A significantly reduced mean tricuspid valve E/A peak flow velocity ratio, decreased tricuspid valve mean deceleration gradient in the E phase and loss of diastasis time were all present in our ASO patient group, indicating delayed right ventricular relaxation during diastole (Table 2, Figure 1). In addition, the tricuspid valve mean deceleration gradient in the E phase and loss of diastasis were positively correlated with right ventricular mass ($r = 0.35$, $P = 0.04$ and $r = 0.45$, $P < 0.01$, respectively), as would be expected because delayed relaxation is associated with hypertrophy accompanying stiffening of the right ventricular myocardium.

Figure 1.

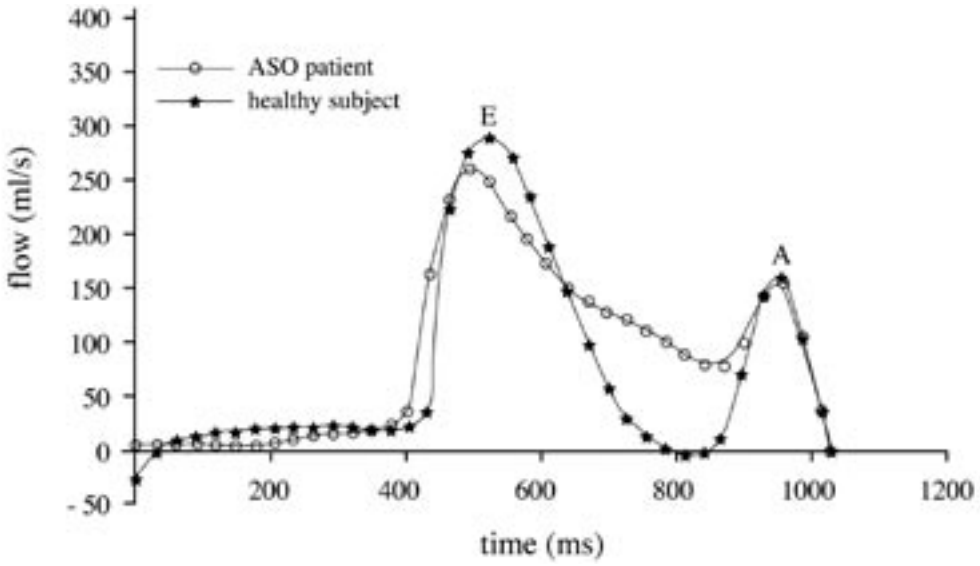


**Figure 1.** Right ventricular inflow curves across the tricuspid valve in an ASO patient and a matched healthy subject. The biphasic inflow pattern consists of two peaks, representing the early inflow (E) and the late atrial kick (A). Note the decreased mean deceleration gradient after the E peak in the ASO patient compared with the matched healthy subject.

## Discussion

Cardiac MRI was used to assess pulmonary flow dynamics and right ventricular function in patients late after the arterial switch operation without significant anatomical narrowing of the pulmonary arteries, as compared with matched healthy subjects. This study revealed frequently increased peak flow velocities in the pulmonary trunk, even in the absence of significant anatomical narrowing of the pulmonary arteries. Further hemodynamic consequences were delayed pulmonary flow propagation, right ventricular hypertrophy and right ventricular relaxation abnormalities as early markers of disease, whereas systolic right ventricular function remained well preserved.

### Pulmonary artery characteristics

ASO patients often have increased peak flow velocities at the level of the pulmonary trunk compared with healthy subjects. Various reasons for this have been postulated. Reduction of cross sectional area is induced by stretching of the pulmonary arteries following the Lecompte maneuver (2,5,7). The non-spiral configuration of the pulmonary arteries after this maneuver

has been reported to promote the formation of stenotic plaques through an altered wall shear stress distribution (2), while scarring at the anastomosis site often results in circumferential narrowing (5-7,9). Recent reports of patients with repaired coarctation also indicate that, even in the absence of significant stenosis at the site of anastomosis, loss of distensibility because of stiff scar tissue is a major contributor to an increased peak flow velocity (10,11). It is likely that local scar tissue with loss of distensibility made a major contribution to increased peak flow velocities in our ASO patients, in addition to possible minor degrees of narrowing at the site of anastomosis or peripheral pulmonary branches. In this study the pulmonary trunk was slightly smaller in the ASO patient group than in the matched healthy subjects. Previous studies indicated normal dimensions of the pulmonary trunk and peripheral pulmonary branches before the ASO, excluding a congenital deformity (5,6).

**Right ventricular function**

In this study, systolic right ventricular function was well preserved late after the ASO. These findings are supported by previous reports (1,20).

The right ventricular mass was significantly greater in the ASO patients than in the healthy controls, indicating right ventricular hypertrophy. This often occurs as a compensatory mechanism for increased right ventricular afterload (9,21), which in this study was reflected by increased peak flow velocities across the pulmonary trunk. Increased right ventricular afterload was also indicated by the delayed propagation of the systolic pulmonary flow (17). Ischemic damage caused by coronary insufficiency has been suggested as another explanation for compensatory right ventricular hypertrophy after ASO (20). However, none of our patients had perioperative ischemic events according to the available patient records, so ventricular hypertrophy from ischemic damage was not suspected.

Delayed right ventricular relaxation was indicated by decreased tricuspid valve E/A peak flow velocity ratio, reduced tricuspid valve mean deceleration gradient of the E phase and loss of diastasis time in our ASO patient group. In contrast to mild to moderate degrees of isolated pulmonary stenosis, which have little impact on right ventricular function (9), a supravalvar increase in peak flow velocity proved to have negative repercussions for right ventricular function in this study. Delayed right ventricular relaxation is related to hypertrophy accompanying stiffening of the myocardium (20) and can be seen as an early marker of diastolic dysfunction which may precede right ventricular systolic dysfunction (20,22). The impact of right ventricular diastolic dysfunction is considerable, as published reports suggest that its prognostic value is equal to impaired left ventricular diastolic function (20,22,23). Impaired left ventricular diastolic function is a major contributor in one third of patients with congestive heart failure (16,22,24) and causes diminished exercise performance (24,25). Aging contributes to diastolic dysfunction by an increase in ventricular mass and a loss of elastic myocardial properties over time (16,24). Thus impaired right ventricular relaxation

might pose a future risk for right ventricular dysfunction in our patient group, with negative implications for prognosis.

The evaluation by MRI of right ventricular function and pulmonary flow dynamics late after the ASO revealed an increased peak flow velocity across the pulmonary trunk, even in the absence of significant pulmonary stenosis at the surgical anastomosis. Further hemodynamic consequences were right ventricular hypertrophy and right ventricular relaxation abnormalities as early markers of disease, though systolic right ventricular function was still well preserved.

## References


1. Gutberlet M, Boeckel T, Hosten N, et al. Arterial switch procedure for D-transposition of the great arteries: quantitative midterm evaluation of hemodynamic changes with cine MR imaging and phase-shift velocity mapping-initial experience. Radiology. 2000; 214 (2): 467-475.
2. Tang T, Chiu IS, Chen HC, et al. Comparison of pulmonary arterial flow phenomena in spiral and Lecompte models by computational fluid dynamics. J Thorac Cardiovasc Surg. 2001; 122 (3): 529-534.
3. Formigari R, Santoro G, Guccione P, et al. Treatment of pulmonary artery stenosis after arterial switch operation: stent implantation vs. balloon angioplasty. Catheter Cardiovasc Interv. 2000; 50 (2): 207-211.
4. McMahon CJ, Ravekes WJ, Smith EO, et al. Risk Factors for Neo-Aortic Root Enlargement and Aortic Regurgitation Following Arterial Switch Operation. Pediatr Cardiol. 2004; 24 (4): 329-335.
5. Massin MM, Nitsch GB, Dabritz S, et al. Growth of pulmonary artery after arterial switch operation for simple transposition of the great arteries. Eur J Pediatr. 1998; 157 (2): 95-100.
6. Santoro G, Di Carlo D, Formigari R, et al. Late onset pulmonary valvar stenosis after arterial switch operation for transposition of the great arteries. Heart. 1998; 79 (3): 311-312.
7. Weiss F, Habermann CR, Lilje C, et al. MRI of pulmonary arteries in follow-up after arterial-switch-operation (ASO) for transposition of great arteries (d-TGA). Rofo. 2005; 177 (6): 849-855.
8. Lecompte Y, Neveux JY, Leca F, et al. Reconstruction of the pulmonary outflow tract without prosthetic conduit. J Thorac Cardiovasc Surg. 1982; 84 (5): 727-733.
9. Beek FJ, Beekman RP, Dillon E, et al. MRI of the pulmonary artery after arterial switch operation for transposition of the great arteries. Pediatr Radiol. 1993; 23 (5): 335-340.
10. Verhaaren H, De Mey S, Coomans I, et al. Fixed region of nondistensibility after coarctation repair: in vitro validation of its influence on Doppler peak velocities. J Am Soc Echocardiogr. 2001; 14 (6): 580-587.
11. Seifert BL, DesRochers K, Ta M, et al. Accuracy of Doppler methods for estimating peak-to-peak and peak instantaneous gradients across coarctation of the aorta: An In vitro study. J Am Soc Echocardiogr. 1999; 12 (9): 744-753.
12. Meire HB, Cosgrove D. Vascular ultrasound. In: Grainger & Allison's, editors. Diagnostic Radiology. New York, NY: Churchill Livingstone. 1997: 2459-2481.
13. Pruessmann KP, Weiger M, Boesiger P. Sensitivity encoded cardiac MRI. J Cardiovasc Magn Reson. 2001; 3 (1): 1-9.
14. van der Geest RJ, Reiber JH. Quantification in cardiac MRI. J Magn Reson Imaging. 1999; 10 (5): 602-608.
15. Paelinck BP, Lamb HJ, Bax JJ, et al. Assessment of diastolic function by cardiovascular magnetic resonance. Am Heart J. 2002; 144 (2): 198-205.
16. Van Straten A, Vliegen HW, Hazekamp MG, et al. Right ventricular function after pulmonary valve replacement in patients with tetralogy of Fallot. Radiology. 2004; 233 (3): 824-829.

17. Grotenhuis HB, Kroft LJM, Vliegen HW, et al. Magnetic Resonance Imaging of function and flow in post-operative Congenital Heart Disease. In: Higgins C.B., de Roos A, editors. MRI and CT of the Cardiovascular System. Philadelphia, Pa: Lippincott, Williams & Wilkins. 2006: 411-428.
18. Pluim BM, Lamb HJ, Kayser HW, et al. Functional and metabolic evaluation of the athlete's heart by magnetic resonance imaging and dobutamine stress magnetic resonance spectroscopy. Circulation. 1998; 97 (7): 666-672.
19. Van Straten A, Vliegen HW, Lamb HJ, et al. Time course of diastolic and systolic function improvement after pulmonary valve replacement in adult patients with tetralogy of Fallot. J Am Coll Cardiol. 2005; 46 (8): 1559-1564.
20. Taylor AM, Dymarkowski S, Hamaekers P, et al. MR coronary angiography and late-enhancement myocardial MR in children who underwent arterial switch surgery for transposition of great arteries. Radiology. 2005; 234 (2): 542-547.
21. Yu CM, Sanderson JE, Chan S, Yeung L, Hung YT, Woo KS. Right ventricular diastolic dysfunction in heart failure. Circulation. 1996; 93 (8): 1509-1514.
22. Pepi M, Agostoni P, Marenzi G, et al. The influence of diastolic and systolic function on exercise performance in heart failure due to dilated cardiomyopathy or ischemic heart disease. Eur J Heart Fail. 1999; 1 (2): 161-167.
23. Meluzin J, Spinarova L, Hude P, et al. Prognostic importance of various echocardiographic right ventricular functional parameters in patients with symptomatic heart failure. J Am Soc Echocardiogr. 2005; 18 (5): 435-444.
24. Mandinov L, Eberli FR, Seiler C, et al. Diastolic heart failure. Cardiovasc Res. 2000; 45 (4): 813-825.
25. Singh GK, Greenberg SB, Yap YS, et al. Right ventricular function and exercise performance late after primary repair of tetralogy of Fallot with the transannular patch in infancy. Am J Cardiol. 1998; 81 (11): 1378-1382.

Heynric B. Grotenhuis
Jaap Ottenkamp
Liesbeth de Bruijn
Jos J.M. Westenberg
Hubert W. Vliegen
Lucia J.M. Kroft
Albert de Roos

# chapter 07

**Aortic Elasticity and Size are associated with Aortic Regurgitation and Left Ventricular Dysfunction in Tetralogy of Fallot after Pulmonary Valve Replacement.**

Heart. Accepted for publication.

## Abstract

**Purpose:** Aortic wall pathology and concomitant aortic dilatation have been described in tetralogy of Fallot (TOF) patients, which may negatively affect aortic valve and left ventricular (LV) systolic function. In this study, aortic dimensions, aortic elasticity, aortic valve competence and biventricular function were assessed in repaired TOF patients after pulmonary valve replacement (PVR) by using magnetic resonance imaging (MRI).

**Materials and Methods:** MRI was performed in 16 patients with TOF after PVR (10 male; mean age ± standard deviation: 31 years ± 15) and 16 age- and gender matched healthy subjects.

**Results:** TOF patients showed aortic root dilatation (mean difference 7.8 - 8.8 mm, $P < 0.01$ at all 4 predefined levels) and reduced aortic elasticity (pulse wave velocity in aortic arch: 5.5 m/s ± 1.2 vs 4.6 m/s ± 0.9, $P = 0.04$; aortic root distensibility: $1.4*10^{-3}$ mm $Hg^{-1}$ ± 1.7 vs $5.7*10^{-3}$ mm $Hg^{-1}$ ± 3.6, $P < 0.01$). Minor degrees of aortic regurgitation (AR) (AR fraction 6% ± 8 vs 1% ± 1, $P < 0.01$) and reduced LV ejection fraction were present (51% ± 8 vs 58% ± 6, $P = 0.01$), whereas right ventricular (RV) ejection fraction was within normal limits (47% ± 8 vs 52% ± 7, $P = 0.06$). Degree of AR fraction was associated with dilatation of the aortic root ($r = 0.39$ - $0.49$, $P < 0.05$) and reduced aortic root distensibility ($r = 0.44$, $P = 0.02$), while reduced LV ejection fraction was correlated with degree of AR and RV ejection fraction ($r = 0.41$, $P = 0.02$, and $r = 0.49$, $P < 0.01$, respectively).

**Conclusion:** Aortic root dilatation and reduced aortic elasticity are frequently present in patients with TOF, in addition to minor degrees of AR and reduced LV systolic function. Aortic wall pathology in repaired TOF patients may therefore represent a separate mechanism leading to LV dysfunction, in addition to adverse right-to-left ventricular interaction.

## Introduction

Aortic root dilatation frequently occurs in tetralogy of Fallot (TOF) patients, ranging in incidence between 15% and 88% depending on the definition (1-5). Aortic root dilatation may lead to serious complications such as aortic regurgitation, aneurysm formation and even aortic dissection, necessitating aortic valve and aortic root surgery (3,5,6). Therefore, meticulous non-invasive follow-up of the aorta is clinically highly desirable (2,3,5,6).

Recent reports indicate that aortic dilatation and concomitant reduced aortic elasticity may have a negative effect on aortic valve function, by loss of central coaptation and increased stress on the aortic valve leaflets during opening and closing, respectively (7-14). Reduced aortic elasticity is also associated with LV dysfunction and impaired coronary blood flow (15,16). Aortic wall pathology in repaired TOF patients may therefore represent a separate mechanism leading to LV dysfunction, in addition to possible adverse right-to-left ventricular interaction (17-19).

Distensibility and pulse wave velocity (PWV) in the aorta have been shown to be markers of aortic vessel wall condition, since they are mainly due to the elastic properties of the aorta (15,20,21), for which magnetic resonance imaging (MRI) has been established as an accurate non-invasive imaging tool (7,8,22). In addition, MRI is a reliable and accurate method for assessment of aortic dimensions, aortic valve competence and biventricular function (19,23,24).

We hypothesized that aortic root dilatation in patients after repair of TOF can be attributed to aortic wall pathology, as measured by abnormal aortic distensibility and PWV, and that abnormal aortic elastic properties may negatively affect aortic valve and LV systolic function. In our study we examined TOF patients after pulmonary valve replacement (PVR), to minimize the possible confounding effect of adverse right-to-left ventricular interaction due to pulmonary regurgitation (PR) (17-19). Accordingly, the purpose of the current study was to prospectively assess aortic dimensions, aortic elasticity, aortic valve competence and biventricular systolic function in repaired TOF patients after PVR by using MRI.

## Materials and Methods

### Patients

The local medical ethics committee approved the study and informed consent was obtained from all participants prior to enrollment in the study.

Sixteen patients with TOF and 16 age- and gender matched healthy subjects were prospectively studied with MRI at our institution. All TOF patients (10 male, 6 female; mean age ± standard deviation: 31 years ± 15) were recruited from our local congenital heart disease database. Inclusion criteria consisted of diagnosis of TOF, previous history of PVR, willingness to comply with the study procedures and written informed consent. Exclusion criteria comprised of evidence of aortic valve stenosis (aortic velocity > 2.5m/s on echocardiography)

(25), pulmonary regurgitation exceeding 10% (1 patient), aortic coarctation and/or other forms of congenital heart disease than TOF, Marfan syndrome or a family history of Marfan syndrome, usage of medication such as beta-blockers and general contraindications to MRI.

Age- and gender-matched healthy subjects were selected from our local database of healthy subjects. Characteristics and functional status as expressed as New York Heart Association class of the patients and healthy subjects were obtained from the patient records (Table 1).

Table 1: Characteristics of tetralogy of Fallot patients and healthy subjects

| Characteristics | patients (n = 16) | healthy subjects (n = 16) |
|---|---|---|
| male / female | 10 / 6 | 10 / 6 |
| age at MRI (years) * | 31 ± 15 | 31 ± 16 |
| height (cm) * | 172 ± 10 | 179 ± 10 |
| weight (kg) * | 70 ± 14 | 73 ± 16 |
| body surface area ($m^2$) * and † | 1.7 ± 0.2 | 1.9 ± 0.4 |
| blood pressure systolic (mm Hg) * | 118 ± 14 | 121 ± 13 |
| blood pressure diastolic (mm Hg) * | 72 ± 7 | 73 ± 12 |
| cardiac frequency (beats per minute) * | 65 ± 8 | 67 ± 9 |
| New York Heart Association class I / II | 15 / 1 | 16 / 0 |
| age at shunt procedure, median (years) | 1.2 (0.8 to 2.4) | |
| age at initial TOF repair, median (years) | 2.1 (1.8 to 3.0) | |
| age at PVR, median (years) | 27 (23 to 35) | |
| interval surgery - PVR (years) * | 24 ± 4 | |
| interval PVR - MRI (years) * | 4 ± 4 | |

* Data are expressed as mean ± standard deviation.
† According to the formula: √ (height (cm) × weight (kg) / 3600).
Abbreviations: MRI = magnetic resonance imaging; TOF = tetralogy of Fallot; PVR = pulmonary valve replacement.

**Surgical technique**

Initial repair was performed in TOF patients with a transatrial-transpulmonary approach, using cardiopulmonary bypass and moderate hypothermia. A transannular patch was used in 10 patients. Fourteen patients had previously undergone Blalock-Taussig shunt insertion and 1 patient had received a Potts shunt prior to initial repair.

Pulmonary valve replacement in all TOF patients was performed using cryopreserved pulmonary homografts. Homografts were inserted in the orthotopic pulmonary position with maximal resection of the RV outflow tract patch material.

**MRI**

MRI was performed with a 1.5-T system (NT 15 Gyroscan Intera; Philips Medical Systems, The Netherlands) by one researcher (with 4 years experience in cardiac MRI). Imaging sequences were previously described (7,8).

Aortic root dimensions were assessed by acquisition of double-oblique transverse images perpendicular to the aorta, at the levels of the annulus of the aortic valve, the sinus of Valsalva, the sinotubular junction and the ascending aorta; the latter at the level of the crossing of the right pulmonary artery (7,8).

Aortic distensibility was measured at the level of the sinotubular junction (7,8). Distensibility (mm $Hg^{-1}$) is defined as: $(A_{max} - A_{min}) / (A_{min} \times (P_{max} - P_{min}))$, with $A_{max}$ and $A_{min}$ the maximal and minimal lumen areas ($mm^2$) of the sinotubular junction, and $P_{max}$ and $P_{min}$ the systolic and diastolic blood pressures (mm Hg) (7,8). The minimal lumen area was obtained during the iso-volumetric contraction phase (just before the beginning of the systolic upslope) and the maximal lumen area was obtained at the peak of aortic flow passing through the ascending aorta (7,8). Simultaneous blood pressure measurements were non-invasively obtained using a semiautomatic MRI-compatible sphygmomanometer (Invivo Research, USA) (26).

A velocity-encoded MRI sequence was performed just distal to the aortic valve for timing of the acquisition of the cross-sectional minimal and maximal area measurements and for determination of aortic valve regurgitation (AR fraction). AR fraction was calculated with the following formula: regurgitant volume / systolic forward volume × 100%, where volume is measured in milliliters. A similar flow sequence was used for assessment of pulmonary valve regurgitation (PR), with a through-plane velocity encoded of up to 150 cm/s (27).

PWV of the aorta was measured between the ascending and proximal descending aorta, and between the proximal descending aorta and the abdominal aorta just proximal to the bifurcation (8). A transverse velocity-encoded MRI sequence was applied at the level of the pulmonary trunk to measure through-plane flow in the ascending aorta and proximal descending aorta, while a second slice was prescribed in the abdominal aorta just proximal to the bifurcation (8). PWV was calculated as $\Delta x/\Delta t$ (expressed in m/s), where $\Delta x$ is the aortic path length between the measurement sites and $\Delta t$ is the transit time between the arrival of the systolic wave front at these sites (8).

Systolic biventricular function was assessed with a steady-state free-precession cine sequence in the short-axis plane by using breath holds. A total of 12 consecutive slices were obtained (40 phases per cardiac cycle) without slice gap (28).

**Postprocessing**

Diameter- and distensibility measurements of the aortic root, as well as systolic biventricular function images were analyzed with the software package MASS (Medis, The Netherlands) (28). The following parameters were determined for both ventricles: end-diastolic volume (EDV), end-systolic volume (ESV), stroke volume (SV), ejection fraction (EF); and LV mass (7,8,28). Indexation

was performed according to the Mosteller formula (BSA = √ (height (cm) × weight (kg) / 3600)), where BSA is the body surface area in square meters (7,28).

Flow velocity-encoded MRI data were analyzed with the software package FLOW (Medis, The Netherlands) (29). Flow curves were obtained with this method for aortic flow and pulmonary flow during the cardiac cycle.

The manual drawing of all MRI contours and analysis of the other results was performed by one researcher (with 4 years experience in cardiac MRI), which was subsequently checked by a radiologist (with 10 years experience in cardiac MRI), who was unaware of the clinical condition of the examined TOF patients.

**Statistical analysis**

Statistical analysis was performed using software (SPSS for Windows, version 12.0.1; SPSS, USA). All data are presented as mean values ± standard deviation, unless stated otherwise. Two-tailed Mann-Whitney U test was used to express differences between the patient and healthy subjects. Correlation between variables was expressed with Spearman rank correlation coefficient. Statistical significance was indicated by a P value of less that 0.05.

## Results

Results of the TOF patients and healthy subjects are summarized in Table 2.

**Aortic dimensions and elasticity**

Diameters of the aortic root at all 4 levels were significantly increased in TOF patients as compared to the healthy subjects ($P < 0.01$ for all). Dilatation was most pronounced at the level of the sinus of Valsalva, with a decrease in mean difference towards the level of the ascending aorta (Figures 1 and 2). Elasticity of the proximal aorta was found to be reduced in TOF patients, as PWV in the aortic arch was significantly increased and distensibility at the level of the sinotubular junction was significantly reduced. PWV in the descending aorta was relatively normal. Dilatation at all levels of the aortic root was significantly correlated with reduced distensibility of the aortic root ($r = 0.66 - 0.72$, $P < 0.01$ for all).

Figure 1. Aortic dilatation.

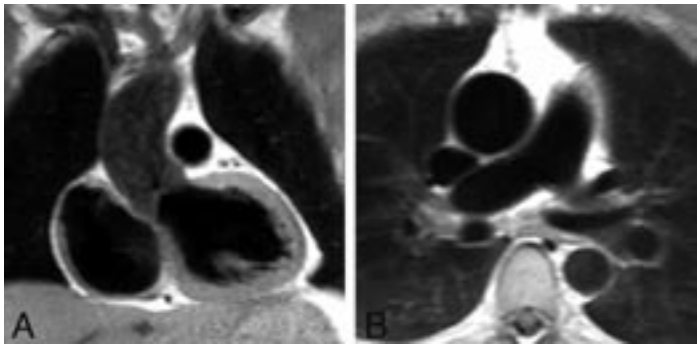


**Figure 1 a-b.** Coronal **(a)** and transverse **(b)** black-blood turbo spin-echo MRI images of the ascending aorta in a 46-year old male with repaired tetralogy of Fallot, showing a dilated ascending aorta with a maximum diameter of 4.2 cm.

Figure 2. Aortic insufficiency.

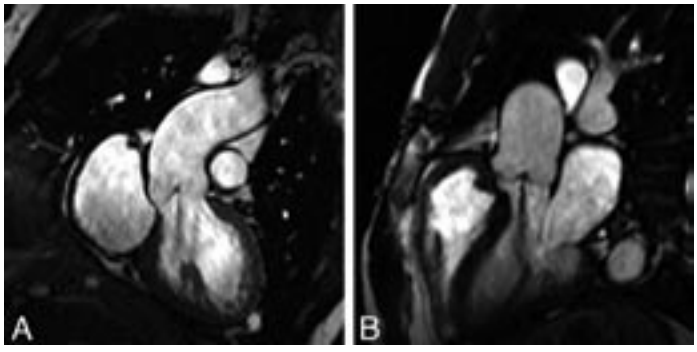


**Figure 2 a-b.** Oblique coronal **(a)** and sagittal **(b)** gradient-echo images of the ascending aorta in the same 46-year old male with repaired tetralogy of Fallot, showing a dilated ascending aorta and central aortic valve regurgitation.

### Aortic and pulmonary valve competence

In 7 of 16 TOF patients minor degrees of AR were found, with AR fraction ranging between 5% and 12% (Figure 2). In none of the healthy subjects AR fraction exceeded 5%. Dilatation and reduced elasticity of the aortic root were associated with the degree of AR, as aortic root dilatation (r ranging 0.39 - 0.49, $P \leq 0.04$ for all 4 levels) and reduced distensibility of the aortic root ($r = 0.44$, $P = 0.01$) were all correlated with degree of AR fraction. Minor degrees of PR were present in 4 patients, with PR fraction ranging between 6% and 10%.

**LV and RV function**

Systolic LV function - expressed by LV EF - was found to be significantly decreased in patients after TOF as compared to the healthy subjects, whereas RV ejection fraction was within normal limits. Reduced LV ejection fraction was correlated with degree of AR and RV ejection fraction ($r = 0.41$, $P = 0.02$, and $r = 0.49$, $P < 0.01$, respectively). LV and RV dimensions (EDV and ESV) were within normal limits in the TOF patient group, although RV ESV of the TOF patient group was significantly larger as compared to the healthy subjects. Mean LV mass was normal in the patient group as compared to the healthy subjects.

Table 2: Results of tetralogy of Fallot patients and healthy subjects.

| Parameters | patients | healthy subjects | P value | mean difference |
|---|---|---|---|---|
| diameter annulus (mm) | 36.0 ± 4.6 | 27.2 ± 3.2 | < 0.01 | 8.8 |
| diameter sinus of Valsalva (mm) | 39.3 ± 5.4 | 30.4 ± 3.1 | < 0.01 | 8.8 |
| diameter sinotubular junction (mm) | 35.9 ± 4.9 | 27.7 ± 3.6 | < 0.01 | 8.2 |
| diameter ascending aorta (mm) | 33.6 ± 5.6 | 25.8 ± 3.8 | < 0.01 | 7.8 |
| distensibility at STJ (in $10^{-3}$ mm $Hg^{-1}$) | 1.4 ± 1.7 | 5.7 ± 3.6 | < 0.01 | |
| PWV aortic arch (m/s) | 5.5 ± 1.2 | 4.6 ± 0.9 | 0.04 | |
| PWV descending aorta (m/s) | 4.9 ± 1.9 | 4.5 ± 1.1 | 0.48 | |
| aortic regurgitation fraction (%) | 6 ± 8 | 1 ± 1 | < 0.01 | |
| LV EF (%) | 51 ± 8 | 58 ± 6 | < 0.01 | |
| LV EDV ($m/m^2$) * | 99 ± 25 | 98 ± 29 | 0.87 | |
| LV ESV ($m/m^2$) * | 47 ± 15 | 41 ± 14 | 0.28 | |
| LV SV ($m/m^2$) * | 53 ± 15 | 57 ± 18 | 0.51 | |
| LV mass ($g/m^2$) * | 55 ± 16 | 51 ± 15 | 0.46 | |
| pulmonary regurgitation fraction (%) | 4 ± 4 | 2 ± 2 | < 0.01 | |
| RV EF (%) | 47 ± 8 | 52 ± 7 | 0.06 | |
| RV EDV ($ml/m^2$) * | 117 ± 36 | 101 ± 28 | 0.17 | |
| RV ESV ($ml/m^2$) * | 63 ± 25 | 48 ± 13 | 0.04 | |

Note: data are expressed as mean ± standard deviation.

* indexed for body surface area, according to the formula: $\sqrt{}$ (height (cm) × weight (kg) / 3600).

Abbreviations: STJ = sinotubular junction; PWV = pulse wave velocity; LV = left ventricle; EF = ejection fraction; EDV = end-diastolic volume indexed for body surface area; ESV = end-systolic volume indexed for body surface area; SV = stroke volume indexed for body surface area; RV = right ventricle.

## Discussion

The main findings of our study are: 1. patients after TOF repair show aortic root dilatation and reduced elasticity of the proximal aorta; 2. aortic root dilatation and reduced elasticity of the proximal aorta are associated with minor degrees of aortic regurgitation; 3. reduced LV systolic function is present in TOF patients clinically doing well after pulmonary valve replacement, and is associated with the degree of aortic regurgitation and RV ejection fraction.

**Aortic dimensions**

Significant dilatation of the aortic root was present in our patient group with repaired TOF, being most pronounced at the levels of the annulus and the sinus of Valsalva. Increased blood flow from both ventricles to the overriding aorta before surgical repair may pose increased stress on the aortic wall, which may lead to aortic root dilatation (1,3,5,6). In addition, histological changes of the aortic media have been reported resembling those observed in Marfan syndrome (5,6,30). Strong correlation between histological aortic wall changes and the ascending aortic circumference suggests a causative mechanism for subsequent aortic root dilatation (5). Whether aortic wall pathology results from an intrinsic medial abnormality inherent to TOF itself, is secondary to the antecedent volume load through the aorta before TOF repair, or perhaps a combination of the two, remains however difficult to distinguish (1,3,5,6).

Aortic dilatation has been reported to be progressive in TOF patients with aortic dilatation, with an increase of aortic dilatation at a rate of 1.7 mm/year, in contrast to 0.03 mm/year in a control TOF patient group without aortic dilatation (1). Of even greater concern are recent case reports of aortic dissection late after repair of TOF in two adults whose aortic roots exceeded 6.0 cm in diameter (31,32). Close monitoring of aortic dimensions is therefore mandatory during follow-up - especially when a dilated ascending aorta is present - although clear guidelines for an exact timeframe of follow-up are not available (1,32). Evaluation of aortic dilatation may be performed every 6 months to determine the rate of progression, which can be extended to annual evaluation when the aortic size is stable over time, analogue to patients with Marfan syndrome (33). As MRI is already a well-accepted imaging modality for follow-up of RV function in TOF patients, assessment of aortic and LV parameters may be included in the imaging protocol. Aortic root surgery may be considered for patients with repaired TOF in case of progressive AR and aortic root dilatation exceeding 5.5 cm, particularly when the primary indication for surgery is PVR (1). At present, there is no clear consensus to our knowledge on beta-blocker administration for prevention of progressive dilatation of the aortic root in repaired TOF patients such as in patients with Marfan syndrome, nor at what stage aortic root surgery should be performed (1).

**Aortic elasticity**

Reduced elasticity of the proximal aorta in our patient group indicated that TOF is not only associated with aortic dilatation (1,3,5), but also with reduced aortic elasticity. In Marfan syndrome and bicuspid aortic valve disease, increased aortic stiffness has been reported due to fragmentation of elastic wall components (26). Considering the many histological similarities between these entities and TOF (6), aortic wall abnormalities in TOF patients may be responsible for reduced aortic elasticity as well (1,3,5,6,30). Our patient group showed diminished elasticity of the aortic root and the aortic arch, suggesting that only the proximal part of the aorta is affected in TOF patients. In patients with Marfan syndrome, aortic stiffness has proven to be an independent predictor of progressive aortic dilatation (26). Evaluation of the elastic properties of the ascending aorta in patients with TOF might therefore be used analogously to identify patients who are at risk of progressive dilatation and other aortic sequelae.

Arterial stiffness has been shown to be a cardiovascular risk factor on its own, being associated with impaired coronary blood flow and LV dysfunction (15). In addition, a strong and independent association has been demonstrated between increased arterial stiffness and the presence of coronary artery disease (34). Senzaki et al. recently described augmented aortic wave reflections and increased aortic and peripheral arterial stiffness in a group of TOF patients, which contributes to pulsatile load on the LV and adversely affects LV ejection (30). Prognosis of patients with increased arterial stiffness in patients with TOF may therefore be worse as compared to healthy subjects, since other cardiovascular risk factors act cumulatively over a lifetime (15,34).

**Aortic valve competence**

Aortic root dilatation and decreased aortic distensibility are closely related to aortic valve function, with the potential to cause AR (7-9). Though fewer than half of our TOF patients exhibited mild degrees of AR, dilatation and reduced elasticity of the aortic root were associated with the degree of AR. Increased dimensions of the aortic annulus may lead to loss of coaptation of the aortic valve leaflets, which may subsequently result in varying degrees of central AR (2,9,10). In addition, aortic valve dynamics are related to distensibility of the aortic root. During systole, as the aortic valve opens, the aortic root should expand simultaneously (11,12). Any disturbance in this synchronized process results in increased stress on the aortic valve leaflets (12-14), which may ultimately result in degeneration of the aortic valve leaflets and consequent AR.

**LV function**

LV systolic function was significantly reduced in our TOF patients. In a recent study of Geva et al., moderate to severe LV dysfunction was the strongest independent variable associated with impaired clinical status in long-term survivors of TOF repair (19).

Despite the fact that most of our patients were identified as New York Heart Association functional class I, reduced LV ejection fraction may therefore be of negative prognostic value. LV dysfunction has been explained by adverse right-to-left ventricular interaction: longstanding PR in repaired TOF patients will lead to RV dilatation, which is associated with increased LV end-systolic volume and impaired septal contractility, having an adverse effect on LV systolic performance (17-19). In our study, TOF patients after PVR were investigated with only minor degrees of PR, to minimize the possible confounding effect of adverse right-to-left ventricular interaction.

In this study, LV systolic dysfunction was also associated with the degree of AR, which may be considered as the endpoint in a sequence of events. Increased LV mass may occur as a consequence of AR, to maintain normal LV filling pressures (9). In the case of limited AR, the increased preload will lead to a normal LV volume/mass ratio with adequate preservation of LV EF (9). When AR progresses, the concomitant increased wall stress will result in LV systolic dysfunction and reduced LV ejection fraction (9). Therefore, aortic dilatation and increased aortic stiffness due to aortic wall pathology in repaired TOF patients may have a contributive effect on the development of AR and LV dysfunction, in addition to adverse right-to-left ventricular interaction (17-19).

Our study has limitations. First, our study design is observational and therefore longitudinal follow-up studies are required to define the prognostic value of our findings. Secondly, relatively weak correlation coefficients between the investigated variables were found, so other contributive factors may play a role as well.

In conclusion, our study findings revealed frequent aortic root dilatation and reduced elasticity of the proximal aorta in patients after repair of TOF, associated with minor degrees of aortic regurgitation and reduced LV systolic function. Aortic wall pathology in repaired TOF patients may therefore represent a separate mechanism leading to LV dysfunction, in addition to adverse right-to-left ventricular interaction. Our study showed the feasibility of MRI as an integrated imaging tool to monitor aortic and LV function parameters, which may facilitate the early detection of LV dysfunction in patients after repaired TOF. Assessment of aortic and LV function parameters should be part of already routine MRI of RV function in TOF patients.

## References


1. Niwa K, Siu SC, Webb GD, et al. Progressive aortic root dilatation in adults late after repair of tetralogy of Fallot. Circulation. 2002; 106: 1374-1378.
2. Chong WY, Wong WH, Chiu CS, et al. Aortic root dilation and aortic elastic properties in children after repair of tetralogy of Fallot. Am J Cardiol. 2006; 97: 905-909.
3. Niwa K. Aortic root dilatation in tetralogy of Fallot long-term after repair-histology of the aorta in tetralogy of Fallot: evidence of intrinsic aortopathy. Int J Cardiol. 2005; 103: 117-119.
4. Cheung YF, Ou X, Wong SJ. Central and peripheral arterial stiffness in patients after surgical repair of tetralogy of Fallot: implications for aortic root dilatation. Heart. 2006; 92: 1827-1830.
5. Tan JL, Davlouros PA, McCarthy KP, et al. Intrinsic histological abnormalities of aortic root and ascending aorta in tetralogy of Fallot: evidence of causative mechanism for aortic dilatation and aortopathy. Circulation. 2005; 112: 961-968.
6. Niwa K, Perloff JK, Bhuta SM, et al. Structural abnormalities of great arterial walls in congenital heart disease: light and electron microscopic analyses. Circulation. 2001; 103: 393-400.
7. Grotenhuis HB, Westenberg JJ, Doornbos J, et al. Aortic root dysfunctioning and its effect on left ventricular function in Ross procedure patients assessed with magnetic resonance imaging. Am Heart J. 2006; 152: 975-978.
8. Grotenhuis HB, Ottenkamp J, Westenberg JJ, et al. Reduced aortic elasticity and dilatation are associated with aortic regurgitation and left ventricular hypertrophy in nonstenotic bicuspid aortic valve patients. J Am Coll Cardiol. 2007; 49: 1660-1665.
9. Bekeredjian R, Grayburn PA. Valvular heart disease: aortic regurgitation. Circulation. 2005; 112: 125-134.
10. Thubrikar MJ, Labrosse MR, Zehr KJ, et al. Aortic root dilatation may alter the dimensions of the valve leaflets. Eur J Cardiothorac Surg. 2005; 28: 850-855.
11. Thubrikar MJ, Heckman JL, Nolan SP. High speed cine-radiographic study of aortic valve leaflet motion. J Heart Valve Dis. 1993; 2: 653-661.
12. Schmidtke C, Bechtel J, Hueppe M, et al. Size and distensibility of the aortic root and aortic valve function after different techniques of the Ross procedure. J Thorac Cardiovasc Surg. 2000; 119: 990-997.
13. Thubrikar MJ, Nolan SP, Aouad J, et al. Stress sharing between the sinus and leaflets of canine aortic valve. Ann Thorac Surg. 1986; 42: 434-440.
14. Thubrikar M, Skinner JR, Aouad J, et al. Analysis of the design and dynamics of aortic bioprostheses in vivo. J Thorac Cardiovasc Surg. 1982; 84: 282-290.
15. Cruickshank K, Riste L, Anderson SG, et al. Aortic pulse-wave velocity and its relationship to mortality in diabetes and glucose intolerance: an integrated index of vascular function? Circulation. 2002; 106: 2085-2090.
16. Mandinov L, Eberli FR, Seiler C, et al. Diastolic heart failure. Cardiovasc Res. 2000; 45: 813-25.
17. Niezen RA, Helbing WA, van der Wall EE, et al. Biventricular systolic function and mass studied with MR imaging in children with pulmonary regurgitation after repair for tetralogy of Fallot. Radiology. 1996; 201: 135-140.

18. Davlouros PA, Kilner PJ, Hornung TS, et al. Right ventricular function in adults with repaired tetralogy of Fallot assessed with cardiovascular magnetic resonance imaging: detrimental role of right ventricular outflow aneurysms or akinesia and adverse right-to-left ventricular interaction. J Am Coll Cardiol. 2002; 40: 2044-2052.
19. Geva T, Sandweiss BM, Gauvreau K, et al. Factors associated with impaired clinical status in long-term survivors of tetralogy of Fallot repair evaluated by magnetic resonance imaging. J Am Coll Cardiol. 2004; 43: 1068-1074.
20. Wilton E, Jahangiri M. Post-stenotic aortic dilatation. J Cardiothorac Surg. 2006; 1: 7-18.
21. Rogers WJ, Hu YL, Coast D, et al. Age-associated changes in regional aortic pulse wave velocity. J Am Coll Cardiol. 2001; 38: 1123-1129.
22. Groenink M, de Roos A, Mulder BJ, et al. Changes in aortic distensibility and pulse wave velocity assessed with magnetic resonance imaging following beta-blocker therapy in the Marfan syndrome. Am J Cardiol. 1998; 82: 203-208.
23. Constantine G, Shan K, Flamm SD, et al. Role of MRI in clinical cardiology. Lancet. 2004; 363: 2162-2171.
24. Melina G, Rajappan K, Amrani M, et al. Aortic distensibility after aortic root replacement assessed with cardiovascular magnetic resonance. J Heart Valve Dis. 2002; 11: 67-74.
25. Otto CM, Lind BK, Kitzman DW, et al. Association of aortic-valve sclerosis with cardiovascular mortality and morbidity in the elderly. N Engl J Med. 1999; 341: 142-147.
26. Nollen GJ, Groenink M, Tijssen JG, et al. Aortic stiffness and diameter predict progressive aortic dilatation in patients with Marfan syndrome. Eur Heart J. 2004; 25: 1146-1152.
27. Van Straten A, Vliegen HW, Lamb HJ, et al. Time course of diastolic and systolic function improvement after pulmonary valve replacement in adult patients with tetralogy of Fallot. J Am Coll Cardiol. 2005; 46: 1559-1564.
28. van der Geest RJ, Reiber JH. Quantification in cardiac MRI. J Magn Reson Imaging. 1999; 10: 602-608.
29. van der Geest RJ, Niezen RA, van der Wall EE, et al. Automated measurement of volume flow in the ascending aorta using MR velocity maps: evaluation of inter- and intraobserver variability in healthy volunteers. J Comput Assist Tomogr. 1998; 22: 904-911.
30. Senzaki H, Iwamoto Y, Ishido H, et al. Arterial Hemodynamics in Patients after Repair of tetralogy of Fallot: Influence on Left Ventricular Afterload and Aortic Dilation. Heart. 2008; 94: 70-74.
31. Kim WH, Seo JW, Kim SJ, et al. Aortic dissection late after repair of tetralogy of Fallot. Int J Cardiol. 2005; 101: 515-516.
32. Rathi VK, Doyle M, Williams RB, et al. Massive aortic aneurysm and dissection in repaired tetralogy of Fallot, diagnosis by cardiovascular magnetic resonance imaging. Int J Cardiol. 2005; 101: 169-170.
33. Milewicz DM, Dietz HC, Miller DC. Treatment of aortic disease in patients with Marfan syndrome. Circulation. 2005; 111: 150-157.
34. Arnett DK, Evans GW, Riley WA. Arterial stiffness: a new cardiovascular risk factor? Am J Epidemiol. 1994; 140: 669-682.

Mark G. Hazekamp
Heynric B. Grotenhuis
Paul H. Schoof
Marry E. Rijlaarsdam
Jaap Ottenkamp
Robert A.E. Dion

# chapter 08

**Results of the Ross operation in a Paediatric Population.**
Eur J Cardiothorac Surg. 2005; 27 (6): 975-979.

## Abstract

**Purpose**: To analyse the results of the mid-term clinical and echocardiographic follow-up of the pediatric Ross operation.

**Materials and Methods**: Echo-Doppler follow-up of 53 consecutive pediatric Ross procedures was performed between 1994 and 2003. Median age was 9.7 years at time of operation (2 weeks - 17.7 years). Six patients were younger than 3 months. Median age at follow-up was 15.6 years. Aortic valve/left ventricular outflow tract (LVOT) anomalies were congenital in 49 (92%). Seventy percent had previous surgery or balloon valvuloplasty. Root replacement was used in all. Thirteen patients (25%) had LVOT enlargement. Mean cross-clamp time was 113 (69 - 189) minutes.

**Results**: Early mortality occurred in 3 patients after emergency surgery following balloon failure (n = 1) and extended Ross following interrupted arch / VSD repair (n = 2). Late mortality was due to LV fibroelastosis in 2 patients and complicated pulmonary artery stenting in another. RVOT reoperations were required because of late homograft obstruction in 2 patients and because of pulmonary artery stenosis in another. Five patients (9.4%) were reoperated for pulmonary autograft dilatation (n = 3) and for leaflet fibrosis or perforation (n = 2). Autografts were repaired in two patients, while a mechanical valve was inserted in 3 cases. At 9 years the actuarial survival and event free survival were 89% and 74%, respectively. At last follow-up 90% of autograft diameters indexed to body surface area was above the 90th percentile of normal aortic root diameters. LVOT and RVOT gradients were low and autograft insufficiency was trivial to mild in 84% and mild to moderate in 16%. Autograft stenosis was not noticed.

**Conclusion**: The pediatric Ross procedure remains an important tool but autograft dilatation also occurs in the pediatric population. The significance of this finding has yet to be determined.

## Introduction

The use of the pulmonary autograft was first reported in 1967 by Ross for the treatment of aortic valve disease in adults (1). Since that time, the Ross procedure has been increasingly applied to the pediatric population, including neonates and infants (2-6). Several advantages of the pulmonary autograft are of benefit for both the adult and pediatric patient group: the high rates of freedom of reoperation and the lack of need for anticoagulation (2-6). Especially for the pediatric population there are additional beneficial effects, like the potential for growth of the autograft and the ready availability of an inherently proper sized pulmonary autograft (2,3,5-9). However, pulmonary autograft growth and dilatation cannot be easily distinguished from each other and several reports indicate that both dilatation and growth occur in the growing subject (10). Despite conflicting reports about autograft dilatation causing aortic insufficiency, excess dilatation necessitating reoperation is one of the main concerns following the Ross operation (3-8).

We have reviewed our consecutive Ross operations in all patients younger than 18 year with an emphasis on maximal pulmonary autograft diameters in relation to body surface. Part of our experience has been described previously (11).

## Material and methods

### Patient population

From February 1994 to March 2003, 53 consecutive Ross procedures have been performed in patients younger than 18 years in our institution. The preoperative indication for the Ross procedure was aortic stenosis (AS) in 12 patients (23%), aortic regurgitation (AR) in 14 patients (26%) and a combination in 27 patients (51%). The underlying left ventricular outflow tract (LVOT) pathology was congenital in 48 patients (90%) while 3 patients had a pulmonary autograft procedure as a consequence of rheumatic heart disease and 2 following endocarditis of the aortic valve (AV). Bicuspid aortic valve was present in 64% of all cases. Median age at operation was 9.7 years (range: 2 weeks - 17. 7 years), with a mean age of 9.15 ± 5.07 years. Six patients were operated at an age of 3 months or less. Forty-six patients were male (87%).

Thirty-seven patients (70%) had undergone surgery or percutaneous intervention(s) prior to the Ross procedure (Table 1). Of this group 11 patients (20%) had undergone more than one procedure prior to the pulmonary autograft procedure.

Informed consent was obtained from all included patients, with approval of the institutional ethics committee.

Table 1. Previous interventions.

| Intervention | number |
|---|---|
| Balloon dilatation | 11 |
| Aortic valvotomy | 15 |
| Resection subaortic stenosis | 13 |
| Aortic valve repair | 3 |
| VSD closure | 8 |
| Coarctation or interrupted arch repair | 9 |
| Arterial switch operation | 1 |

**Operative technique**

In all patients the pulmonary autograft was implanted using the root replacement technique. Reinforcement of proximal and distal suture lines with a strip of autologous pericardium was used in most patients. Continuous sutures were used in all. In all cases cardiopulmonary bypass with moderate hypothermia was used. Autograft harvesting was usually performed after aortic cross-clamping and antegrade administration of St Thomas cardioplegic solution. The mean cross-clamp time was 113 min (range: 69 - 189 min). Right ventricular outflow tract (RVOT) reconstruction was performed with cryopreserved pulmonary homografts (n = 47; mean diameter 22 mm), cryopreserved aortic homografts (n = 3; mean diameter 15 mm) or Contegra bovine jugular vein grafts (Medtronic Inc., USA) (n = 3; mean diameter 15 mm). The distal RVOT suture line was usually done during myocardial arrest while the proximal suture lines were performed on beating heart.

In 13 patients (25%) the aortic annular or LVOT diameter was considered as being too small and annular enlargement was performed in association with septal muscle myectomy and/or resection of subaortic fibrous tissue. In 3 of these 13 patients the LVOT was further enlarged by septal patch insertion (Ross-Konno procedure).

Associated procedures during the Ross operation were enucleation or resection of a discrete subaortic stenosis in 8 patients, ventricular septal defect (VSD) closure in 2 patients and mitral valve replacement in 1 patient. One patient with a VSD and aortic insufficiency repaired has previously been described elsewhere (12).

### Follow-up

Follow-up was performed by analysis of operative reports, patient records and echo-Doppler studies at last follow-up. Body weight and height data at the time of last follow-up were collected and used to determine body surface area (BSA expressed in $m^2$). The maximal diameter of the pulmonary autograft at sinus of Valsalva (SOV) level obtained by echocardiography was noted at the same last visit. Maximal autograft diameters were indexed for BSA and compared to normal values for aortic SOV diameters in relation to body surface area and age, as indexed by Roman (13). The degrees of pulmonary autograft and RVOT conduit insufficiency were indexed as being trivial, mild, moderate or severe. Gradients over the LVOT and RVOT were expressed in maximal Doppler gradients (mm Hg).

Of the 47 surviving patients 5 were lost to follow-up. Four of these patients came from non-European countries. With the exception of these 5 patients, recent follow-up data were available in all other patients.

### Statistical analysis

Statistical analysis was performed with the use of SPSS-11. Descriptive statistics are expressed as median and range. Means are provided with standard deviations. Unpaired student t-test was used for comparison of unpaired data. $P < 0.05$ was considered to indicate statistically significant difference. The Kaplan-Meyer method was used to determine event-free survival curves.

## Results

### Postoperative complications

In the postoperative period 5 patients required a resternotomy for bleeding, while late pericardial effusions needed drainage in 3 patients. Complete heart block requiring pacemaker implantation occurred in 2 patients.

### Early mortality

Early mortality occurred in 3 patients (5.6%) at the age of 1, 2 and 4 months. One neonate with critical valvular AS developed massive AR directly after balloon dilatation and underwent a Ross procedure on an emergency basis. This patient died in the intensive care unit as a result of multiple organ failure. Two other infants had been referred with LVOT obstruction following previous repair of interrupted aortic arch and VSD, 1 and 3 months before the Ross operation. One of them died as a result of preoperative poor left ventricular (LV) function. The other patient developed myocardial ischemia related to the coronary artery reimplantation and died early.

**Late mortality**

Three patients died 13 months, 5 and 6 years after the Ross operation (5.6%). One patient with valvular AS received a Ross procedure at the age of 2.5 months following a failed attempt of balloon dilatation. Severe pulmonary hypertension persisted after surgery and this patient died 13 months later. A second patient received a Ross procedure at the age of 7 years but suddenly died at 5 years of follow-up. Pulmonary hypertension had been diagnosed in this patient several years postoperatively. In these 2 patients autopsy showed severe LV endocardial fibroelastosis. LV dimensions were within normal limits at the time of the Ross procedure. A third patient had a Ross operation at the age of 16 years. Pulmonary artery patch augmentation was performed after one year to relief distal RVOT homograft stenosis. Complications of stent placement for recurrent RVOT obstruction subsequently led to mortality 6 years after the Ross procedure.

**Reoperation**

A total of 8 patients required reoperation. Five patients (9.4%) were reoperated for insufficiency and/or dilatation of the pulmonary autograft. Two patients were reoperated for valvular failure of the pulmonary autograft. One patient presented with a valvular insufficiency 3 years after the Ross procedure: at reoperation a delineated perforation near the hinge of the right coronary autograft cusp was observed and subsequently repaired with an autologous pericardial patch. A second patient returned with fibrosis and shortening of one of the autograft leaflets 2 years after the Ross procedure. In this patient who had undergone an arterial switch operation in the past, an insufficient aortic valve had been replaced by the pulmonary autograft that in fact was the aortic valve before the arterial switch operation (14). At reoperation the autograft was replaced by a mechanical prosthesis.

Autograft dilatation with mild to severe AR led to reoperation in 3 patients. Maximal autograft diameter (at sinus Valsalva level) was 63 mm in one patient. This patient underwent a Bentall procedure with insertion of a mechanical valve prosthesis. Mechanical valve replacement was performed in a second patient and valve sparing root remodelling was done in the third patient. The age at the time of the Ross procedure had been 5.5, 3 and 6 years, respectively.

Three patients were reoperated for right-sided homograft obstruction. Two homografts were replaced 5 and 8 years after the Ross operation (Ross performed at the age of 1 month and 4.8 years, respectively). In a third patient distal homograft obstruction required patch enlargement 1 year after the Ross procedure.

**Midterm survival**

Kaplan-Meyer analysis showed a survival and event free survival rate of 89 and 74% at 9 years of follow-up, respectively (Figure 1).

Figure 1. Survival and event free survival**.**

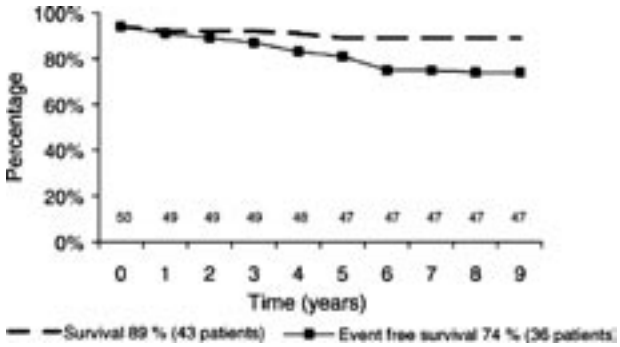


**Functional status**

The mean follow-up was 5.5 years (range: 0.9 - 8.2 years). At last follow-up all survivors were in New York Heart Association class I, without using medication.

**Autograft function**

Maximal autograft diameters (at sinus level) were indexed to body surface area ($m^2$) and compared to normal values for aortic root diameters in infants, children and young adults (Figure 2). At last follow-up 90% of autograft diameters indexed to body surface area was above the 90th percentile of normal aortic root diameters. Median diameter was 37 mm (range: 22 - 45 mm). Bicuspid aortic valve vs tricuspid valve showed no significant difference for risk of developing aortic root dilatation (P = 0.218).

Figure 2. Autograft diameter vs body surface area.

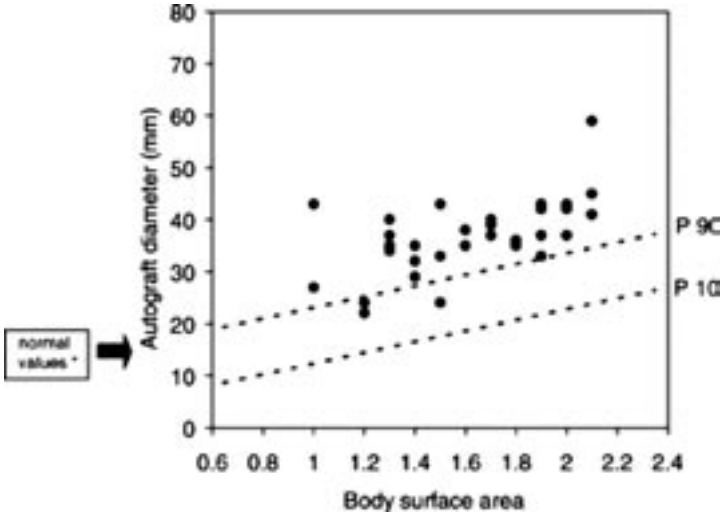

In all patients mean LVOT gradients were less than 5 mm Hg, including all patients with an extended Ross or Ross-Konno procedure. Moderate pulmonary autograft insufficiency at last follow-up was observed in 6 patients (11%), while 17 patients had mild autograft regurgitation.

**Homograft function**

RVOT obstruction was rare in our patients; in only 3 cases a moderate degree of stenosis was noticed, with a maximum Doppler RVOT gradient ranging between 37 and 45 mm Hg. Mean maximal RVOT gradient of the entire population was 23 mm Hg, ranging between 7 and 45 mm Hg. Moderate homograft insufficiency was observed in only 4 patients, while 13 patients had only trivial to mild homograft regurgitation.

## Discussion

In the pediatric group aortic valvular disease can frequently be treated without the need for valve replacement. Balloon dilatation, open commissurotomy, cusp shaving as well as repair procedures for insufficient valves are the first choice. Subaortic obstruction is also frequently amenable to resection of fibrous or muscular tissue. Valve replacement may be postponed for years in this way. Seventy percent of our patients had undergone one or more procedures prior to their Ross operation (Table 1) leading in this series to a mean age of 9.15 years at the time of the autograft procedure.

When aortic valve replacement in children can no longer be postponed, replacement with the pulmonary autograft has important advantages. The use of anticoagulants can be avoided as well as the occurrence of early failure as observed with homografts in children. Above all the autograft increases in size commensurate with body growth (10). Therefore, the pulmonary autograft is superior to any other available aortic valve substitute for the growing child.

Alternative surgical options to the Ross procedure should however, always be considered. Mechanical valves can be used in older children if a size of 21 mm or larger can be inserted. Severe LVOT obstruction can be repaired sometimes without the need for aortic valve replacement. However, in our series aortic valve pathology or hypoplastic annulus was present in all Ross-Konno patients.

During our 10-year experience we came across some additional technical benefits of the Ross procedure. Enlargement of annulus or septum which is often required in congenital aortic valve disease, is easily accomplished when the root is removed and may be accomplished without the insertion of patch material, using the extended muscular rim of the autograft. Moreover, any associated subaortic VSD can be addressed in a similar fashion by using the muscular rim of the autograft to make an extended inflow anastomosis including the VSD (12). In tunnel-form LVOT obstruction incision of the muscular septum

and subsequent enlargement with patch material (Ross-Konno procedure) will provide a satisfactory solution in almost all cases.

In 1 patient with neo-aortic valve insufficiency following the arterial switch operation a 'switch-back' procedure was performed. The valve was replaced with the neopulmonary valve, which originally was the anatomic aortic valve. Bringing back the native aortic valve to the LV certainly has a lot of intuitive appeal (14).

Early mortality in our series occurred only in neonatal patients or young infants. Six patients underwent the Ross procedure at an age of 3 months or less. Mortality in this age group was relatively high with 4 of 6 patients dying (3 in-hospital deaths and 1 late death). One patient died as a result of multiple organ failure following an emergency Ross procedure. Balloon dilatation had resulted in severe aortic valve insufficiency and cardiac arrest. Two patients had valvular and subvalvular LVOT obstruction following repair of interrupted aortic arch type B and VSD 1 and 3 months earlier. One of them had severely depressed LV function and died of low output failure following the Ross procedure. Ischemia probably caused by unrecognized left coronary artery kinking led to mortality in the other patient with previous IAA/VSD repair. Finally, one patient died 13 months after a Ross procedure (performed at the age of 2 months) due to severe pulmonary hypertension and LV failure. Autopsy confirmed the presence of severe LV fibroelastosis. Prior to the Ross operation diastolic LV dysfunction with a minor suspicion of fibroelastosis was present. LV-dimensions were within normal ranges.

LVOT obstruction following IAA/VSD repair is common and the use of the Ross-Konno procedure is very attractive. Care should be taken with coronary artery transfer as the diameter of the pulmonary autograft will usually be considerably larger than that of the aortic root. Starnes et al. reported their experience with the pulmonary autograft procedure for residual LVOT obstruction following IAA/VSD repair with good results. They even suggest that for IAA/VSD and small LVOT a primary Ross-Konno procedure with arch repair may be the procedure of choice (2,15-17).

Endocardial fibroelastosis has been reported as being a risk factor for an adverse outcome in neonatal critical aortic stenosis (18). Biventricular repair may not always be the ideal solution for this subgroup and the Norwood procedure and subsequent univentricular repair can be a better option.

Dilatation and autograft valve failure as has been described in several series of adult patients (3-8) also occurred in our pediatric population. The majority of patients showed annular diameters in excess of 90th percentile of normal aortic root diameters and 3 patients were even reoperated for valve failure in association with excessive root dilatation. The meaning of this observation is not clear, as progression of autograft dilatation was not common in this series. Serial assessment by echocardiography and careful clinical follow-up will provide more insight in the coming years. Although exact criteria for reoperation

because of dilatation are not available, the rate at which dilatation occurs and maximal diameter related to body surface area should be taken in consideration.

In some patients the superior capacity of juvenile tissues to remodel appears to be inadequate to prevent aneurysmal dilatation and valve failure of the pulmonary autograft. Although one might believe that a Ross procedure performed in the neonatal period would suffer less from autograft dilatation than a Ross performed at a later age, some evidence exists that autograft dilatation can also occur following a neonatal Ross operation (Ziemer, personal communication 2003). Initial bicuspid aortic valve appeared to be no risk factor for developing dilatation either; despite suggestions in literature our study showed no difference in dilatation between the two groups (19).

Reinforcing proximal and distal autograft suture lines with autologous pericardial strips was used in most of our patients, but apparently did not provide protection from dilatation. The use of large coronary buttons to replace the native pulmonary sinuses and reinforcement of the 'non-coronary' sinus wall of the pulmonary autograft by leaving the noncoronary aortic sinus in situ, have been reported to be of benefit (20).

Root dilatation is not the only mechanism of autograft failure. In one of our patients leaflet fibrosis occurred leading to replacement by a mechanical prosthesis. Leaflet dysfunction without associated root dilatation has been described by others before (21). The mechanism of autograft leaflet shortening by fibrosis is not known. It may be the result of improper tissue handling at the time of operation but autograft leaflet failure may also be the result of a (connective) tissue disorder.

In summary, we believe that the Ross procedure is of great use in the pediatric population as it provides a unique growing aortic valve substitute together with the above-described additional technical advantages such as an adequate solution for otherwise difficult to treat obstructive LVOT's. Nevertheless, in our opinion the Ross procedure should only be considered when valve-sparing techniques can no longer provide a solution for pediatric aortic valve disease.

## References


1. Ross DN, Replacement of aortic and mitral valves with a pulmonary autograft, Lancet. 1967; 2 (7523): 956-958.
2. Ohye RG, Gomez CA, Ohye BJ, Goldberg CS and Bove AL, The Ross/Konno procedure in neonates and infants: intermediate-term survival and autograft function, Ann Thorac Surg. 2001; 72 (3): 823-830.
3. Elkins RC, Lane MM and McCue C, Ross operation in children: late results, J Heart Valve Dis. 2001; 10 (6): 736-741.
4. Elkins RC, Lane MM, McCue C and Ward KE, Pulmonary autograft root replacement: mid-term results, J Heart Valve Dis. 1999; 8 (5): 499-503.
5. Alphonso N, Baghai M, Dhital K, Mood G, Tulloh R, Austin C and Anderson D, Midterm results of the Ross procedure, Eur J Cardiothorac Surg. 2004; 25 (6): 925-930.
6. Hraska V, Krajci M, Haun C, Ntalakoura K, Razek V, Lacour-Gayet F, Weil J and Reichenspurner H, Ross and Ross-Konno procedure in children and adolescents: mid-term results, Eur J Cardiothorac Surg. 2004; 25 (5): 742-747.
7. Paparella D, David TE, Armstrong S and Ivanov J, Mid-term results of the Ross procedure, J Card Surg. 2001; 16 (4): 338-343.
8. David TE, Omran A, Ivanov J, Armstrong S, de Sa MA, Sonnenberg B and Webb G, Dilation of the pulmonary autograft after the Ross procedure, J Thorac Cardiovasc Surg. 2000; 119 (2): 210-220.
9. Elkins RC, The Ross operation: a 12-year experience, Ann Thorac Surg. 1999; 68 (3): S14-S18.
10. Schoof PH, Hazekamp MG, van Wermeskerken GK, de Heer E, Bruijn JA, Gittenberger-de Groot AC and Huysmans HA, Disproportionate enlargement of the pulmonary autograft in the aortic position in the growing pig, J Thorac Cardiovasc Surg. 1998; 115 (6): 1264-1272.
11. Braun J, Hazekamp MG, Schoof PH, Ottenkamp J and Huysmans HA, Short-term follow up of the Ross operation in children, J Heart Valve Dis. 1998; 7 (6): 615-619.
12. Schoof PH, Hazekamp MG and Huysmans HA, Pulmonary autograft in ventricular septal defect-aortic insufficiency complex, Ann Thorac Surg. 1996; 61 (3): 1005-1006.
13. Roman MJ, Devereux RB, Kramer-Fox R and O'Loughlin J, Two-dimensional echocardiographic aortic root dimensions in normal children and adults, Am J Cardiol. 1989; 64 (8): 507-512.
14. Hazekamp MG, Schoof PH, Suys BE, Hutter PA, Meijboom EJ, Ottenkamp J and Huysmans HA, Switch back: using the pulmonary autograft to replace the aortic valve after arterial switch operation, J Thorac Cardiovasc Surg. 1997; 114 (5): 844-846.
15. Starnes VA, Luciani GB, Wells WJ, Allen RB and Lewis AB, Aortic root replacement with the pulmonary autograft in children with complex left heart obstruction, Ann Thorac Surg. 1996; 62 (2): 442-448.
16. Luciani GB, Ackerman RJ, Chang AC, Wells WJ and Starnes VA, One-stage repair of interrupted aortic arch, ventricular septal defect, and subaortic obstruction in the neonate: a novel approach, J Thorac Cardiovasc Surg. 1996; 111 (2): 348-358.

17. Luciani GB and Starnes VA, Pulmonary autograft after repair of interrupted aortic arch, ventricular septal defect, and subaortic stenosis, J Thorac Cardiovasc Surg. 1998; 115 (1): 266-267.
18. Lofland GK, McCrindle BW, Williams WG, Blackstone EH, Tchervenkov CI, Sittiwangkul R and Jonas RA, Critical aortic stenosis in the neonate: a multi-institutional study of management, outcomes, and risk factors. Congenital Heart Surgeons Society, J Thorac Cardiovasc Surg. 2001; 121 (1): 10-27.
19. de Sa M, Moshkovitz Y, Butany J and David TA, Histologic abnormalities of the ascending aorta and pulmonary trunk in patients with bicuspid aortic valve disease: clinical relevance to the ross procedure, J Thorac Cardiovasc Surg. 1999; 118 (4), 588-594.
20. Black MD, van Son JA and Hanley FL, Modified pulmonary autograft aortic root replacement: the sinus obliteration technique, Ann Thorac Surg. 1995; 60 (5): 1434-1436.
21. Walker T, Heinemann MK, Schneider W, Wehrmann M, Bultmann B and Ziemer G, Early failure of the autograft valve after the Ross procedure, J Thorac Cardiovasc Surg. 2001; 122 (1): 187-188.

Heynric B. Grotenhuis
Jos J.M. Westenberg
Joost Doornbos
Lucia J.M. Kroft
Paul H. Schoof
Mark G. Hazekamp
Hubert W. Vliegen
Jaap Ottenkamp
Albert de Roos

# chapter 09

**Aortic Root Dysfunctioning and its Effect on Left Ventricular Function in Ross Procedure Patients assessed with Magnetic Resonance Imaging.**

Am Heart J. 2006; 152 (5): 975 e1-8.

## Abstract

**Purpose:** This study evaluated the diameters and distensibility of the aortic root as well as the degree of aortic regurgitation (AR) and its effect on left ventricular (LV) function in patients 8.2 ± 3.1 years after they underwent the Ross procedure, with a comparison of these parameters between patients and matched healthy subjects.

**Materials and Methods:** Eighteen Ross procedure patients (16 male patients, age (mean ± SD) 19.2 ± 3.8 years) and 18 matched healthy subjects (16 male patients, age (mean ± SD) 19.7 ± 4.2 years) underwent magnetic resonance imaging (MRI). Measurements for diameters (at 4 levels) and the distensibility of the aortic root were performed using a steady-state free precession sequence. Aortic flow was assessed with a velocity-encoded phase-contrast sequence. Left ventricular systolic function was assessed with a gradient-echo sequence in the short-axis plane. Comparison of parameters was performed using the Mann-Whitney U test. Correlations between diameters, distensibility, AR fraction and LV systolic function were expressed with Spearman rank correlation coefficients. Linear regression analysis was used to identify predictors of LV systolic dysfunction.

**Results:** Aortic root diameters were increased in Ross procedure patients as compared with healthy subjects (mean difference 6.3 - 11.6 mm, $P \leq 0.02$ at all 4 levels). Distensibility of the aortic root was lower in patients (1.9 ± 1.1 vs 7.8 ± 3.3 mm $Hg^{-1}$, $P < 0.01$). An AR fraction > 5% was present in 14 of the 18 patients (mean AR fraction 8% ± 5% vs 1% ± 1%, $P < 0.01$). Left ventricular ejection fraction was lower in patients (50% ± 6% vs 57% ± 6%, $P < 0.01$). Dilatation, decreased distensibility and AR fraction were correlated with impaired LV systolic function ($P < 0.05$ for all). The AR fraction predicted impaired LV systolic function ($P < 0.01$).

**Conclusion:** MRI shows dilatation and decreased distensibility of the aortic root, AR, and consequent impaired LV systolic function in patients after the Ross procedure.

## Introduction

The first successful clinical application of a pulmonary autograft for aortic valve replacement was performed by Donald Ross (1) in 1967. During this procedure, the stenotic or insufficient aortic valve is replaced by a pulmonary autograft whereas the right ventricular outflow tract is reconstructed using a pulmonary homograft. This so-called Ross procedure is nowadays widely used in the pediatric population because of the associated excellent survival, the low rate of reoperation and the lack of need for lifelong anticoagulation therapy (2-4). The procedure's additional beneficial effects are the potential for growth of the autograft and the ready availability of an inherently proper-sized pulmonary autograft (2-4).

Recent reports indicate that not only growth but also dilatation of the autograft frequently occurs during follow-up (4,5). Excessive dilatation in patients, which necessitates a reoperation, is therefore one of the main concerns after the Ross procedure (4). The effect of dilatation on autograft wall integrity and its implications for a possible reoperation are unknown. Distensibility reflects the condition of the vascular wall because distensibility directly depends on the elastic properties of the vascular wall (6,7). Furthermore, aortic valve dynamics relates to the distensibility of the aortic root (8,9). Decreased distensibility of the aortic root increases leaflet stress, predisposing patients to the risk of aortic valve dysfunction (10-12).

Echocardiography, currently used in clinical routine to study aortic dimensions and distensibility, has limitations, including restricted imaging quality with increasing patient age. Another important drawback of echocardiography when applied to measure the diameter of the aortic root is the fixed imaging plane, which does not correct for aortic and cardiac motion (13). The sinus of Valsalva of the aortic root will move through the fixed acquisition plane during physiologic motion, which may result in unreliable diameter measurements over the cardiac cycle (13).

Magnetic resonance imaging (MRI) is a well-accepted imaging tool for postsurgical congenital heart disease that provides unlimited field of view (FOV) and accurate assessment of cardiac anatomy and cardiac function (13,14). Moreover, MR measurements can be corrected for through-plane motion to improve the assessment of aortic root distensibility (13).

Accordingly, motion-corrected MRI was used in the current study for evaluating the dimensions and distensibility of the aortic root in relationship with autograft valve competence and left ventricular (LV) systolic function in Ross procedure patients as compared with age- and sex-matched healthy subjects.

## Materials and Methods

### Patient population

The study was approved by the local ethics committee and informed consent was obtained from all participants before their enrollment in the study. Between October 2004 and March 2005, 18 Ross procedure patients and 18 matched healthy subjects were prospectively studied with MRI at our institution. Patients aged between 12 and 25 years (n = 29) were selected from our local database of 53 Ross procedure patients. Patient inclusion criteria included having an aortic valve pathology corrected with the Ross procedure in the past, being between 12 and 25 years old, being willing to comply with the study procedures and providing written informed consent. Patient exclusion criteria composed of having had a Konno extension to the Ross procedure (ie, relief of LV outflow obstruction by septal patch insertion) (3 patients), undergoing reoperation and/or reintervention in the autograft area between the Ross procedure and MR investigation (1 patient) and having other general contraindications to a cardiovascular MR examination. Seven patients denied participation for personal reasons.

Age- and sex-matched healthy subjects were selected from our database of subjects in whom cardiac pathology had been excluded in the past by physical examination and echocardiography. The characteristics of the 2 groups and functional status as expressed in New York Heart Association class were obtained from patient records (Table 1).

Table 1. Patient and volunteer characteristics.

| Characteristics | patients (n = 18) | healthy subjects (n = 18) |
|---|---|---|
| male / female | 16 (89) / 2 (11) | 16 (89) / 2 (11) |
| age at Ross operation (years) * | 11.3 ± 5.3 | |
| interval between the operation and the MRI (years) * | 8.2 ± 3 | |
| height (cm) * | 173 ± 12 | 179 ± 10 |
| weight (kg) * | 66 ± 15 | 71 ± 16 |
| Body Surface Area ($m^2$) * and † | 1.8 ± 0.9 | 1.9 ± 1.0 |
| bicuspid aortic valve before Ross | 14 (78) | none |
| preoperative: AR / AS / combined AR and AS | 3 / 1 / 14 (17 / 6 / 78) | |

Note: unless otherwise indicated, data are number of patients, and data in parentheses are percentages.
* Data are mean ± standard deviation.
† According to the Mosteller formula: √ (height (cm) × weight (kg) / 3600).
MRI = magnetic resonance imaging; AR = aortic regurgitation; AS = aortic stenosis.

**Operative technique**

The Ross procedure was performed on patients with an aortic valve pathology (median age at surgery 10.8 years, age (mean ± SD) 11.3 ± 5.3 years) using cardiopulmonary bypass with moderate hypothermia. In all patients, the pulmonary autograft was implanted using the root replacement technique (15). Reinforcement of proximal and distal suture lines with a strip of autologous pericardium was used for most patients. Autograft harvesting was usually performed after aortic cross-clamping. Associated procedures during the Ross procedure were enucleation or resection of a discrete subaortic stenosis (3 patients) and ventricular septal defect closure (2 patients).

**MRI**

MRI studies were performed with a 1.5-T system (NT 15 Gyroscan Intera, Phillips Medical Systems, The Netherlands). Scout images were obtained in transverse, coronal and sagittal planes using a standard multislice turbo spin-echo sequence.

Two sets of orthogonal scout cine images of the aortic root were obtained for planning of the acquisition planes for diameter measurements of the aortic root. Four diameter measurements were subsequently obtained at the levels of the annulus of the aortic valve, the sinus of Valsalva, the sinotubular junction and the ascending aorta (AA), with the AA at the level of the pulmonary trunk (Figure 1). A steady-state free precession sequence (balanced turbo field-echo pulse sequence) was used, with the following scan parameters: FOV 220 mm; voxel size 1.25 × 1.25 × 6.00 mm; flip angle (FA) 50°; repetition time (TR) 3.2 ms; echo time (TE) 1.23 ms; gate width 34.2 ms. Diameter measurements were acquired during diastole, with a trigger delay for all measurements set at 600 ms.

Figure 1.

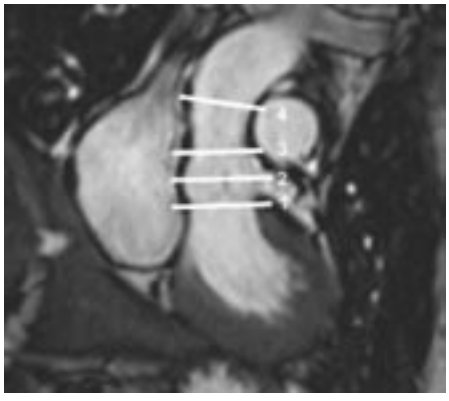


**Figure 1.** Four diameter measurements of the aortic root using a steady-state free precession cine sequence were performed at the level of the annulus of the aortic valve (1), the sinus of Valsalva (2), the sinotubular junction (3) and the AA at the level of the pulmonary trunk (4).

Distensibility is defined as follows (16):

$$\text{Dist (mm Hg}^{-1}) = ((A_{max} - A_{min}) / (A_{min} \times (P_{max} - P_{min})))$$

with $A_{max}$ and $A_{min}$ as the maximal and minimal cross-sectional lumen areas (in mm squared) of the aortic root, respectively, and $P_{max}$ and $P_{min}$ as the systolic and diastolic blood pressures (in mm of mercury), respectively. In our study, the maximal and minimal cross-sectional lumen areas were obtained at the level of the sinotubular junction (Figure 2). Imaging at this level ensured optimal imaging quality as a result of the absence of aortic valve movements, in comparison with the aortic annulus and the sinus of Valsalva.

Blood pressure was noninvasively obtained using a semiautomatic MRI-compatible sphygmomanometer (Invivo Research, USA). In each patient, right brachial artery systolic and diastolic blood pressures were measured 3 times during the measurements for distensibility, and the average of the measurements was used for calculations (17). In all investigated subjects, the used cuff size depended on patient size.

A pilot study on 5 healthy subjects showed that the minimal lumen area is to be expected early in the cardiac cycle during the isovolumetric contraction phase, whereas the maximal area is to be expected when the peak of aortic flow passes through the AA (Figure 2). For this, cross-sectional lumen area measurements were obtained throughout the cardiac cycle at the level of the sinotubular junction.

Accordingly, first, the flow was measured at the level of the AA with a phase-contrast sequence for timing of the acquisition of the cross-sectional minimal and maximal area measurements. The phase-contrast study consisted of a gradient-echo sequence, with the following scan parameters: FOV 300 mm; matrix size 128 × 128 mm (with a reconstructed voxel size of 1.17 × 1.17 × 8.00 mm); FA 20°; TR 4.8 ms; TE 2.8 ms; velocity encoding value 1.5 m/s (using retrospective gating). The high temporal resolution ranging between 7 and 12 ms enabled optimal timing of the acquisition of the minimal and maximal cross-sectional area measurements. The same study was also used for determination of aortic valve competence (aortic regurgitation (AR) fraction).

Minimal and maximal lumen area MRI studies were performed after manually positioning the acquisition planes perpendicularly to the aorta at the level of the sinotubular junction, at time points of minimal flow and maximal flow through the aortic root, respectively. This approach enabled correction for through-plane motion of the aortic root during contraction. The scan parameters were identical to the diameter measurements; gate delay was individually applied for optimal timing of the acquisition. Examples of the positioning of the acquisition plane at minimal and at maximal aortic flow are respectively shown in Figure 2.

Left ventricular systolic function was assessed with a steady-state free precession cine sequence. A short-axis stack of 14 to 18 contiguous slices was used (FOV 400 mm, voxel

Figure 2.

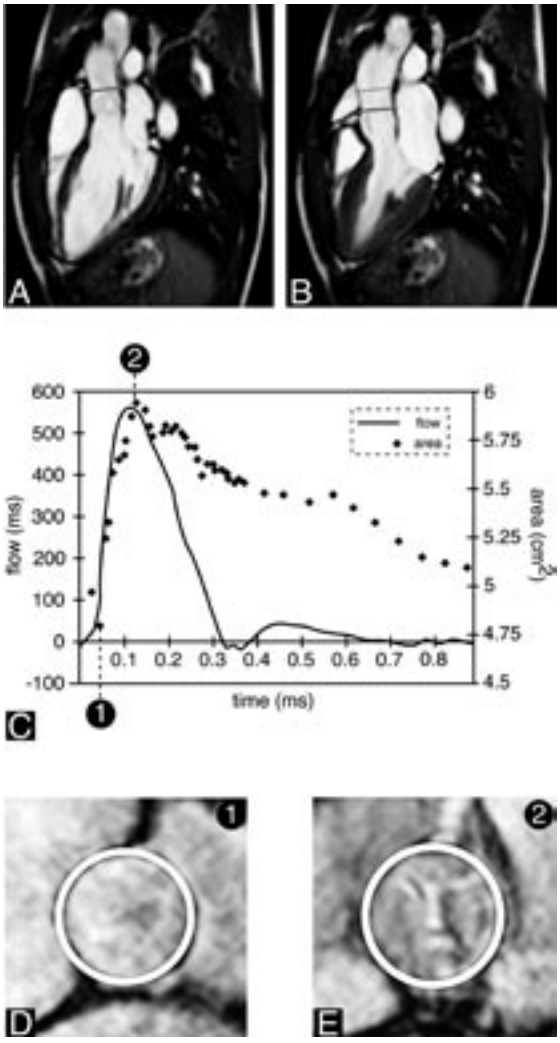


**Figure 2a-e.** Aortic root distensibility. **(a,b)** MR images show section positioning at minimal and maximal aortic flow for distensibility measurements; in this way, we corrected for through-plane motion of the aortic root during contraction. Note the difference in position of the aortic root in both images due to cardiac motion. Gate delay is 35 ms in **a** and 120 ms in **b**. **(c)** Graph shows aortic flow curve - obtained by using a phase-contrast study - and corresponding lumen areas at the level of the sinotubular junction throughout the cardiac cycle in 17-year-old female healthy control subject. Minimal lumen area (1) is obtained at isovolumetric contraction, and maximal lumen area (2) is obtained at moment of peak flow. **(d,e)** Gated steady-state free precession MR images show the minimal aortic lumen area (to be expected early in the cardiac cycle during the isovolumetric contraction phase) (1) and the maximal aortic lumen area (to be expected when the peak of aortic flow passes through the ascending aorta) (2), respectively. Lumen areas are manually traced (circles).

size 1.6 × 1.6 × 8.00 mm, no slice gap, FA 70°, TR 3.2 ms and TE 1.6 ms), covering the base of the heart to the apex.

**Postprocessing**

All images were quantitatively analyzed on a Sun workstation (Sun Microsystems, USA) with 2 software packages that were previously validated (18,19). All contours were manually drawn by 2 independent observers (HBG, with 2 years of experience and LJMK, with 8 years of experience).

The diameter measurements, measurements of the distensibility of the aortic root and the short-axis gradient-echo images of both ventricles were analyzed with the software package MASS (Medis, The Netherlands) (18). Diameters of the aortic root were obtained by direct measurement of the lumen at each level of the aortic root. A dilated aortic root is defined as the diameter at the level of the sinus of Valsalva > 4.0 cm (20). Endovascular aortic contours were drawn for minimal and maximal lumen area measurements. Intraobserver and interobserver variations of our image analyses of the minimal and maximal lumen area measurements were determined in 10 of our Ross procedure patients by repeated analysis by one observer (blinded to the first analysis with an interval > 2 weeks) and by additional image analysis of a second observer (blinded to the results obtained by the first observer).

Left ventricular end-diastolic volume (LV EDV) and LV end-systolic volume (LV ESV) were obtained by drawing contours around the lumen of the LV at end-diastole and at end-systole in all sections of the cine sequence (18) and were subsequently indexed for body surface area (BSA) according to the Mosteller formula: $\sqrt{}$ (height (cm) × weight (kg) / 3600) (indicated by LV $EDV_i$ and LV $ESV_i$, respectively). Left ventricular ejection fraction (LV EF) was calculated by dividing the LV stroke volume by the LV EDV (18). Left ventricular mass was calculated as previously described after drawing LV endocardial and epicardial contours (21) and was subsequently indexed for BSA (indicated by LV $mass_i$).

Aortic velocity maps were analyzed by using the software package FLOW (Medis, The Netherlands) (19). Endovascular contours were drawn for the aorta, and flow data were obtained from the velocity data of each voxel in all phases. Flow curves were obtained with this method for flow in the aorta during a cardiac cycle. The aortic regurgitant fraction was calculated with the following formula: Regurgitant Flow Volume / Systolic Forward Flow Volume × 100%. Aortic regurgitation was considered to be significant if the regurgitant fraction was > 5% of the systolic forward flow.

**Statistical analysis**

Statistical analysis was performed with the use of SPSS for Windows (version 12.0.1, SPSS, USA). All data are presented as mean value ± 1 SD, unless stated otherwise. The Mann-Whitney U test was used to express differences in variables between patients and healthy

subjects. Correlations between variables were expressed with Spearman rank correlation coefficients. Intraobserver and interobserver variations were studied for the analysis of minimal and maximal lumen area measurements (for distensibility calculations) by calculating the coefficient of variation (defined as the standard deviation of the differences between the 2 series of measurements divided by the mean of both measurements) with CI. The Wilcoxon signed rank test was used to express any difference between the mean differences of the distensibility measurements. Linear regression analysis was used to identify predictors of impaired LV systolic function with backward elimination procedures. Statistical significance was indicated by a P value < 0.05.

## Results

The Ross procedure patients and healthy subjects were matched for age and sex. Other parameters such as height, mass and BSA were not significantly different between the groups (Table 1). All patients were in New York Heart Association class I. Results are summarized in Table 2.

Table 2. Results for the 18 Ross procedure patients and 18 age- and sex-matched healthy subjects.

| Parameters | patients | healthy subjects | P value | mean difference |
|---|---|---|---|---|
| diameter annulus (mm) | 33.6 ± 6.9 | 26.3 ± 2.7 | < 0.01 | 7.3 |
| diameter sinus of Valsalva (mm) | 41.4 ± 5.7 | 29.8 ± 3.1 | < 0.01 | 11.6 |
| diameter sinotubular junction (mm) | 34.2 ± 6.9 | 26.2 ± 2.7 | < 0.01 | 8.0 |
| diameter ascending aorta (mm) | 31.0 ± 6.2 | 24.7 ± 3.0 | < 0.01 | 6.3 |
| distensibility (in $10^{-3}$ mm $Hg^{-1}$) * | 1.9 ± 1.1 | 7.8 ± 3.3 | < 0.01 | |
| aortic regurgitation fraction (%) | 8 ± 5 | 1 ± 1 | < 0.01 | |
| LV EF (%) | 50 ± 6 | 57 ± 6 | < 0.01 | |
| LV $EDV_i$ ($ml/m^2$) | 67 ± 17 | 56 ± 11 | 0.03 | |
| LV $ESV_i$ ($ml/m^2$) | 34 ± 8 | 33 ± 34 | 0.09 | |
| LV $mass_i$ ($g/m^2$) | 33 ± 8 | 28 ± 6 | 0.04 | |

Note: data are expressed as mean ± standard deviation.
* Distensibility was measured at the level of the sinotubular junction.
Abbreviations: LV = left ventricle, EF = ejection fraction, $EDV_i$ = end-diastolic volume indexed for body surface area, $ESV_i$ = end-systolic volume indexed for body surface area.

The Ross procedure patients showed increased diameters of the aortic root at all 4 levels as compared with the healthy subjects (Table 2, Figure 3). Dilatation of the sinus of Valsalva > 4 cm was present in 11 of the 18 patients. It was most pronounced at the level of the sinus of Valsalva, which decreased toward the AA (Table 2, Figure 3). Dilatation at the level of the sinus of Valsalva was significantly correlated with younger age at surgery: the diameter difference between the sinus of Valsalva and the annulus significantly increased when the patient was younger at operation ($r = 0.57$, $P < 0.01$). The preoperative presence of a bicuspid aortic valve, AR, aortic stenosis (AS), or combined AR and AS was not related to dilatation of the aortic root ($r = 0.27$ - $0.42$ for all 4 levels, $P > 0.05$).

Figure 3.

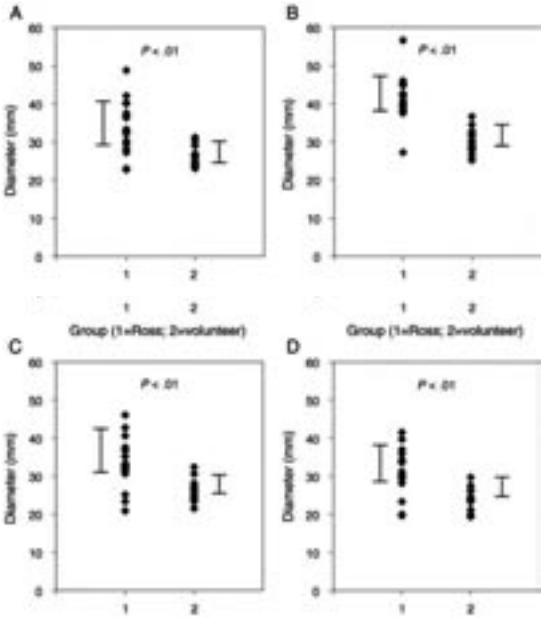


**Figure 3 a-d. (a-d)** show the diameter measurements for the Ross procedure patients and healthy subjects at the 4 levels of the aortic root: annulus; sinus of Valsalva; sinotubular junction; and AA. Diameters are expressed in mm.

Distensibility at the level of the sinotubular junction was clearly decreased in Ross procedure patients as compared with the healthy subjects (Table 2, Figure 4). A significant correlation was found between the dilatation at the level of the sinotubular junction and decreased distensibility at the same level ($r = 0.70$, $P < 0.01$). The preoperative presence of a bicuspid aortic valve, AR, AS, or combined AR and AS were not related to impaired distensibility ($r = 0.05$ - $0.36$, $P > 0.05$).

Figure 4.

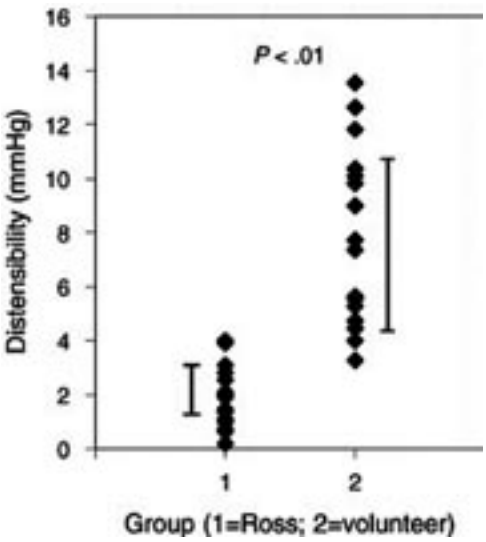


**Figure 4.** Distensibility of the aortic root in the Ross procedure patients as compared with that in the healthy subjects. Distensibility is expressed in $10^{-3}$ mm $Hg^{-1}$.

Ross procedure patients were characterized by the frequent presence of AR, as 14 of the 18 patients showed an AR fraction > 5%. The AR fraction ranged from 5% to 17%, representing mild degrees of AR. Aortic regurgitation fraction (expressed in percentages, Table 2) was significantly correlated with increased diameters of the aortic root at all 4 levels (r = 0.46-0.63, P < 0.01 for all) and with impaired distensibility (r = 0.66, P < 0.01). The preoperative presence of a bicuspid aortic valve, AR, AS, or combined AR and AS did not predispose patients to AR (r = 0.02 - 0.50, P > 0.05).

Left ventricular systolic function expressed as LV EF was significantly lower in Ross procedure patients as compared with healthy subjects (Table 2). Mean LV $EDV_i$ was significantly increased in patients as compared with healthy subjects (Table 2) and significantly correlated to the AR fraction (r = 0.41, P = 0.02). The mean LV $ESV_i$ values were not significantly different between Ross procedure patients and healthy subjects (Table 2). Left ventricular $mass_i$ was significantly increased in Ross procedure patients as compared with healthy subjects (Table 2). Increased LV $mass_i$ was correlated with increased LV $EDV_i$ (r = 0.67, P < 0.01).

Decreased LV EF was correlated with the degree of dilatation at the level of the sinus of Valsalva (r = 0.47, P < 0.01), the degree of reduced distensibility of the aortic root (r = 0.43, P = 0.01) and the AR fraction (r = 0.57, P <0.01). Linear regression showed that AR fraction predicted reduced LV systolic function (r = 5.0, P < 0.01).

Intraobserver and interobserver variations of our image analyses of the distensibility measurements were determined: mean differences for intraobserver and interobserver results of the minimal and maximal lumen area measurements ranged from 0.03 to 0.12 $mm^2$ (SD 0.19 - 0.28, P = 0.31 - 0.78). The coefficient of variation never exceeded 1% for both intraobserver and interobserver variations (CI 0.4 - 0.6).

## Discussion

In this study, cardiac MRI was used to evaluate the dimensions and distensibility of the aortic root (autograft) as well as aortic valve (autograft) competence in relation to LV systolic function in Ross procedure patients as compared with age- and sex-matched healthy subjects. The main findings of the current study revealed dilatation of the aortic root, decreased distensibility of the aortic root, frequent mild AR and reduced LV systolic function in the Ross procedure patients at a mean of 8 years after they had their operation. Impaired LV systolic function was significantly correlated with dilatation and decreased distensibility of the aortic root, as well as the AR, indicating a relationship between autograft dysfunction and decreased LV systolic function. Furthermore, AR appeared to predict the presence of decreased LV systolic function.

**Autograft dilatation**

Significant dilatation of the aortic root was found in our Ross procedure patient group as compared with the control group. After a mean follow-up period of 8 years, 11 of the 18 patients showed dilatation, with a diameter > 4.0 cm at the level of the sinus of Valsalva, which is in line with the findings of Simon-Kupilik et al. (22), who found a 7-year freedom from dilatation of 45%. Our patients were however significantly younger; therefore, absolute diameters of the aortic root could underestimate the diameter as compared with body size. Dilatation was most pronounced at the level of the sinus of Valsalva, with a decrease of dilatation toward the AA. This has been reported before; however, relative loss of anatomical landmarks of the aortic root caused by dilatation hampered definition of aortic root levels when using echocardiography (20). In this study, MRI allowed to overcome this practical limitation as a result of optimal planning of the acquisition planes.

Younger age at operation also predisposed patients to aortic root dilatation. This observation is in accordance with the results of previous studies (12,20,22). Possible explanations are the greater likelihood of a mismatch of aortic and pulmonary roots and physiologic dilatation (i.e., root growth) in children who undergo the Ross procedure (4,20). The latter process is supported by animal studies and similar observations of the

behavior of an autologous pulmonary root late after the repair of other congenital cardiac lesions (5,23).

The association between the initial presence of a bicuspid aortic valve and autograft dilatation is a matter of controversy (4,20,24-26). We found no supportive evidence for such a possible association, suggesting that other factors could play a role in the appearance of autograft dilatation. Degenerative lesions of the pulmonary artery media could occur after autograft implantation as a result of an altered microvascular supply, its exposure to the hemodynamic stress of the systemic circulation, severity of prior AR and variables related to the operative technique (26).

**Autograft distensibility**

Distensibility of the aortic root was evaluated in this study with a motion-corrected MR approach. We found a significantly decreased mean distensibility of the aortic root in the Ross procedure patient group. Reduced distensibility of the aortic root reflects an impaired condition of the vascular wall because distensibility directly depends on the elastic properties of the vessel wall (6,7,13,16). This study revealed that dilatation of the aortic root was the most important cause of impaired distensibility, as can be observed in elderly individuals and patients with the Marfan syndrome (16).

**Aortic regurgitation**

In the current study, mild degrees of AR were a common finding in the Ross procedure patient group. Both increased diameter of the aortic annulus and decreased distensibility of the aortic root were significantly correlated with AR fraction. David et al. (27) pointed out that dilatation of the aortic root has the potential to cause AR in adults; in our study, this relationship was found in children after the Ross procedure. The dynamics of the aortic valve is related to the distensibility of the aortic root (12). Aortic valve opening occurs in concert with root expansion during the beginning of systole (8,9,12). Disturbance of this interrelation greatly determines the stress on valve leaflets (10-12). In contrast to a recent echocardiography study (12), this study showed that decreased distensibility of the aortic root was correlated with the AR fraction. We therefore hypothesize that decreased aortic root distensibility in Ross procedure patients increases leaflet stress and thus predisposes the patients to aortic valve dysfunction.

**Left ventricular systolic function**

In this study, decreased LV systolic function in the Ross procedure patient group was significantly correlated with dilatation of the aortic root, impaired distensibility of the aortic root and AR fraction, whereas the AR fraction proved to predict reduced LV systolic function. The AR fraction was correlated with increased LV $EDV_i$, indicating increased diastolic filling of

the LV as a result of the AR. Increased LV $EDV_i$ was also correlated with increased LV $mass_i$, which might suggest compensatory LV hypertrophy caused by the volume overload of the LV.

We hypothesize that the dysfunctioning autograft negatively influences LV systolic function: dilatation of the aortic root appears to result in decreased aortic distensibility and aortic valve dysfunctioning, subsequently leading to reduced LV systolic function and compensatory LV hypertrophy. We therefore suggest that impaired LV systolic function as a result of autograft dysfunction may be a long-term consequence of the Ross procedure.

MRI allows for comprehensive evaluation of aortic root function, aortic valve function and LV systolic function in patients after the Ross procedure, especially when motion-corrected MR is applied for the evaluation of the distensibility of the aortic root.

**Limitations**

Preoperative and follow-up measurements were not available; therefore, progression of findings could not be documented.

## References


1. Ross, DN. Replacement of Aortic and Mitral Valves With a Pulmonary Autograft. Lancet. 1967; 2 (7523): 956-958.
2. Elkins RC, Lane MM, and McCue C. Ross Operation in Children: Late Results. J Heart Valve Dis. 2001; 10 (6): 736-741.
3. Ohye RG, Gomez GA, Ohye BJ, et al. The Ross/Konno Procedure in Neonates and Infants: Intermediate-Term Survival and Autograft Function. Ann Thorac Surg. 2001; 72 (3): 823-830.
4. Hraska V, Krajci M, Haun C, et al. Ross and Ross-Konno Procedure in Children and Adolescents: Mid-Term Results. Eur J Cardiothorac Surg. 2004; 25 (5): 742-747.
5. Schoof, PH, Hazekamp MG, van Wermeskerken GK, et al. Disproportionate Enlargement of the Pulmonary Autograft in the Aortic Position in the Growing Pig. J Thorac Cardiovasc Surg. 1998; 115 (6): 1264-1272.
6. Rerkpattanapipat P, Hundley WG, Link KM, et al. Relation of Aortic Distensibility Determined by Magnetic Resonance Imaging in Patients > or =60 Years of Age to Systolic Heart Failure and Exercise Capacity. Am J Cardiol. 2002; 90 (11): 1221-1225.
7. Okazaki Y, Takarabe K, Furukawa K, et al. Distensibility of the Pulmonary Autograft Under Systemic Pressure. J Heart Valve Dis. 2002; 11 (2): 231-235.
8. Thubrikar MJ, Heckman JL, and Nolan SP. High Speed Cine-Radiographic Study of Aortic Valve Leaflet Motion. J Heart Valve Dis. 1993; 2 (6): 653-661.
9. Sievers HH, Storde U, Rohwedder EB, et al. Superior Function of a Bicuspid Over a Monocuspid Patch for Reconstruction of a Hypoplastic Pulmonary Root in Pigs. J Thorac Cardiovasc Surg. 1993; 105 (4): 580-590.
10. Thubrikar MJ, Nolan SP, Aouad J, et al. Stress Sharing Between the Sinus and Leaflets of Canine Aortic Valve. Ann Thorac Surg. 1986; 42 (4): 434-440.
11. Thubrikar M, Skinner JR, Aouad J, et al. Analysis of the Design and Dynamics of Aortic Bioprostheses in Vivo. J Thorac Cardiovasc Surg. 1982; 84 (2): 282-290.
12. Schmidtke C, Bechtel J, Hueppe M, et al. Size and Distensibility of the Aortic Root and Aortic Valve Function After Different Techniques of the Ross Procedure. J Thorac Cardiovasc Surg. 2000; 119 (5): 990-997.
13. Melina G, Rajappan K, Amrani M, et al. Aortic Distensibility After Aortic Root Replacement Assessed With Cardiovascular Magnetic Resonance. J Heart Valve Dis. 2002; 11 (1): 67-74.
14. Constantine G, Shan K, Flamm SD, et al. Role of MRI in Clinical Cardiology. Lancet. 2004; 363 (9427): 2162-2171.
15. Stelzer P, Jones DJ and Elkins RC. Aortic Root Replacement With Pulmonary Autograft. Circulation. 1989; 80 (5 Pt 2): III209-III213.
16. Groenink M, de Roos A, Mulder BJ, et al. Changes in Aortic Distensibility and Pulse Wave Velocity Assessed With Magnetic Resonance Imaging Following Beta-Blocker Therapy in the Marfan Syndrome. Am J Cardiol. 1998; 82 (2): 203-208.

17. Nollen GJ, Westerhof, BE, Groenink M, et al. Aortic Pressure-Area Relation in Marfan Patients With and Without Beta Blocking Agents: a New Non-Invasive Approach. Heart. 2004; 90 (3): 314-318.
18. van der Geest RJ and Reiber JH. Quantification in Cardiac MRI. J Magn Reson Imaging. 1999; 10 (5): 602-608.
19. van der Geest RJ, Niezen RA, van der Wall EE, et al. Automated Measurement of Volume Flow in the Ascending Aorta Using MR Velocity Maps: Evaluation of Inter- and Intraobserver Variability in Healthy Volunteers. J Comput Assist Tomogr. 1998; 22 (6): 904-911.
20. van der Geest RJ and Reiber JH. Quantification in Cardiac MRI. J Magn Reson Imaging. 1999; 10 (5): 602-608.
21. Luciani GB, Casali G, Favaro A, et al. Fate of the Aortic Root Late After Ross Operation. Circulation. 2003; 108 Suppl 1: II61-II67.
22. van der Geest RJ, Lelieveldt BP and Reiber JH. Quantification of Global and Regional Ventricular Function in Cardiac Magnetic Resonance Imaging. Top Magn Reson Imaging. 2000; 11 (6): 348-358.
23. Simon-Kupilik N, Bialy J, Moidl R, et al. Dilatation of the Autograft Root After the Ross Operation. Eur J Cardiothorac Surg. 2002; 21 (3): 470-473.
24. Hutter PA, Thomeer BJ, Jansen P, et al. Fate of the Aortic Root After Arterial Switch Operation. Eur J Cardiothorac Surg. 2001; 20 (1): 82-88.
25. Schmidtke C, Bechtel M, Hueppe M, et al. Time Course of Aortic Valve Function and Root Dimensions After Subcoronary Ross Procedure for Bicuspid Versus Tricuspid Aortic Valve Disease. Circulation. 2001; 104 (12 Suppl 1): I21-I24.
26. Koul B, Lindholm CJ, Koul M, et al. Ross Operation for Bicuspid Aortic Valve Disease in Adults: Is It a Valid Surgical Option? Scand Cardiovasc J. 2002; 36 (1): 48-52.
27. Luciani GB, Barozzi L, Tomezzoli A, et al. Bicuspid Aortic Valve Disease and Pulmonary Autograft Root Dilatation After the Ross Procedure: a Clinicopathologic Study. J Thorac Cardiovasc Surg. 2001; 122 (1): 74-79.

Heynric B. Grotenhuis
Albert de Roos
Jaap Ottenkamp
Paul H. Schoof
Hubert W. Vliegen
Lucia J.M. Kroft

# chapter 10

**MR Imaging of Right Ventricular Function after the Ross Procedure for Aortic Valve Replacement - Initial Experience.**
Radiology. 2008; 246 (2): 394-400.

## Abstract

**Purpose:** To prospectively assess right ventricular (RV) function after the Ross procedure by using magnetic resonance imaging (MRI).

**Materials and Methods:** The local ethics committee approved the study and informed consent was obtained from all participants prior to enrollment in the study. Seventeen patients (15 male, two female; mean age ± standard deviation, 19 years ± 3.9; imaging performed 8.3 years after surgery ± 3.2) and 17 matched controls (15 male, two female; mean age ± standard deviation, 20 years ± 3.9) were studied by using MRI. Standard velocity-encoded and multisection multiphase imaging sequences were used to assess homograft valve function, systolic and diastolic RV function, and RV mass. The two-tailed Mann-Whitney U test and the Spearman rank correlation coefficient were used for statistical analysis.

**Results:** Minor degrees of homograft stenosis (peak flow velocity between 1.5 and 3.0 m/s across the homograft valve) were found in 12 of 17 patients but not in controls ($P < 0.001$). A larger RV mass was present in Ross procedure patients than in controls (17.0 g/m$^2$ ± 4.8 vs 10.9 g/m$^2$ ± 5.6, $P = 0.004$). In addition, impaired diastolic RV function was found, as shown by a decreased mean tricuspid valve early filling phase-atrial contraction phase (E/A) peak flow velocity ratio (1.56 ± 0.75 vs 2.05 ± 0.58, $P = 0.03$). Peak velocity across the homograft valve correlated with RV mass ($r = 0.38$, $P = 0.03$) and tricuspid valve E/A peak flow velocity ratio ($r = 0.39$, $P = 0.02$). RV systolic function was normal in Ross procedure patients (mean RV ejection fraction, 52% ± 8 vs 51% ± 5; $P = 0.74$).

**Conclusion:** RV hypertrophy and RV diastolic dysfunction are frequently observed in patients after the Ross procedure, even in the absence of overt homograft stenosis. RV systolic function is still preserved.

## Introduction

Aortic valve replacement, according to the Ross procedure, is frequently performed in the pediatric population (1,2). During this operation, the stenotic or regurgitant aortic valve is replaced by a pulmonary autograft, while a homograft valve is inserted in the pulmonary position (1). Potential advantages of this procedure are the use of the patient's own valve with favorable hemodynamic characteristics, avoidance of anticoagulant therapy, and the alleged growth potential of the autograft valve in children (2,3). Long-term survival is satisfactory, although frequent dilatation of the autograft in the aortic position and diminished left ventricular (LV) function have been reported (2-4).

The longevity of the homograft valve in pulmonary position is reported to be limited owing to frequent homograft stenosis: shrinkage of the homograft annulus occurs because of a postoperative immune-mediated response to the homograft, as well as calcification and thickening of the valve leaflets (2,3,5-10). As a result, homograft stenosis is the main cause for a reoperation after the Ross procedure, necessary in approximately 10% of all cases at long-term follow-up (2,3,10,11).

Little is known about the effect of early homograft stenosis on right ventricular (RV) function. Insight into this relationship is relevant as RV function has prognostic value concerning patient survival and exercise tolerance (12,13) and may contribute to optimal timing for replacement of a dysfunctioning homograft valve.

Echocardiography is a widely used imaging tool in clinical practice but has limitations in assessment of RV function owing to the complex RV geometry (12). Magnetic resonance imaging (MRI) has been established as an accurate noninvasive tool for the assessment of the pulmonary valve and RV function (14-16). To our knowledge, MRI has not previously been used to study the relationship between homograft valve function and systolic and diastolic RV function in patients after the Ross procedure.

We hypothesized that minor degrees of homograft stenosis occur frequently in patients after the Ross procedure and that the associated increased RV afterload may negatively affect RV function. Thus, the objective of our study was to prospectively assess RV function after the Ross procedure by using MRI.

## Materials and Methods

### Patients

The medical ethics committee of Leiden University Medical Center (Leiden, The Netherlands) approved the study and informed consent was obtained from all participants prior to their enrollment in the study. Seventeen Ross procedure patients (mean age ± standard deviation, 19 years ± 3.9; imaging performed 8.3 years after surgery ± 3.2) and 17 age- and gender-matched healthy controls were prospectively studied with MRI at our institution (Table 1).

Tabel 1. Characteristics of patients and controls.

| Characteristics | patients (n = 17) | controls (n = 17) |
|---|---|---|
| male / female | 15 / 2 | 15 / 2 |
| range of age at MRI by birth sex (years) | 12.9 - 25.1/13.8 - 20.6 | 12.8 - 25.8/14.1 - 21.2 |
| age at Ross procedure (years) * | 10.8 ± 5.2 | |
| interval between the operation and the MRI (years) * | 8.3 ± 3.2 | |
| height (cm) * | 174 ± 13 | 179 ± 10 |
| weight (kg) * | 65 ± 15 | 72 ± 16 |
| Body Surface Area ($m^2$) * and † | 1.8 ± 0.3 | 1.9 ± 0.3 |

* Data are mean ± standard deviation.
† According to the Mosteller formula: √ (height (cm) × weight (kg) / 3600).
Abbreviations: MRI = magnetic resonance imaging.

Ross procedure patients were recruited from our local database of 53 Ross procedure patients. The inclusion criterion was aortic valve previously corrected with the Ross procedure. Exclusion criteria included age younger than 12 years and older than 25 years (n = 25), a Konno extension to the Ross procedure (i.e., relief of LV outflow obstruction by using septal patch insertion, n = 3), repeat operation and/or intervention in the homograft area between the Ross procedure and MR investigation (n = 1) and general contraindications to a cardiovascular MR examination. Seven patients declined to participate for personal reasons.

Age- and gender-matched healthy controls were selected from our database of individuals with a harmless heart murmur in which congenital cardiac disease had been excluded in the past by physical examination and echocardiography. Patient characteristics and functional status, as classified on the basis of the New York Heart Association functional class standards, were obtained from the patient records (Table 1). All patients were identified as New York Heart Association functional class I, without using medication.

LV function analysis of the patient group used in this study and their matched healthy controls have previously been described (4).

**Operative technique**

The Ross procedure was performed in patients with aortic valve disease (median age at surgery, 10.8 years; mean age, 10.8 years ± 5.2) by using cardiopulmonary bypass with moderate hypothermia by 2 surgeons (P.H.S. and a nonauthor, with 11 years experience each with the Ross procedure) (3). In all patients the pulmonary autograft was implanted by using the root replacement technique (17). Reinforcement of proximal and distal suture lines with a strip of autologous pericardium was used in all patients except 1. Autograft harvesting was performed after aortic cross-clamping. The RV outflow tract was reconstructed with a cryopreserved pulmonary homograft valve in all patients. Associated procedures during the Ross procedure were enucleation or resection of a discrete subaortic stenosis in 3 patients and ventricular septal defect closure in 2.

**MRI**

MRI studies were performed with a 1.5-T system (NT 15 Gyroscan Intera; Philips Medical Systems, The Netherlands).

Flow dynamics across the homograft valve were assessed by using velocity-encoded MRI just distal to the homograft valve. In the control group, velocity-encoded MRI was performed just distal to the pulmonary valve (15). Imaging parameters were: repetition time in ms / echo time in ms, 8.6 / 5.3; field of view, 400 mm; flip angle, 20°; voxel size, 2.34 × 2.61 × 8.00 mm. The sequence was encoded for a through-plane velocity of up to 150 cm/s. In case of aliasing owing to flow velocity exceeding 150 cm/s, the imaging was repeated with through-plane velocity encoding up to 300 cm/s. Temporal resolution was 25.6 ms.

Systolic biventricular function was assessed with a steady-state free precession cine sequence in the short-axis plane by using breath holds (15). Imaging parameters were: repetition time in ms / echo time in ms, 3.2 / 1.6; field of view, 400 mm; flip angle, 70°; voxel size, 1.6 × 1.6 × 8.00 mm; and no section gap (14,15).

Diastolic RV function was assessed by using velocity-encoded MRI across the tricuspid valve (15,18). Imaging parameters were: repetition time in ms / echo time in ms, 9.4 / 6; flip angle, 20°; voxel size, 2.34 × 2.61 × 8.00 mm. The sequence was encoded for a through-plane velocity of up to 100 cm/s. Temporal resolution was 25.6 ms.

**Postprocessing**

All images were quantitatively analyzed on a workstation with a Pentium 4 processor (Intel, USA).

Systolic RV and LV function were analyzed with the software package MASS (Medis, The Netherlands) (14,15). Biventricular end-diastolic volume (EDV) and end-systolic volume (ESV) were assessed by drawing the RV and LV endocardial contours at end-diastole and end-systole in all sections, as described previously (14). At end-diastole, epicardial borders of the RV free wall were drawn to obtain the RV mass (15). The interventricular septum was included in the LV analysis. Indexation was performed according to the Mosteller formula (BSA = √ (height

(cm) × weight (kg) / 3600)), where BSA is the body surface area in square meters. The following parameters were then determined: EDV, ESV, stroke volume, ejection fraction (EF) and ventricular mass (14).

Flow velocity-encoded MR data were analyzed with the software package FLOW (Medis, The Netherlands) (15,16). Flow curves were obtained with this method for homograft or pulmonary artery flow during the cardiac cycle. Contours were drawn for the homograft (patients) or pulmonary artery (controls) lumen, and flow data were subsequently obtained from the velocity data of each voxel in all phases. Peak flow velocity was determined with a time-velocity analysis that revealed the voxel with maximum peak flow throughout the cardiac cycle. Peak flow velocity across the homograft valve or pulmonary valve was considered substantially increased if maximum blood flow velocity ($V_{max}$) exceeded 1.5 m/s (19).

Pressure gradients across the homograft and pulmonary valves were subsequently calculated by using the simplified Bernoulli equation: $\Delta P = 4V^2$, where $\Delta P$ is the pressure gradient across the valve (mm of mercury), 4 is the estimated loss coefficient, and V is the peak flow velocity (m/s) (20). The regurgitant fraction was calculated with the following formula: regurgitant flow / systolic forward flow × 100%, where flow is measured in mm. Valve regurgitation was considered substantial if the regurgitant fraction exceeded 5% of the systolic forward flow (14).

Analysis of diastolic RV function by measuring flow through the tricuspid valve was performed by using the same method (14). Peak flow velocity curves were obtained for calculation of early filling phase, atrial contraction phase and early filling phase / atrial contraction phase (E/A) peak flow velocity ratios. Calculation of mean deceleration gradients of the early filling phase was used for analysis of the early filling phase slopes. The times of the early filling phase, atrial contraction phase and diastasis were also measured (16).

The manual drawing of all MR contours and analysis of the other results were performed by one researcher (H.B.G., with 3 years experience in cardiac MRI) and were subsequently checked by a radiologist (L.J.M.K., with 9 years experience in cardiac MRI), who was unaware of the patient's conditions.

**Statistical analysis**

Statistical analysis was performed by using software (SPSS for Windows, version 12.0.1; SPSS, USA). All data are expressed as mean value ± 1 standard deviation, unless stated otherwise. The Mann-Whitney U test was used to express differences in variables between the patients and controls. Correlation between variables was expressed with the Spearman rank correlation coefficient. Statistical significance was indicated by a P value of less than 0.05.

## Results

### Homograft and pulmonary valve characteristics

In 12 (82%) of 17 Ross procedure patients, the homograft valve $V_{max}$ exceeded 1.5 m/s (compared with none from the control group), indicating minor degrees of homograft stenosis (Figure 1, Table 2). Calculated pressure gradients derived from these peak flow velocities were 16.8 mm Hg ± 9.0 in patients (range: 4.3 - 36.0 mm Hg) and 4.0 mm Hg ± 1.5 in controls (range: 2.1 - 7.6 mm Hg; $P < 0.001$). No regurgitant flow across the homograft valve in any patient or the pulmonary valve in any control was present.

Figure 1.

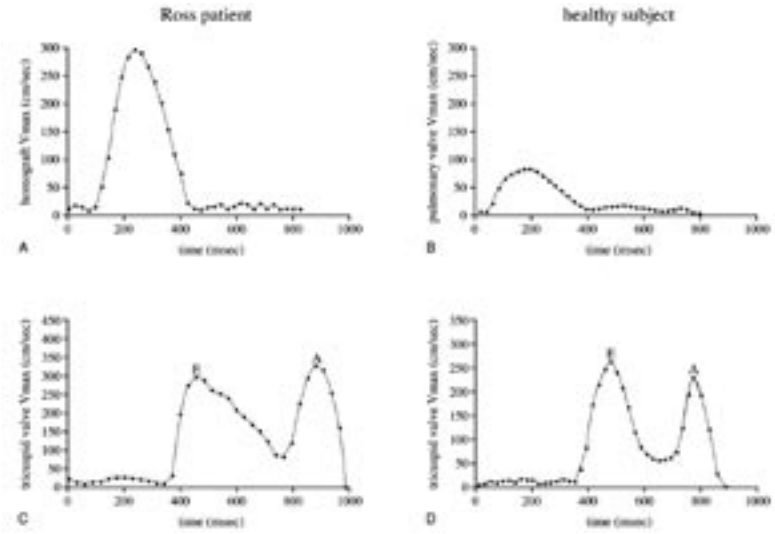


**Figure 1a-d.** Graphs show peak flow velocity curves across pulmonary homograft valve in **(a)** Ross patient and **(b)** control. Time between surgery and MR was 7.5 years. Note markedly increased peak flow velocity during systole in Ross patient (maximum velocity, 300 cm/s), indicating homograft stenosis (derived pressure gradient, 36 mm Hg). RV inflow curves across tricuspid valve in **(c)** Ross patient and **(d)** control. Biphasic inflow pattern has early filling and atrial contraction phase peaks. Note decreased tricuspid valve E/A peak flow velocity ratio and decreased mean deceleration gradient in early filling phase in Ross patient as compared with control, indicating delayed RV relaxation.

Table 2. Results in Ross procedure Patients and Controls.

| parameters | patients | controls | P value |
|---|---|---|---|
| $V_{max}$ (m/s)* | 1.97 ± 0.56 | 0.99 ± 0.18 | < 0.001 |
| pressure gradient (mm Hg)* | 16.8 ± 9.0 | 4.0 ± 1.5 | < 0.001 |
| RV EF (%) | 52 ± 8 | 51 ± 5 | 0.74 |
| RV SV (ml/m$^2$) | 54 ± 8 | 52 ± 8 | 0.84 |
| RV EDV (ml/m$^2$) | 106 ± 13 | 107 ± 16 | 0.64 |
| RV ESV (ml/m$^2$) | 53 ± 14 | 52 ± 8 | 0.69 |
| RV mass (g/m$^2$) | 17.0 ± 4.8 | 11.7 ± 4.9 | 0.004 |
| TV E/A peak-flow ratio | 1.56 ± 0.75 | 2.05 ± 0.58 | 0.03 |
| TV mean dec gradient of E phase (l/s$^2$) | -2.67 ± 1.09 | -3.05 ± 1.03 | 0.39 |
| TV diastasis time (ms) | 46 ± 54 | 74 ± 89 | 0.55 |
| LV EF (%) | 50 ± 6 | 57 ± 5 | 0.001 |
| LV EDV (ml/m$^2$) | 67 ± 16 | 56 ± 11 | 0.03 |
| LV ESV (ml/m$^2$) | 34 ± 8 | 33 ± 4 | 0.99 |
| LV mass (g/m$^2$) | 33.0 ± 8.6 | 28.4 ± 5.9 | 0.04 |

Note: data are expressed as mean ± standard deviation.
* homograft and pulmonary artery in patients and controls, respectively.
Abbreviations: $V_{max}$ = maximum velocity, RV = right ventricle; EF = ejection fraction; SV = stroke volume indexed for Body Surface Area; EDV = end-diastolic volume indexed for Body Surface Area; ESV = end-systolic volume indexed for Body Surface Area; TV = tricuspid valve; E = early filling phase; A = atrial contraction phase; dec = deceleration; LV = left ventricle.

**Biventricular Function**

Systolic function - expressed as RV EF and RV stroke volume - was not found to be different between Ross procedure patients and controls (Table 2). Also, RV dimensions (EDV and ESV) were not found to be different between the two groups (Table 2). Mean RV mass of the Ross patient group was significantly larger than in controls (Table 2). In addition, a significantly lower mean tricuspid valve E/A peak flow velocity ratio in Ross procedure patients as compared with the controls reflected a delayed RV relaxation (Figure 1, Table 2). Mean deceleration gradients of the early filling phase, and the times of the early filling phase, atrial contraction phase, and diastasis were not significantly different between the two groups (Table 2). In the Ross patient group, higher peak flow velocities across the homograft valve were significantly correlated with RV mass ($r = 0.38$, $P = 0.03$) (Figure 2) and with the E/A peak flow velocity ratio across the tricuspid valve ($r = 0.39$, $P = 0.02$) (Figure 3).

Figure 2.

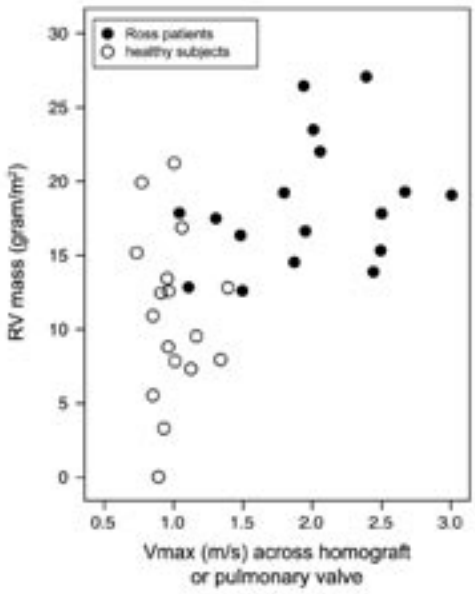


Figure 3.

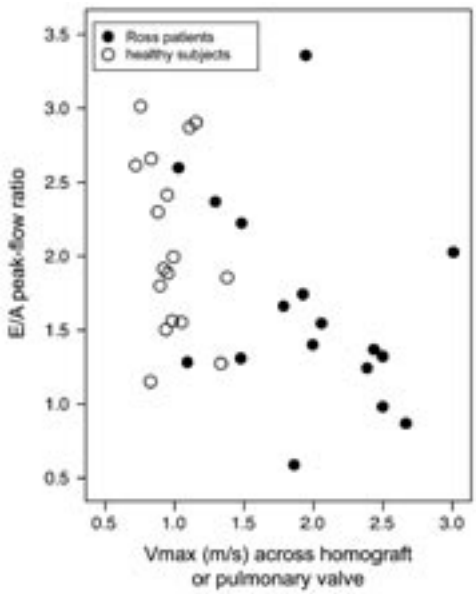


**Figure 2.** Scatterplot shows distribution of relationship between peak flow velocity across homograft or pulmonary valve vs indexed RV mass in Ross procedure patients and controls. Mild degrees of homograft stenosis represented by higher peak flow velocities across homograft valve were responsible for RV hypertrophy as compensatory mechanism owing to increased RV afterload.

**Figure 3.** Scatterplot shows distribution of relationship between peak flow velocity across homograft or pulmonary valve vs E/A peak flow ratio across tricuspid valve in Ross procedure patients and controls. Diastolic RV dysfunction in Ross group (lower mean tricuspid valve E/A peak flow velocity ratio) results from increased RV afterload and concomitant RV hypertrophy.

LV systolic function, expressed as LV EF, was diminished in the Ross procedure patients as compared with controls (Table 2). Mean LV EDV and LV mass were significantly larger in the Ross procedure patients as compared with controls (Table 2), while mean LV ESV was not significantly different between the two groups. RV EF and LV EF were not significantly correlated in the Ross patient group ($r = 0.21$, $P = 0.12$). In addition, LV mass was not significantly correlated with RV mass ($r = 0.28$, $P = 0.10$) or with peak flow velocity across the homograft valve ($r = 0.12$, $P = 0.48$).

## Discussion

Our study findings revealed RV hypertrophy and diastolic dysfunction in patients after the Ross procedure, in the presence of mild degrees of homograft stenosis. Systolic RV function was preserved.

Ross procedure patients showed higher peak flow velocities across the homograft valve, with calculated pressure gradients up to 36 mm Hg reflecting mild degrees of homograft stenosis (19), whereas all values were below 8 mm Hg in our controls. Despite favorable survival rates and low incidence of reoperation when compared to other valve substitutes such as mechanical valves and xenografts, degeneration and calcification of the homograft valve can cause homograft stenosis (2,3,5-10).

Homograft valve regurgitation occurs only in a minority of cases (2,5), as is consistent with our data. Homograft stenosis is caused by an early postoperative immune-mediated response to the homograft that leads to shrinkage of the homograft annulus (2,3,5-10) and calcification and thickening of the valve leaflets (2,3,8,10). Stenosis predominantly occurs during the first 2 years after surgery (9,10), although others have reported progression at a later stage (2,3,5,6). A gradient exceeding 9 mm Hg at 1 year follow-up could be used to predict the late occurrence of homograft stenosis (10).

Other predictive variables for homograft valve durability are related to homograft antigenicity and to the size of the inserted homograft valve (6,10). Reduced viability of the donor cells within the homografts has been shown to be favorable; older donor age and a longer duration of graft cryopreservation were associated with a lower rate of homograft stenosis (6,10). Oversizing of the homograft by 2 - 3 mm facilitates homograft valve performance (6,10). Nevertheless, somatic outgrowth remains an important contributor to homograft valve failure in the pediatric population (2,10), as may have been the case in our patient group with a mean age at surgery of 10.8 years.

Systolic RV function was adequately preserved in our patients after the Ross procedure and all were identified as New York Heart Association functional class I. However, mean RV mass was significantly higher as compared with that in the controls, indicating RV hypertrophy in the Ross patient group. RV hypertrophy often occurs as a compensatory mechanism owing to increased RV afterload (21), which in our study was related to mild degrees of homograft stenosis, as represented by higher peak flow velocities across the homograft valve.

As homograft stenosis can progress over time owing to continuing degeneration of the homograft valve or somatic outgrowth, RV hypertrophy may increase during follow-up. In addition, higher LV mass may have contributed to RV hypertrophy (22), although LV mass and RV mass were not significantly correlated in our Ross patient group. Also, a direct correlation was

found between homograft peak flow velocity and RV mass, but not with LV mass, illustrating the functional effect of homograft stenosis on the RV.

Impaired RV diastolic function was reflected by a significantly lower mean tricuspid valve E/A peak flow velocity ratio as compared with those values in controls. RV diastolic dysfunction is a consequence of hypertrophy owing to stiffening of the myocardium and may precede RV systolic dysfunction (21). Impaired diastolic function is a primary cause in 30 - 40% of patients with congestive heart failure (18,21) and is associated with diminished exercise performance (13). As physiologic loss of elastic myocardial properties and increasing ventricular mass during lifetime contribute to diastolic dysfunction (18,21), current RV diastolic dysfunction in our Ross patient group might pose a future risk for progressive RV dysfunction. Further studies are needed to address the long-term effects of our results.

Homograft replacement is suggested from a pressure gradient of 50 mm Hg or more or when signs of RV dysfunction are present (3). Therefore, serial follow-up assessment of homograft valve and RV function with noninvasive imaging techniques is useful for early detection of homograft valve dysfunction, which may facilitate selecting patients for possible reoperation. In addition, exercise testing may help assess the functional implications of homograft and RV dysfunction. Although transthoracic echocardiography is the most commonly used imaging technique, it has limitations such as a reduced acoustic window with increased patient age and difficulty helping to assess RV function, owing to the complex RV geometry.

MRI overcomes these limitations, as accurate assessment of homograft valve function and systolic and diastolic RV function can be achieved in one imaging session with low inter- and intraobserver variability (15,23,24). MRI should primarily be used for patient follow-up owing to its good reproducibility (15,23,24), as identification of patients with RV dysfunction remains difficult considering the variation in RV function parameters as depicted in Figures 2 and 3 and the fact that clear cut-off values for RV dysfunction are still lacking. Although MRI will not replace transthoracic echocardiography as the imaging technique of choice owing to higher costs and reduced availability, it should be considered when echocardiographic imaging is difficult or when actual homograft replacement is considered.

Our study had limitations. We used a limited number of patients and controls, although the low inter- and intraobserver variability of cardiac MRI allowed for relatively small sample sizes (25). No preoperative or follow-up measurements were available in our observational study, so progression of findings could not be documented. Further research is required to define cut-off values of homograft valve and RV function for optimal timing of homograft replacement in patients after the Ross procedure.

In conclusion, cardiac MRI revealed mild degrees of homograft stenosis in patients after the Ross procedure, as evidenced by higher peak flow velocities across the homograft valve. Hemodynamic consequences were RV hypertrophy and diastolic dysfunction, whereas systolic

RV function was preserved. Our study showed the feasibility of MRI as an integrated imaging tool to monitor homograft valve and RV function in patients after the Ross procedure, which may facilitate the early detection of homograft valve dysfunction. MRI may facilitate better selection of patients who need reoperation after the Ross procedure for homograft valve dysfunction.

## References


1. Ross DN. Replacement of aortic and mitral valves with a pulmonary autograft. Lancet. 1967; 2: 956-958.
2. Takkenberg JJ, Dossche KM, Hazekamp MG et al. Report of the Dutch experience with the Ross procedure in 343 patients. Eur J Cardiothorac Surg. 2002;22:70-7.
3. Bohm JO, Botha CA, Horke A et al. Is the Ross operation still an acceptable option in children and adolescents? Ann Thorac Surg. 2006;82:940-7.
4. Grotenhuis HB, Westenberg JJ, Doornbos J et al. Aortic root dysfunctioning and its effect on left ventricular function in Ross procedure patients assessed with magnetic resonance imaging. Am Heart J. 2006;152:975-8.
5. Gulbins H, Kreuzer E, Reichart B. Homografts: a review. Expert Rev Cardiovasc Ther. 2003;1:533-9.
6. Raanani E, Yau TM, David TE, Dellgren G, Sonnenberg BD, Omran A. Risk factors for late pulmonary homograft stenosis after the Ross procedure. Ann Thorac Surg. 2000;70:1953-7.
7. Sinzobahamvya N, Wetter J, Blaschczok HC, Cho MY, Brecher AM, Urban AE. The fate of small-diameter homografts in the pulmonary position. Ann Thorac Surg. 2001;72:2070-6.
8. Ward KE, Elkins RC, Overholt ED et al. Evaluation of cryopreserved homografts in the right ventricular outflow tract after the Ross procedure: intermediate-term follow up. J Heart Valve Dis. 1997;6:130-3.
9. Carr-White GS, Kilner PJ, Hon JK et al. Incidence, location, pathology, and significance of pulmonary homograft stenosis after the Ross operation. Circulation. 2001;104:I16-I20.
10. Feier H, Collart F, Ghez O et al. Risk factors, dynamics, and cutoff values for homograft stenosis after the Ross procedure. Ann Thorac Surg. 2005;79:1669-75.
11. Khambadkone S, Coats L, Taylor A et al. Percutaneous pulmonary valve implantation in humans: results in 59 consecutive patients. Circulation 2005;112:1189-97.
12. Carr-White GS, Kon M, Koh TW et al. Right ventricular function after pulmonary autograft replacement of the aortic valve. Circulation. 1999;100:II36-II41.
13. Singh GK, Greenberg SB, Yap YS, Delany DP, Keeton BR, Monro JL. Right ventricular function and exercise performance late after primary repair of tetralogy of Fallot with the transannular patch in infancy. Am J Cardiol. 1998;81:1378-82.
14. Van Straten A, Vliegen HW, Hazekamp MG et al. Right ventricular function after pulmonary valve replacement in patients with tetralogy of Fallot. Radiology. 2004;233:824-9.
15. van der Geest RJ, Reiber JH. Quantification in cardiac MRI. J Magn Reson Imaging. 1999;10:602-8.
16. Pluim BM, Lamb HJ, Kayser HW et al. Functional and metabolic evaluation of the athlete's heart by magnetic resonance imaging and dobutamine stress magnetic resonance spectroscopy. Circulation. 1998;97:666-72.
17. Stelzer P, Jones DJ, Elkins RC. Aortic root replacement with pulmonary autograft. Circulation. 1989;80:III209-III213.

18. Paelinck BP, Lamb HJ, Bax JJ, van der Wall EE, de Roos A. Assessment of diastolic function by cardiovascular magnetic resonance. Am Heart J. 2002;144:198-205.
19. Gutberlet M, Boeckel T, Hosten N et al. Arterial switch procedure for D-transposition of the great arteries: quantitative midterm evaluation of hemodynamic changes with cine MR imaging and phase-shift velocity mapping-initial experience. Radiology. 2000;214:467-75.
20. Oshinski JN, Parks WJ, Markou CP et al. Improved measurement of pressure gradients in aortic coarctation by magnetic resonance imaging. J Am Coll Cardiol. 1996;28:1818-26.
21. Mandinov L, Eberli FR, Seiler C, Hess OM. Diastolic heart failure. Cardiovasc Res. 2000;45:813-25.
22. Niezen RA, Helbing WA, van der Wall EE, van der Geest RJ, Rebergen SA, de Roos A. Biventricular systolic function and mass studied with MR imaging in children with pulmonary regurgitation after repair for tetralogy of Fallot. Radiology. 1996;201:135-40.
23. van der Geest RJ, de Roos A, van der Wall EE, Reiber JH. Quantitative analysis of cardiovascular MR images. Int J Card Imaging. 1997;13:247-58.
24. van der Geest RJ, Niezen RA, van der Wall EE et al. Automated measurement of volume flow in the ascending aorta using MR velocity maps: evaluation of inter- and intraobserver variability in healthy volunteers. J Comput Assist Tomogr. 1998;22:904-11.
25. Bellenger NG, Davies LC, Francis JM, Coats AJ, Pennell DJ. Reduction in sample size for studies of remodeling in heart failure by the use of cardiovascular magnetic resonance. J Cardiovasc Magn Reson. 2000;2:271-8.

# chapter 11

**Summary & Conclusions**
**Samenvatting & Conclusies**
**List of Publications**
**Dankwoord**

## Summary & Conclusions

The aim of this thesis was to evaluate the functional implications of aortic wall pathology on aortic valve competence and left ventricular (LV) function in patients with a bicuspid aortic valve, transposition of the great arteries, tetralogy of Fallot and patients after the Ross procedure, using magnetic resonance imaging (MRI) techniques. MRI was also used to test whether a similar interaction is present between pulmonary artery dynamics and the right ventricle (RV) in the above mentioned entities.

Chapter 1 provides a general introduction to the thesis, with a short description of the potential negative interaction between aortic wall disease and aortic valve- and LV function in the above mentioned entities.

Chapter 2 reviews the 5 most commonly affected entities of inherited connective tissue disorders and classical congenital heart disease with intrinsic aortic wall abnormalities, with description of the potential role of MRI in their evaluation and management. Marfan syndrome is the prototype for aortic wall disease, which is associated with complications like aneurysm formation and aortic dissection. Recent reports in the literature indicate that aortic wall abnormalities are also present in a wide range of other entities like transposition of great arteries and tetralogy of Fallot, each with its own pathogenic substrate and clinical repercussions. Using MRI for the assessment of aortic dimensions and elasticity (as indicators for aortic wall pathology), as well as aortic valve competence and LV function, allows for accurate monitoring of aortic and LV conditions.

Chapter 3 describes in vivo validation and testing of reproducibility of aortic pulse wave velocity as assessed with MRI ($PWV_{MRI}$). In this study, $PWV_{MRI}$ and pulse wave velocity as assessed by invasive pressure recordings (gold-standard) were compared in 18 patients scheduled for diagnostic catheterization. Non-invasive $PWV_{MRI}$ assessment of the proximal aorta, distal aorta and total aorta appeared to be in good agreement with the gold-standard as derived by invasive pressure measurements. Reproducibility of $PWV_{MRI}$ was tested in 10 healthy volunteers, who underwent repeated measurement of $PWV_{MRI}$ on a single occasion. Reproducibility of $PWV_{MRI}$ was high despite a substantial physiological variation in aortic pulse wave velocity. $PWV_{MRI}$ results should therefore be considered in combination with other parameters like blood pressure and MRI-assessed variables such as LV function and LV mass for depiction of cardiovascular disease.

Chapter 4 describes the effects of aortic wall pathology on aortic valve and LV function in patients with a non-stenotic bicuspid aortic valve. In this study, twenty patients with bicuspid

aortic valve disease and 20 age- and gender-matched healthy subjects were prospectively studied with MRI. Reduced aortic elasticity and aortic root dilatation were frequently observed, as indicators of proximal aortic wall disease. Furthermore, reduced aortic wall elasticity was associated with severity of aortic regurgitation and degree of LV hypertrophy, indicating that intrinsic aortic wall abnormalities in bicuspid aortic valve disease result in a negative cascade that affects aortic elasticity, aortic dimensions, aortic valve competence and LV function.

Chapter 5 describes the interaction between aortic elasticity and dimensions, aortic valve competence and LV function in 15 patients after the arterial switch operation and 15 age- and sex-matched control subjects. A similar cascade as in the previous chapter was observed, revealing frequent aortic root dilatation and reduced elasticity of the proximal aorta, associated with minor degrees of aortic regurgitation, reduced LV systolic function and enlarged LV dimensions. Therefore, despite the fact that the arterial switch operation has significantly reduced the number of sequelae associated with surgical correction of transposition of the great arteries, the current findings might pose a prognostic risk for patients after the arterial switch operation.

Chapter 6 describes the results of pulmonary flow dynamics in relationship with RV function in 17 patients with transposition of the great arteries, late after the arterial switch operation and 17 matched healthy controls. Supravalvar pulmonary artery stenosis has been reported to be the most frequent complication after arterial switch operation. This study reveals that increased peak-flow velocities are present across the pulmonary trunk even in patients without significant stenosis at the surgical anastomosis. Loss of distensibility due to local scar-tissue as well as minor degrees of narrowing at the site of anastomosis or peripheral pulmonary branches are probably the underlying reason. RV hypertrophy and RV relaxation abnormalities were found to be hemodynamic consequences, whereas systolic RV function is well preserved.

Chapter 7 reports on the relationship between the aorta, aortic valve and LV function in patients with repaired tetralogy of Fallot. In our study we examined 16 tetralogy of Fallot patients after pulmonary valve replacement, to minimize the possible confounding effect of adverse right-to-left ventricular interaction due to pulmonary regurgitation, and 16 matched healthy controls. This study revealed frequent aortic root dilatation and reduced elasticity of the proximal aorta, associated with minor degrees of aortic regurgitation and reduced LV systolic function. The current findings suggest that aortic wall pathology in repaired tetralogy of Fallot patients may represent a separate mechanism leading to aortic valve and LV dysfunction.

Chapter 8 describes the outcome of 53 consecutive patients who have previously undergone the Ross procedure in our institution for a dysfunctioning aortic valve. During the Ross procedure, a stenotic or insufficient aortic valve is replaced by a pulmonary autograft, with reconstruction of the right ventricular outflow tract using a pulmonary homograft. Early mortality occurred in 3 patients (5.6%), while 3 patients died 13 months, 5 and 6 years after the Ross operation, respectively (5.6%). Functional status of all survivors was excellent, although the majority of our patients showed autograft dilatation with concomitant aortic regurgitation. Therefore, the Ross procedure is considered to be of use especially in the pediatric population as it provides a growing aortic valve substitute, but should only be considered when valve-sparing techniques can no longer provide a solution for pediatric aortic valve disease.

Chapter 9 studies aortic dimensions and elasticity, aortic valve competence and LV function in 18 patients after the Ross procedure and 18 age- and sex-matched healthy subjects. Frequent dilatation of the autograft has been reported in literature during follow-up. The current study reveals not only dilatation, but also decreased distensibility of the aortic root, concomitant aortic regurgitation and reduced LV ejection fraction at a mean of 8 years of follow-up. Long-term sequelae after the Ross are therefore not only limited to the aorta, but extend towards the aortic valve and LV.

Finally, Chapter 10 evaluates the relationship between pulmonary flow dynamics and RV function in 17 patients after the Ross procedure and 17 age- and gender matched healthy subjects. Pulmonary homograft stenosis is the main cause for re-operation after the Ross procedure, necessary in approximately 10% of all cases at long-term follow-up. Little is however known about the effect of early homograft stenosis on RV function. In this study, MRI revealed mild degrees of homograft stenosis in most patients after the Ross procedure at a mean of 8.3 years of follow-up, with hemodynamic consequences like RV hypertrophy and RV diastolic dysfunction. Systolic RV function was still preserved. Therefore, as MRI is able to detect even subtle homograft valve and RV dysfunction, it may facilitate better selection of patients who need re-operation after the Ross procedure for homograft valve dysfunction.

## General conclusions

The MRI studies described in this thesis aimed to clarify the relation between aortic wall pathology, as expressed by measurements of aortic elasticity and dimensions, and aortic valve and LV function in different entities with intrinsic aortic wall abnormalities. MRI was also used to test whether a similar interaction is present between pulmonary artery dynamics and the right ventricle.

**We have shown that:**

1. non-invasive MRI assessment of the pulse wave velocity of the aorta is in good agreement with the gold-standard as derived by invasive pressure measurements and can be assessed with high reproducibility.
2. intrinsic aortic wall abnormalities result in a negative cascade of reduced aortic elasticity and increased aortic dimensions, and associated aortic valve- and LV dysfunction.
3. disturbed pulmonary flow dynamics by local stenosis or loss of distensibility result in pulmonary valve- and right ventricular dysfunction.
4. integrated MRI assessment of aortic elasticity and aortic dimensions, as well as aortic valve competence and LV function may be useful in the work-up of patients with intrinsic aortic wall abnormalities like bicuspid aortic valve disease, transposition of the great arteries, tetralogy of Fallot and patients after the Ross procedure.

## Samenvatting & Conclusies

Dit proefschrift beschrijft de rol van MRI (Magnetic Resonance Imaging) bij het in kaart brengen van de relatie tussen de dimensies en elasticiteit van de aorta en de aortaklep- en linker hartkamerfunctie bij patiënten met een bicuspide aortaklep, transpositie van de grote vaten, tetralogie van Fallot en patiënten na de Ross operatie. Tevens werd met behulp van MRI gekeken naar de interactie tussen de pulmonaal arterie en de rechter hartkamer bij dezelfde ziektebeelden.

Hoofdstuk 1 biedt algemene achtergrondinformatie over de interactie tussen de aorta, de aortaklep- en linker hartkamerfunctie bij bovengenoemde ziektebeelden.

In hoofdstuk 2 wordt de huidige stand van zaken besproken bij de 5 meest voorkomende aangeboren hartafwijkingen en bindweefselaandoeningen met intrinsieke aortawandafwijkingen, met beschrijving van de potentiële rol van MRI bij het vaststellen en de follow-up van deze ziektebeelden. Het is bekend dat veranderingen in de aortawand bij patiënten met de ziekte van Marfan kunnen leiden tot complicaties zoals aneurysma vorming en dissectie van de aorta. De ziekte van Marfan kan daarbij worden beschouwd als een prototype voor andere aangeboren hartafwijkingen waarbij veranderingen in de aortawand optreden. Als gevolg van deze aortawandafwijkingen kan er een cascade op gang komen, met uiteindelijk linker hartkamerdisfunctie tot gevolg: verlies van matrixstructuur en elastische componenten in de aortawand leidt tot dilatatie en een afgenomen elasticiteit van de aorta. De negatieve effecten zijn een versnelde aortaklepdegeneratie en een verhoging van de afterload voor de linker hartkamer. Progressie van deze cascade zal uiteindelijk resulteren in een overbelasting van de linker hartkamer. Met behulp van MRI kan op betrouwbare en nauwkeurige wijze deze cascade in kaart worden gebracht, hetgeen van nut kan zijn bij een verbeterde selectie van patiënten voor chirurgische interventie en voor het meten van veranderingen in aortafunctie tijdens farmacotherapie.

In hoofdstuk 3 wordt de in vivo validatie beschreven van metingen van de polsgolfsnelheid in de aorta gemeten met behulp van MRI ($PWV_{MRI}$). $PWV_{MRI}$ en de polsgolfsnelheid gemeten met behulp van invasieve drukmetingen werden met elkaar vergeleken bij 18 patiënten die een diagnostische hartkatheterisatie ondergingen. Non-invasieve $PWV_{MRI}$ van de proximale aorta, distale aorta en totale aorta bleken goed overeen te komen met de invasieve drukmetingen. Daarnaast werd de reproduceerbaarheid getest van $PWV_{MRI}$ door bij 10 gezonde vrijwilligers de $PWV_{MRI}$ tweemaal te meten op dezelfde dag. De reproduceerbaarheid bleek hoog te zijn, ondanks een fysiologische variatie van de aortale polsgolfsnelheid. Geconcludeerd wordt dat MRI een betrouwbare methode is voor het meten van polsgolfsnelheid in de aorta. MRI heeft

bovendien de voordelen dat de methode niet-invasief is en dat er geen gebruik wordt gemaakt van röntgentechnieken.

In hoofdstuk 4 wordt de relatie beschreven tussen de dimensies en de elasticiteit van de aorta en de aortaklep- en linker hartkamerfunctie bij patiënten met een niet-stenotische bicuspide aortaklep. In deze MRI-studie werden 20 patiënten met een bicuspide aortaklep vergeleken met 20 gezonde vrijwilligers. Bij een groot deel van het aantal onderzochte patiënten werd een afgenomen elasticiteit en dilatatie van de aorta vastgesteld, hetgeen was geassocieerd met de mate van aortaklepinsufficiëntie en linker hartkamerhypertrofie. Aangezien deze laatste twee factoren op de lange termijn zijn gerelateerd aan diastolische en systolische disfunctie van de linker hartkamer, kunnen deze bevindingen prognostische betekenis hebben voor het optreden van hartfalen op latere leeftijd. Follow-up van dimensies en elasticiteit van de aorta, in combinatie met aortaklep- en linker hartkamerfunctie wordt daarom aanbevolen voor deze groep van patiënten.

In hoofdstuk 5 wordt de interactie beschreven tussen de aorta, de aortaklep en de linker hartkamer bij 15 patiënten geboren met transpositie van de grote vaten, bij wie ter correctie een arteriële switch operatie (ASO) werd uitgevoerd. Een vergelijkbare cascade zoals in het vorige hoofdstuk wordt bij de ASO patiëntengroep beschreven: aortawortel dilatatie en afgenomen aorta-elasticiteit zijn geassocieerd met aortaklep- en linker hartkamerdisfunctie. Ondanks het feit dat het gebruik van de ASO een duidelijke afname heeft gegenereerd van het aantal complicaties in vergelijking met de in het verleden gebruikte chirurgische technieken, kunnen de genoemde factoren mogelijk leiden tot het optreden van hartfalen op latere leeftijd bij de onderzochte groep ASO patiënten.

In hoofdstuk 6 wordt de relatie beschreven tussen de pulmonale circulatie en de rechter hartkamerfunctie, bij 17 patiënten die geboren zijn met transpositie van de grote vaten - gecorrigeerd middels de ASO - en 17 gezonde vrijwilligers. Supravalvulaire pulmonaalklepstenose is de meest frequente complicatie na de ASO. Deze studie toont aan dat verhoogde snelheden van het bloed in de pulmonaal arterie in patiënten aanwezig kunnen zijn zonder een significante stenose. Verlies van elasticiteit van de pulmonaal arterie ten gevolge van lokaal littekenweefsel en een lichte mate van vernauwing ter plaatse van de pulmonalis hoofdstam en de perifere takken worden verondersteld als meest waarschijnlijke oorzaken. Rechter hartkamerhypertrofie en diastolische disfunctie werden vastgesteld als vroege aanwijzingen van rechter hartkamerdisfunctie, terwijl de systolische functie van de rechter hartkamer relatief was gespaard.

In hoofdstuk 7 wordt de relatie behandeld tussen de aorta, de aortaklep en de linker hartkamer bij tetralogie van Fallot patiënten na een pulmonaalklepvervanging. Deze studie toonde frequente dilatatie en een afgenomen elasticiteit van de aorta aan, welke zijn geassocieerd met aortaklepinsufficiëntie en een afgenomen linker hartkamerfunctie. Linker hartkamerdisfunctie bij tetralogie van Fallot patiënten werd tot op heden voornamelijk verklaard door een zogenaamde 'negatieve rechts-links interactie'. Hierbij zou een gedilateerde rechter hartkamer als gevolg van langdurig bestaande pulmonaalklepinsufficiëntie kunnen leiden tot linker hartkamerdisfunctie. Uit deze studie blijkt dat, naast deze verklaring, ook de aortawandpathologie bijdraagt aan aortaklep- en linker hartkamerdisfunctie bij patiënten na chirurgische correctie van tetralogie van Fallot.

In hoofdstuk 8 wordt de lange termijn uitkomst beschreven van 53 patiënten met een disfunctionerende aortaklep die de Ross operatie hebben ondergaan. Gedurende de Ross operatie wordt de lekkende, dan wel vernauwde, aortaklep vervangen door de eigen pulmonaalklep van de patiënt, met plaatsing van een donorklep op de opengevallen pulmonaalklep-positie. In totaal overleden 6 patiënten, van wie 3 patiënten postoperatief (5.6%) en 3 patiënten overleden na respectievelijk 13 maanden, 5 jaar en 6 jaar na de Ross operatie (5.6%). De klinische toestand van de resterende patiënten was weliswaar uitstekend, maar bij de meerderheid was er sprake van dilatatie en insufficiëntie van de pulmonaalklep in aortaklep-positie. De Ross operatie wordt daarom beschouwd als een goed chirurgisch alternatief vooral voor kinderen: de nieuwe klep kan immers meegroeien met het kind. De Ross operatie dient alleen te worden overwogen als klepsparende chirurgische technieken niet mogelijk zijn.

In hoofdstuk 9 wordt de relatie beschreven tussen dimensies en elasticiteit van de aorta en de aortaklep- en linker hartkamerfunctie bij 18 patiënten na de Ross operatie en 18 gezonde vrijwilligers. Dilatatie van de nieuwe aortawortel wordt frequent beschreven in de literatuur. Deze studie toont aan dat niet alleen dilatatie, maar ook een afgenomen elasticiteit van de aortawortel vaak voorkomt, samen met geassocieerde aortaklepinsufficiëntie en systolische linker hartkamerdisfunctie. Nadat de pulmonaalklep in aortaklep-positie is geplaatst, leiden een verstoorde lokale microcirculatie van de vaatwand en de blootstelling aan hogere systeemdrukken van de voormalige pulmonaal arterie vaatwand waarschijnlijk tot een versneld degeneratief proces, resulterend in de beschreven afwijkingen.

In het laatste hoofdstuk van dit proefschrift (hoofdstuk 10) wordt de relatie beschreven tussen de pulmonale flow dynamiek en de rechter hartkamerfunctie bij 17 patiënten na de Ross operatie. Pulmonaalklepstenose is de belangrijkste reden van re-operatie na de Ross operatie, noodzakelijk bij ongeveer 10% van alle patiënten. Er is echter weinig

bekend over het effect van een milde vorm van stenose op de rechter hartkamerfunctie. Deze studie laat zien dat het grootste deel van het aantal Ross patiënten, gemiddeld 8.3 jaar postoperatief, een milde vorm van pulmonaalklepstenose heeft, met rechter hartkamerhypertrofie en diastolische disfunctie tot gevolg. De systolische functie van de rechter hartkamer blijkt vooralsnog relatief te zijn gespaard. Aangezien het met behulp van MRI mogelijk is om zelfs een geringe mate van pulmonaalklepstenose en rechter hartkamerdisfunctie aan te tonen, wordt aanbevolen om MRI te gebruiken voor de follow-up van patiënten met een disfunctionerende pulmonalisdonorklep na de Ross operatie.

## Conclusies

De MRI-studies beschreven in dit proefschrift zijn bedoeld om meer inzicht te verkrijgen in de relatie tussen de dimensies en elasticiteit van de aorta en de aortaklep- en linker hartkamerfunctie bij patiënten met een bicuspide aortaklep, transpositie van de grote vaten, tetralogie van Fallot en patiënten na de Ross operatie. Tevens werd met behulp van MRI gekeken naar de interactie tussen de pulmonaal arterie en de rechter hartkamer bij de genoemde ziektebeelden.

**Deze studies tonen aan dat:**

1. MRI een betrouwbare en reproduceerbare non-invasieve methode is om de polsgolfsnelheid in de aorta vast te stellen.
2. aortawandafwijkingen niet alleen leiden tot dilatatie en een afgenomen elasticiteit van de aorta, maar ook tot aortaklep- en linker hartkamerdisfunctie.
3. een verstoorde pulmonale flow dynamiek, als gevolg van stenose of afgenomen distensibiliteit, leidt tot pulmonaalklep- en rechter hartkamerdisfunctie.
4. MRI metingen van dimensies en elasticiteit van de aorta en aortaklep- en linker hartkamerfunctie van belang zijn voor de follow-up van patiënten met intrinsieke aortawandafwijkingen zoals bij een bicuspide aortaklep, transpositie van de grote vaten, tetralogie van Fallot en patiënten na de Ross operatie.

# List of Publications

## Papers

**Grotenhuis HB**, Ottenkamp J, de Bruijn L, Westenberg JJM, Vliegen HW, Kroft LJM, de Roos A. Aortic elasticity and size are associated with aortic regurgitation and left ventricular dysfunction in tetralogy of Fallot after pulmonary valve replacement.
*Heart, accepted for publication.*

**Grotenhuis HB**, Westenberg JJM, Steendijk P, van der Geest RJ, Ottenkamp J, Bax JJ, Jukema JW, de Roos A. Validation and reproducibility of aortic pulse wave velocity as assessed with velocity-encoded MRI.
*Journal of Magnetic Resonance Imaging, accepted for publication.*

Romeih SAH, Kroft LJM, Bökenkamp R, Schalij MJ, **Grotenhuis HB**, Hazekamp MG, Groenink M, de Roos A, Blom NA. Delayed improvement of right ventricular diastolic function and regression of right ventricular mass after percutaneous pulmonary valve implantation in patients with congenital heart disease.
*American Heart Journal. 2009; 158 (1): 40-46.*

**Grotenhuis HB**, Ottenkamp J, Fontein D, Vliegen HW, Westenberg JJM, Kroft LJM, de Roos A. Aortic elasticity and left ventricular function after arterial switch operation: MR imaging - initial experience.
*Radiology. 2008; 249 (3): 801-809.*

**Grotenhuis HB**, de Roos A, Ottenkamp J, Schoof PH, Vliegen HW, Kroft LJM. MR imaging of right ventricular function after the Ross procedure for aortic valve replacement: initial experience.
*Radiology. 2008; 246 (2): 394-400.*

**Grotenhuis HB**, Ottenkamp J, Westenberg JJM, Bax JJ, Kroft LJM, de Roos A. Reduced aortic elasticity and dilatation are associated with aortic regurgitation and left ventricular hypertrophy in nonstenotic bicuspid aortic valve patients.
*J Am Coll Cardiol. 2007; 49 (15): 1660-1665.*

**Grotenhuis HB**, Kroft LJM, van Elderen SG, Westenberg JJM, Doornbos J, Hazekamp MG, Vliegen HW, Ottenkamp J, de Roos A. Right ventricular hypertrophy and diastolic dysfunction in arterial switch patients without pulmonary artery stenosis.
*Heart. 2007; 93 (12): 1604-1608.*

**Grotenhuis HB**, Westenberg JJM, Doornbos J, Kroft LJM, Schoof PH, Hazekamp MG, Vliegen HW, Ottenkamp J, de Roos A. Aortic root dysfunctioning and its effect on left ventricular function in Ross procedure patients assessed with magnetic resonance imaging.
*Am Heart J. 2006; 152 (5): 975 e1-8.*

Hazekamp MG, **Grotenhuis HB**, Schoof PH, Rijlaarsdam ME, Ottenkamp J, Dion RA. Results of the Ross operation in a pediatric population.
*Eur J Cardiothorac Surg. 2005; 27 (6): 975-979.*

**Grotenhuis HB**, Backx A, Nijveld A. Resection of a cardiac aneurysm in an infant with anomalous origin of the left coronary artery from the pulmonary trunk..
*Cardiol Young. 2004; 14 (1): 106-108.*

**Grotenhuis HB**, Nijveld A, Backx A. Absent pulmonary valve syndrome with intact ventricular septum and patent ductus arteriosus: report of two cases and a short review of the literature.
*Ann Thorac Surg. 2003; 75 (1): 280-282.*

## Oral presentations

Reduced aortic elasticity and dilatation are associated with aortic regurgitation and LV systolic dysfunction in tetralogy of Fallot after pulmonary valve replacement.
*The Association for European Paediatric Cardiology annual congress 2008, Venice, Italy.*

Aortic Pulse Wave Velocity assessed with Velocity-Encoded MRI: a Validation and Reproducibility Study.
*The Society for Cardiovascular Magnetic Resonance annual congress 2008, Los Angeles, USA.*

Reduced aortic elasticity and dilatation are associated with aortic regurgitation and left ventricular dysfunction after the arterial switch operation.
*The Society for Cardiovascular Magnetic Resonance annual congress 2008, Los Angeles, USA.*

Right Ventricular Function and Pulmonary Flow Dynamics Late after the Ross Operation Assessed with MRI.
*Radiological Society of North America annual congress 2007, Chicago, USA.*

Reduced aortic elasticity and dilatation are associated with aortic regurgitation and left ventricular dysfunction after the arterial switch operation.
*The Association for European Paediatric Cardiology annual congress 2007, Warsaw, Poland.*

MRI of aortic wall elasticity, aortic valve competence and LV function in patients with a non-stenotic bicuspid aortic valve.
*The Association for European Paediatric Cardiology annual congress 2007, Warsaw, Poland.*

Frequent pulmonary stenoses are not associated with RV dysfunction in arterial switch patients.
*American Heart Association annual congress 2005, Dallas, USA.*

Autograft dysfunction associated with left ventricular dysfunction after the Ross procedure, assessed with MRI.
*The Association for European Paediatric Cardiology annual congress 2005, Copenhagen, Denmark.*

**Poster presentations**

Reduced aortic elasticity and dilatation are associated with aortic regurgitation and left ventricular dysfunction after the arterial switch operation.
*European Society of Cardiology annual congress 2007, Vienna, Austria.*

Right ventricular function and pulmonary flow dynamics late after the Ross operation, assessed with MRI.
*The Society for Cardiovascular Magnetic Resonance annual congress 2007, Rome, Italy.*

MRI of aortic wall elasticity, aortic valve competence and LV function in patients with a non-stenotic bicuspid aortic valve.
*The Society for Cardiovascular Magnetic Resonance annual congress 2007, Rome, Italy.*

Autograft dysfunction associated with left ventricular dysfunction after the Ross procedure, assessed with MRI.
*Poster Price (first price) of 'Emma Children's Hospital research symposium', Amsterdam, The Netherlands.*

Right ventricular function and pulmonary circulation in arterial switch patients during long-term follow-up, assessed with MRI.
*The Society for Cardiovascular Magnetic Resonance annual congress 2006, Miami,USA.*

Frequent pulmonary stenoses after the arterial switch operation, assessed with MRI.
*World congress for Pediatric Cardiology 2005, Buenos Aires, Argentine.*

Autograft dysfunction associated with left ventricular dysfunction after the Ross procedure, assessed with MRI.
*World congress for Pediatric Cardiology 2005, Buenos Aires, Argentina.*

Frequent pulmonary stenoses after the arterial switch operation, assessed with MRI.
*European Society of Cardiology annual congress 2005, Stockholm,Sweden.*

In-plane pulse wave velocity with MRI in ischemic heart disease: validation of a new technique.
*The Society for Cardiovascular Magnetic Resonance annual congress 2005, San Francisco, USA.*

Aortic autograft dilatation and impaired distensibility in Ross patients, assessed with MRI.
*The Society for Cardiovascular Magnetic Resonance annual congress 2005, San Francisco, USA.*

## Dankwoord

De volgende mensen zou ik graag willen bedanken voor hun hulp bij de totstandkoming van dit proefschrift.

Alle patiënten en gezonde vrijwilligers die hebben deelgenomen aan de studies, als ook de vrijwilligers die hebben geholpen de scantechnieken te optimaliseren.

Alle collega's met wie ik in de afgelopen jaren de onderzoekerskamer heb gedeeld, wat zowel stimulerend als erg leuk was. De mooie congressen (San Francisco), de onderzoekersweekenden (Parijs), de half-twaalf lunch en natuurlijk de gezelligheid op de kamer. Hierdoor kijk ik met een lach op mijn gezicht terug op deze tijd!

Jos, vanaf het begin van mijn promotie traject hebben we fijn samengewerkt, waarbij ik je niet alleen waardeer om je MRI kennis, maar vooral ook om je warmte en interesse.

Gerda, zonder jouw niet-aflatend enthousiasme om alle ouders en kinderen te benaderen voor onze studies had mijn onderzoek zeker langer geduurd, maar bovenal dank voor je inbreng en leuke tijd.

Alle artsen en verpleegkundigen van het catheterisatie lab, voor hun langdurige steun bij het vinden van geschikte patiënten en het verzamelen van data voor deze studie.

Margot, met veel enthousiasme hebben we samen naar hartpreparaten gekeken in het anatomiegebouw, wat sterk heeft geholpen bij mijn begrip van aangeboren hartafwijkingen.

Gerrit, voor al je hulp bij het maken van de figuren in dit proefschrift en verschenen artikelen.

Natascha, Pauline en Margriet, voor jullie interesse en gezelligheid!

Alle collega's van het Emma Kinderziekenhuis / AMC, voor jullie interesse in mijn onderzoek tijdens de opleiding.

Dear Philipp, Reza, Tobias, Gerald, Anil, Aaron, Shak, Vicky, Cathy, Menno, Parantha, Bart and Philip; thanks a lot for the stimulating environment during my stay in the Evelina Children's Hospital and making the 7 months in London a great experience!

Mirelle, voor je artistieke inbreng bij het maken van de cover van dit boekje.

Een speciale dank gaat uit naar de studenten die hun wetenschappelijke stage bij mij hebben verricht (Saskia, Jeroen, Duveken en Liesbeth). Met veel plezier heb ik met jullie samengewerkt!

Beste Jacob, Jan Willem, Marieke, Joost, Wendy, Pieter, Claudia, Bas, Sabina, Jeroen en Bart; hartelijk dank voor jullie vriendschap!

Marieke en Jan Willem, zus en vriend (en broertje), ik ben er trots op dat jullie mijn paranimfen zijn!

Mijn lieve zussen Margit, Brechtje en Marieke.

Lieve Mira, ik hou van je.

Tot slot, lieve Froukje en Dinus, jullie ben ik veel dank verschuldigd, maar ik ben vooral trots op het feit jullie zoon te zijn.